Phenomenology of Supersymmetric Models

James Philip John Hetherington

King's College

A dissertation submitted to the University of Cambridge
for the degree of Doctor of Philosophy
October 2002
As amended after examination, November 2002.

Phenomenology of Supersymmetric Models

James Philip John Hetherington

Abstract

This thesis describes a set of connected studies regarding the phenomenology of supersymmetric models, based around the Minimal Supersymmetric Standard Model (MSSM) and its extensions.

The prospects of discovering supersymmetry at the Large Hadron Collider are re-analysed, in order to re-express coverage in terms of a fine-tuning parameter and to extend the analysis to scalar masses (m_0) above 2 TeV. The discovery reach at high m_0 is of interest because this region has been found to have a focus point, leading to relatively low fine-tuning, and because it remains uncertain how much of the region can be ruled out due to lack of radiative electroweak symmetry breaking. The best fine tuning reach is found in a mono-leptonic channel. All points in minimal supergravity (mSUGRA) with $m_0 < 4000$ GeV, with a fine tuning measure up to 210 or 500 are covered by the search, depending upon whether the definition of fine-tuning excludes or includes the contribution from the top Yukawa coupling. Even for arbitrarily high m_0, mSUGRA can be discovered through gaugino events, provided the gaugino mass parameter $M_{1/2} < 460$ GeV.

The MSSM can include two soft breaking terms which are often neglected: a non-analytic scalar trilinear coupling and a higgsino bilinear term. This is known as Non-Standard Supersymmetry Breaking (NSSB). A set of high-scale boundary conditions consistent with the reparameterisation invariance which the model possesses is obtained.

The three-family renormalisation group equations for the MSSM with these terms are presented. The ranges of the universal high-scale values of these couplings which lead to an acceptable TeV-scale theory are obtained, as is the supersymmetric particle spectrum at this scale. The effect of the new terms on fine-tuning is presented. SOFTSUSY, an existing program for calculating SUSY particle spectra, has been used, with as few modifications as possible to include NSSB terms.

A computer program for automatically determining the one-loop effective potential and one-loop mass matrices of a general supersymmetric model is described. The development of this software is discussed, and results for a variety of models are presented as evidence of its capabilities. These include studies of explicit CP and R-parity violation in the MSSM, where results are obtained that are both consistent with existing studies where expected, and include fuller analyses than previous work. In the study of CP violation, results for the scalar/pseudoscalar coupling ratio of fermions are consistent with previous studies, but the electric dipole moments are found to get large contributions from the light Higgs boson, which is no longer a CP eigenstate. This effect occurs only when the Higgs mass is in violation of LEP mass bounds.

Declaration

This thesis is the result of my own work, except where explicit reference is made to the work of others (see acknowledgments), and has not been submitted for another qualification to this or any other university

James Philip John Hetherington

Acknowledgments

I would like to thank the Particle Physics and Astronomy Research Council for providing financial support during this degree (studentship number PPA/S/S/1999/02798). Thanks to King's College, Cambridge, for seven years of community and belonging.

Thanks to my supervisor, Prof. Bryan Webber, for general consultation, for suggesting the research topic for chapter 4 and for advice regarding HERWIG and the W+jet corrections for the research of chapter 3. Thanks to Dr. Ben Allanach for writing SOFTSUSY and providing support when I was its first non-author user in chapter 4, for the SOFTSUSY fine-tuning calculation in chapter 3, and again, for general consultation. Thanks to Dr. Andy Parker for suggesting the research topic of chapter 3, and for suggestions on how to write to be understood by experimentalists. Thanks to Dr. Peter Richardson and Dr. Agustin Sabio Vera for help and advice. Thanks to Prof. Tim Jones for advice and encouragement.

Thanks to Dr. Chris Lester for friendship, HWPLOT, and being my computer guru when I was new to all this stuff. Thanks to Phil Kendall and Robert Dillon – though this thesis may not have turned out to be a *Tome of Understanding*.

Thanks to all who have proof-read this thesis: Bryan, Ben, Agustin and Peter.

Thanks to my parents, sister, and grandparents.

Thanks to Sue, for Everything.

Contents

List of Figures

List of Tables

Introduction

This constitutes my research for a PhD degree in theoretical high-energy physics. Chapter 1 is an original review of the theoretical background to my research, while chapter 2 is an original review of some of the software I have used during my research. Chapter 3 contains the research from the first year of my PhD: a collaborative (see acknowledgments) study of the ability of the Large Hadron Collider (LHC) to erode our theoretical confidence that supersymmetry may be present in nature. Chapter 4 contains my research into a particular extension of the usual SUSY models known as Non-Standard Supersymmetry Breaking (NSSB). These two studies have been published [1], [2]. Chapter 5 describes the development and use of a program, EFFECTIVE, capable of automatically carrying out many of the calculations necessary in the analysis of new physics models. Chapter 6 gives the results of some studies of CP and R-parity violating extensions of the MSSM using EFFECTIVE, demonstrating the capabilities of the software.

Chapter 1

Theoretical Introduction

1.1 Supersymmetry

1.1.1 Introduction

A possibility for new physics beyond the Standard Model is supersymmetry (SUSY) [3–6]. If fermionic generators are added to the bosonic generators of the Lorentz group, the new space-time symmetry is supersymmetry. As a result of exact supersymmetry, all particles have a partner of equal mass but opposite spin-statistics. Cancellations between bosonic and fermionic loops prevent radiative corrections from driving scalar masses up to the highest scale present, assumed to be the Grand Unification(GUT) or Planck scale, 10^{16} to 10^{19} GeV, thus solving the naturalness problem of the Standard Model [7]. In addition, the renormalised electromagnetic, weak, and strong couplings, whose low energy values are known from data, can be made to converge more nearly to a common value at the grand unification scale [8]. This last point is now believed to be less convincing than it once was [9].

1.1.2 Broken Supersymmetry

Since supersymmetry is not observed amongst the already discovered particles, it must be a broken symmetry. The scale at which supersymmetry is broken, M_{SUSY}, would be the typical mass of the as yet undiscovered superpartners of the Standard Model particles, and represents the scale at which this new physics becomes relevant. Considerations of general new physics beyond the Standard Model [10] can result in upper bounds on new physics scales of order a few TeV. However, in supersymmetric models [6], M_{SUSY} is expected to be at most around 1 TeV. Unless there are large cancellations between SUSY breaking parameters, the electroweak symmetry breaking scale will be of order M_{SUSY}, and the W and Z bosons would have masses inconsistent with their measured values if M_{SUSY} is too large.

If M_{SUSY} is at or below the TeV scale, then supersymmetric particles will almost certainly be discovered at the Large Hadron Collider (LHC), being built at CERN. Indeed, detailed studies of how the SUSY parameters would be measured by the LHC general-purpose experiments ATLAS [11] and CMS [12] have been made.

1.2 The MSSM

The simplest possible SUSY extension of the Standard Model of particle physics, with a superpartner for each standard model particle, and the addition of a second Higgs scalar doublet, is called the Minimal Supersymmetric Standard Model, or MSSM. This model has been the subject of a great deal of research, and is the basis for the studies which suggest that SUSY will be discovered at the LHC if it exists.

1.2.1 Particle Content Of The MSSM

The MSSM has the particle content of the Standard Model plus a supersymmetric partner for each of these, named by prefixing an *s* onto the names of fermions, and suffixing *ino* onto the bosons (table 1.1). In addition, a second Higgs scalar doublet is added, to cancel anomalies and give mass to the down-like quarks (sec. 1.2.2). Here we define a convention, where superscript i represents a family index, a a colour SU(3) fundamental index, b a weak SU(2) fundamental index, c a colour SU(3) adjoint octet index, d a weak SU(2) adjoint triplet index. A + superscript indicates the particles' charge under $U(1)_Y$ of hypercharge in column 2, or the U(1) of electric charge left over from the Higgs mechanism in column 4. From these the gauge representation of the particle in the Standard Model $SU(3)_C \otimes SU(2)_W \otimes U(1)_Y$ group can be recognised. A superscript μ indicates that the particle is a Lorentz vector, a superscript s that it is a left-handed Lorentz spinor. Note that the right-handed particle's symbols refer to their left-handed conjugate fields, hence the conjugation overbar that is part of their names, and the opposite charge from that which might be expected. Table 1.1 defines the naming conventions for the fields in this thesis. To obtain the convention of [5], $H_1 \equiv H_u$, and $H_2 \equiv H_d$.

Many of these particles can mix, and so there also exist names for the mass eigenstates of the theory (table 1.2).

1.2.2 The Superpotential

The MSSM Lagrangian is supposed to include all possible SUSY conserving terms given the particle content. Apart from the gauge interactions, all SUSY conserving renormalisable interaction terms for a general SUSY model can be specified using a "superpotential" [4, 5]. This is an analytic function, formally of the (chiral, or matter) superfields (objects containing the fields and their superpartners, together with a number of aux-

Name	symbol	Alternative Name	symbol
Left Quarks	$Q_L^{iabs-\frac{1}{6}}$	Left-uplike quarks Left-downlike quarks	$u_L^{ias+\frac{2}{3}}$ $d_L^{ias-\frac{1}{3}}$
Right-uplike quarks	$\overline{u}_R^{ias-\frac{2}{3}}$		
Right-downlike quarks	$\overline{d}_R^{ias+\frac{1}{3}}$		
Left leptons	$L_L^{ibs+\frac{1}{2}}$	Electron left Neutrino left	e_L^{is-} ν_L^{is}
Right electrons	$\overline{e}_R^{is+}$		
Left Squarks	$\tilde{Q}_L^{iab-\frac{1}{6}}$	Left-uplike Squarks Left-downlike Squarks	$\tilde{u}_L^{ia+\frac{2}{3}}$ $\tilde{d}_L^{ia-\frac{1}{3}}$
Right-uplike squarks	$\overline{\tilde{u}}_R^{ia-\frac{2}{3}}$		
Right-downlike squarks	$\overline{\tilde{d}}_R^{ia+\frac{1}{3}}$		
Left Sleptons	$\tilde{L}_L^{ib+\frac{1}{2}}$	Selectron left Sneutrino left	$\tilde{e}_L^{i-}$ $\tilde{\nu}_L^{i}$
Right selectrons	$\overline{\tilde{e}}_R^{i+}$		
Higgs one Higgs two	$H_1^{b+\frac{1}{2}}$ $H_2^{b-\frac{1}{2}}$	Real Neutral Higgs 1 Imaginary Neutral Higgs 1 Charged Higgs 1 Real Neutral Higgs 2 Imaginary neutral Higgs 2 Charged Higgs 2	H_1 H_1 H_1^+ H_2 H_2 H_2^-
Higgsino one Higgsino two	$\tilde{H}_1^{bs+\frac{1}{2}}$ $\tilde{H}_2^{bs+\frac{1}{2}}$	Neutral Higgsino 1 Charged Higgsino 1 Neutral Higgsino 2 Charged Higgsino 2	$\tilde{H}_1^{s0}$ $\tilde{H}_1^{s+}$ $\tilde{H}_2^{s0}$ $\tilde{H}_2^{s-}$
B-boson W-boson gluon	B^μ $W^{\mu d}$ $g^{\mu c}$		
Bino Wino gluino	$\tilde{B}^s$ $\tilde{W}^{sd}$ $\tilde{g}^{sc}$		

Table 1.1: The particle content of the MSSM, in terms of interaction eigenstates, using conventions defined in the text.

Name (interaction eigenstate)	symbol	Name (mass eigenstate)	symbol
B-boson	B^μ	Photon	γ^μ
W-3 boson	$W^{\mu 3}$	Z-boson	Z^μ
W-1 boson	$W^{\mu 1}$	W-boson	$W^{\mu +}$
W-2 boson	$W^{\mu 2}$		$W^{\mu -}$
Wino-1	$\tilde{W}^{s1}$	Chargino 1	$\tilde{\chi}_1^{s+}$
Wino-2	$\tilde{W}^{s2}$	Chargino 2	$\tilde{\chi}_2^{s+}$
Charged Higgsino-1	$\tilde{H}_1^{s+}$	Anti-Chargino-1	$\tilde{\chi}_1^{s-}$
Charged Higgsino-2	$\tilde{H}_2^{s-}$	Anti-Chargino-1	$\tilde{\chi}_1^{s-}$
Wino-3	$\tilde{W}^{s3}$	Neutralino 1	$\tilde{\chi}_1^{s0}$
Bino	$\tilde{B}^s$	Neutralino 2	$\tilde{\chi}_2^{s0}$
Neutral Higgsino-1	$\tilde{H}_1^s$	Neutralino 3	$\tilde{\chi}_3^{s0}$
Neutral Higgsino-2	$\tilde{H}_2^s$	Neutralino 4	$\tilde{\chi}_4^{s0}$
Real Neutral Higgs 1	H_1	Light neutral CP-even Higgs	h
Real Neutral Higgs 2	H_2	Heavy neutral CP-even Higgs	H
Imaginary Neutral Higgs 1	H_1	CP-odd Higgs	A
Imaginary neutral Higgs 2	H_2		
Charged Higgs 1	H_1^+	Charged Higgs	H^+
Charged Higgs 2	H_2^-		H^-

Table 1.2: The mixing-groups, in terms of mass and interaction eigenstates of the MSSM.

iliary fields) in the model, but usually taken to be a function of the scalar part of the matter superfields.

The interaction contribution to the Lagrangian arising from the superpotential $W(\phi_i)$ is then (after integrating out auxiliary fields):

$$\mathcal{L} = -\frac{1}{2}(W^{ij}\psi_i\psi_j + W^{*ij}\psi_i^\dagger\psi_j^\dagger) - W^i W^{*i} \tag{1.1}$$

$$W^i = \frac{\delta W}{\delta \phi_i} \tag{1.2}$$

$$W^{ij} = \frac{\delta^2 W}{\delta\phi_i \delta\phi_j} \tag{1.3}$$

where ϕ_i is the ith scalar field in the model, and ψ_i is its spinor superpartner.

The superpotential of the MSSM is thus just that which gives rise to the usual Standard Model Yukawa terms, except that it generates a number of extra interactions as well.

$$W_{\mathrm{MSSM}} = \tilde{\overline{u}}_R^i \tilde{Q}_L^{j\alpha} H_{1\alpha} Y_{ij}^u + \tilde{\overline{d}}_R^i \tilde{Q}_L^{j\alpha} H_{2\alpha} Y_{ij}^d + \tilde{\overline{e}}_R^i \tilde{L}_L^{j\alpha} H_{2\alpha} Y_{ij}^e + \mu H_1^\alpha H_{2\alpha} \quad (1.4)$$

recalling that the SU(2) index α is raised and lowered antisymmetrically. i and j are family indices.

Hence we see that in order to give mass to both the up- and down-type quarks, we need two Higgs doublets with opposite hypercharge, since in order to write an SU(2) gauge invariant superpotential giving, for example, mass to the down-type quarks with H_1, we would need to use H_1^* in the superpotential, but the superpotential must be an analytic function [3]. In addition, without the contribution of both Higgs doublets, cancellation of the higgsino triangle anomaly would not occur.

It should be noted that μ is the only supersymmetry-conserving dimensionful parameter of the MSSM. Later arguments (sec. 1.2.6) will show that in fact, in order for the MSSM to be consistent with known physics, μ must be of order the weak scale. Dimensionful supersymmetry-breaking terms (sec. 1.2.4) can naturally get magnitudes of order the weak scale, as they must, by imagining that the mechanism driving electroweak symmetry breaking also drives supersymmetry breaking: i.e. there is a supersymmetry breaking vacuum expectation value of the appropriate scale. In the MSSM, there is no such mechanism to explain why μ should be around the weak scale– the so called μ-problem of the MSSM. The Next-To-Minimal-SUSY Standard Model (NMSSM) (sec. 1.3.4) is one attempt to provide such a mechanism.

In addition to the superpotential, a general supersymmetric Lagrangian is also expressed in terms of two further functions of the superfields, the Kähler Potential and the Gauge Kinetic Function. Since only one possible form for these functions gives rise to a renormalisable Lagrangian, these common forms are assumed in this thesis [5].

1.2.3 Gauge Interactions

The gauge interactions of the MSSM are generally as expected by analogy with the Standard Model: it has the same $SU(3)_C \otimes SU(2)_W \otimes U(1)_Y$ gauge group. However, there are extra terms arising as a result of the adjoint fermions (gauginos). Here are the extra gauge interaction terms of a SUSY model due to a gauge factor with a coupling g:

$$\begin{aligned}\mathcal{L}_{\text{SUSY,Gauge}} &= -igA^a_\mu \bar{\lambda}^b \overline{\sigma}_\mu f^{abc} \lambda^c \\ &\quad -\sqrt{2}g(\phi_i^* T^a \psi_i \lambda^a + c.c.) \\ &\quad -\frac{1}{2}g^2(\phi_i^* T^a \phi_i)(\phi_j^* T^a \phi_j)\end{aligned} \tag{1.5}$$

λ is the gaugino field, A the gauge boson, ψ is each spinor matter field, ϕ each scalar matter field. T are the generators of the group and f the structure constants. Indices i and j index the particle content of the model, ψ_i is the superpartner of ϕ_i. These terms are in addition to the usual matter-gauge boson and gauge boson-gauge boson interactions from the covariant derivatives.

In the MSSM, g', g_2 and g_3 are the three gauge coupling parameters for the three gauge factors, $U(1)$ $SU(2)_Y$ and $SU(3)_C$ respectively. The symbol $g_1 = g' \times \sqrt{\frac{5}{3}}$ is reserved for the grand-unified theory context, where g_1 is the normalisation of the U(1) coupling which unifies with the other couplings at the unification scale (sec. 1.4).

Note the scalar-quartic term. This is called the "D-term", as it arises, in part, from integrating out the auxiliary field in the gauge supermultiplet, called D.

1.2.4 Supersymmetry Breaking In The MSSM

While models for supersymmetry breaking exist (for a review, see [5]) in the MSSM, we conventionally include all possible renormalisable "soft" supersymmetry-breaking terms in the Lagrangian:

$$\begin{aligned}\mathcal{L}_{\text{MSSM,Soft Breaking}} &= -\frac{1}{2}(M_1\tilde{B}\tilde{B} + M_2\tilde{W}\tilde{W} + M_3\tilde{g}\tilde{g} + c.c.) - m^2_{ij}\phi_i\phi^*_j \\ &\quad -bH_1H_2 - \overline{\tilde{u}^i_R}a^u_{ij}\tilde{Q}^j_L H_1 + \overline{\tilde{d}^i_R}a^d_{ij}\tilde{Q}^j_L H_2 + \overline{\tilde{e}^i_R}a^e_{ij}\tilde{L}^j_L H_2 \qquad (1.6)\end{aligned}$$

ϕ_i is any scalar field in the model, although m^2 is usually diagonal, when its components are labeled $m^2_{H_1}$ and so on.

Why have only these so-called "Soft" terms been included? The soft supersymmetry breaking terms are those which do not destroy the supersymmetric protection against scalar masses gaining corrections of order the cutoff, and are those with positive mass dimension. Then, the limit $M_{\text{SUSY}} \to 0$ of the theory exists, and is supersymmetric. M_{SUSY} is the common value of all the supersymmetry violating terms of mass dimension one, M^2_{SUSY} for parameters of mass dimension two, etc. The non-supersymmetric corrections to the scalar masses vanish in this limit, and therefore, by dimensional analysis near the limit, cannot be proportional to the square of the high-energy cutoff Λ^2:

$$\Delta m^2_H \propto M^a_{\text{SUSY}}\Lambda^{2b} \qquad (1.7)$$

$$2 = a + 2b \qquad (1.8)$$

$$a > 0 \Rightarrow 1 > b \qquad (1.9)$$

The case $b = \frac{1}{2}$ is ruled out because loop integrals never depend linearly on the cutoff. If $a > 0$ is the requirement that the limit $M_{\text{SUSY}} \to 0$ exists.

Note the enormous number of possible soft-breaking terms: one for each scalar field in the model and one for each gauge factor. Models of supersymmetry breaking can be used to reduce this parameter space to a more manageable dimension, and represent sub-categories of the MSSM. Alternatively, studies have been done sampling randomly in the full MSSM parameter space [13].

1.2.5 Minimal Supergravity

The most studied sub-category of the MSSM is minimal supergravity, mSUGRA, sometimes also called the constrained MSSM (CMSSM). Supergravity, where supersymmetry is a local, rather than a global symmetry, at one time motivated unification assumptions amongst the MSSM SUSY breaking parameters, reducing the number of parameters, from the hundred or so of the MSSM, to just four (eq. (1.10)), a soft mass for the scalars, one for the gauginos, a single mass relating the trilinears to the Yukawa couplings and b, which is often relabelled $b = \mu B$. Currently, the suppression of flavour changing neutral currents, not supergravity, is the main motivator for these assumptions.

$$\begin{aligned} m_{\phi_i} &= m_0 \\ M_a &= M_{\frac{1}{2}} \\ a^k_{ij} &= Y^k_{ij} A_0 \\ b &= \mu B \end{aligned} \tag{1.10}$$

In eq. (1.10) we define a convention for the three sets of Yukawa couplings $Y^u Y^d Y^e$ and related objects, using a raised Latin index to indicate this multiplicity.

The idea of a gravity-mediated flavour-blind interaction being responsible for supersymmetry breaking suggests that these constraints should be imposed as boundary conditions on the running SUSY-breaking masses and couplings at high scale, usually taken to be $M_X = 10^{16}$ GeV. Experimental masses of superparticles are obtained by evolving the Lagrangian to the weak scale using the renormalisation group equations (sec. 1.4). A solution consistent with the mSUGRA boundary conditions at M_X and the known Standard Model constraints at M_Z must be found. This constitutes a boundary value differential equation problem, and can be solved numerically (sec. 2.1).

1.2.6 Radiative Electroweak Symmetry Breaking

In the Standard Model, the real part of the neutral Higgs field gets a vacuum expectation value (VEV). An explicit symmetry-breaking potential is included in the Lagrangian $V(h)$.

The MSSM naturally allows for a symmetry-breaking Higgs effective potential: inspection of the Lagrangian reveals that, at tree level:

$$\begin{aligned} V_{\text{Higgs}} &= (|\mu|^2 + m_{H_1}^2)(|H_1^0|^2 + |H_1^+|^2) + (|\mu|^2 + m_{H_2}^2)(|H_2^0|^2 + |H_2^-|^2) \\ &+\mu B(H_1^+ H_2^- - H_1^0 H_2^0) + c.c. \\ &+\frac{1}{8}(g_2^2 + g'^2)(|H_1^0|^2 + |H_1^+|^2 - |H_2^0|^2 + |H_2^-|^2)^2 \\ &+\frac{1}{2} g_2^2 |H_1^+ H_2^{0*} + H_1^0 H_2^{-*}|^2 \end{aligned} \tag{1.11}$$

Thus, provided:

$$\mu^2 B^2 > (|\mu|^2 + m_{H_1}^2)(|\mu|^2 + m_{H_2}^2) \tag{1.12}$$

the minimum of the potential will not be at $\langle H_1^0 \rangle = \langle H_2^0 \rangle = 0$, but instead the two neutral Higgs fields will get VEVs. The ratio of these vacuum expectation values is called $\tan\beta$:

$$\begin{aligned} v_1 &= < H_1^0 > \\ v_2 &= < H_2^0 > \\ v^2 &= v_1^2 + v_2^2 \\ \tan\beta &= v_2/v_1 \end{aligned} \tag{1.13}$$

Note that, as with the standard model, the number of surviving Higgs bosons (5 in the MSSM) after electroweak symmetry breaking is less than the original number of Higgs fields (8 real scalar degrees of freedom), as some are "eaten" by the gauge bosons as the symmetry is broken.

In addition, one must also require that even along the quartically flat directions the potential becomes large for large values of the fields. This constraint is:

$$2|\mu B| < (2|\mu|^2 + m_{H_1}^2 + m_{H_2}^2). \tag{1.14}$$

By differentiation of eq. (1.11) one can obtain:

$$\begin{aligned} \frac{1}{2}M_Z^2 &= \frac{1}{4}(g_2^2 + g'^2)(v_1^2 + v_2^2) \\ &= \frac{m_{H_1}^2 + \mu^2 - (m_{H_2}^2 + \mu^2)\tan^2\beta}{\tan^2\beta - 1} \qquad (1.15) \\ -B\mu &= \frac{1}{2}(m_{H_1}^2 + m_{H_2}^2 + 2|\mu|^2)\sin 2\beta \qquad (1.16) \end{aligned}$$

Now, in the MSSM eq. (1.12) is not generally satisfied by the parameters as they are imposed at M_X (sec. 1.2.5), since universality assumptions motivate equal soft masses for the two Higgs doublets, meaning eq. (1.12) and eq. (1.14) cannot be simulataneously satisfied. However, the renormalisation group equations of the MSSM (sec. 1.4) are such that $m_{\tilde{H}_2}^2$ is normally small around the weak scale. Thus, the quantum corrections driving the renormalisation group running of $m_{\tilde{H}_2}^2$ are what cause electroweak symmetry to be broken in the CMSSM. This is called Radiative Electroweak Symmetry Breaking (REWSB). In some regions of MSSM parameter space, this does not occur, and hence those points of the parameter space are ruled out (sec. 1.2.8).

Note that eq. (1.15) shows that if $m_{\tilde{H}_2}^2$ and $m_{\tilde{H}_1}^2$ are very large, cancellations are required if M_Z is to have its known value. This is part of the reason why M_{SUSY} is assumed to be not much larger than the weak scale, and hence why SUSY is being searched for at collider experiments.

Using the constraints eq. (1.15) and eq. (1.16) one can redefine the parameter set of a SUSY model. For example, for the constrained or supergravity MSSM (sec. 1.2.5), one can take as a parameter set, instead of $m_0, A_0, M_{\frac{1}{2}}, \mu$ and B, the set $m_0, A_0, M_{\frac{1}{2}}, \tan\beta$ and M_Z. In the latter case, because eq. (1.15) depends only on μ^2, we must specify the sign of μ.

1.2.7 Fine-tuning

As mentioned in section 1.2.6, it is possible to avoid the problem of large electroweak boson masses even for large M_{SUSY} if there are cancellations amongst the SUSY masses. In mSUGRA, m_{H_2} has the same origin as the super-partner masses (m_0). Thus as search limits put lower bounds upon super-partners' masses, the lower bound upon m_0 rises, and consequently so does $|m_{H_2}|$. Increasingly fine cancellation is required between the terms of eq. (1.15) in order to provide the measured value of $M_Z \ll |m_{H_2}|$. However, such situations, where the parameters of a theory are carefully tuned to avoid unphysical results, are often thought to be unsatisfactory. Fundamental parameters, it is argued, should be independent, uncorrelated inputs.

These 'naturalness' arguments are often quantified in terms of 'fine tuning' [14]. There are a few different fine-tuning measures, for example, [15,16], and all are intended to be measures of the degree of cancellation required between fundamental parameters. A value of fine-tuning above which a theory becomes unacceptable is often advanced, and used to support the argument that M_{SUSY} should be small.

The authors of [17] discuss a measure of fine-tuning and use it to assess the status of the MSSM if superparticles are not found at the LHC. In [16] fine-tuning motivated upper bounds on MSSM masses are obtained using a complete one-loop effective potential. [18] discusses the use of fine-tuning to compare different high-energy supergravity scenarios, while [19] uses fine-tuning to compare non-minimal supersymmetric models.

Can fine-tuning be used to put an upper bound on the sparticle masses? Will we ever say, "the experimental lower bound on the particle masses is so high, and the MSSM so fine-tuned, that supersymmetry must be wrong"? The use of fine-tuning as a quantitative measure of the theoretical attractiveness of a model is somewhat controversial. Since its status as a possible solution of the naturalness problem of the Standard Model is one of the main reasons for investigating supersymmetry, naturalness arguments have increased relevance to studies of supersymmetry. It is only through assuming enormous cancellations between an uncorrected Higgs mass of order the cutoff scale, and the corrections of order the cutoff scale, that the existence of the weak scale in the Standard Model can be explained.

I therefore contend that fine-tuning is a relevant way to compare SUSY models, experiments, and search channels, and is a useful measure of experimental discovery reach. As experiments push the lower bounds on SUSY parameters upwards, the minimum fine-tuning which SUSY can have increases, and our confidence that the universe is supersymmetric at low energies falls. It is only because of cancellation problems with the standard model that we think SUSY might be there at all. If SUSY is subject to similar criticisms, our reason for believing in it at all is weakened. However, I do not believe that a high fine-tuning in itself can be used to rule a theory out altogether, since accidental cancellations may well be present in the correct theory.

One common definition of fine-tuning c_a, which will be used below, represents the degree to which a parameter a must be carefully adjusted, or 'fine-tuned', in order to achieve consistency with known bounds. Large cancellations lead to high values of fine-tuning:

$$c_a \equiv \left| \frac{\partial \ln M_Z^2}{\partial \ln a} \right|. \tag{1.17}$$

From a choice of a set of fundamental parameters $\{a_i\}$, the fine-tuning of a particular model may defined to be

$$c = \max(c_a) \tag{1.18}$$

Note that a given point in model space may be parameterised in different ways. For example, choosing a^2 rather than a as a parameter halves the fine-tuning due to that parameter.

1.2.8 Constraints On The Valid MSSM Parameter Space

What limits the valid range of values the MSSM or CMSSM parameter space can take?

Most plots of SUSY properties in the (m_0,$M_{1/2}$) plane found in the literature [11,20, 21] show a large excluded triangular region, for large m_0 and small $M_{1/2}$. In this region, mSUGRA does not have the required properties for radiative electroweak symmetry breaking (REWSB).

As the figures in section 2.1.2 show, this constraint, unlike the spectrum of SUSY particle masses ("superspectrum"), is very sensitive to the details of the way it is calculated, and to the value of the top mass. The running top mass is the usual input parameter, which must be calculated from the pole top mass in the renormalisation scheme being used. (The running top mass is specified at the scale m_t^Q such that $m_t^Q = m_t(m_t^Q)$.)

In addition, there are excluded regions due to current experimental bounds on flavour-changing neutral currents, on dipole moment measurements, on existing superparticle and light Higgs boson mass lower bounds from searches.

Assuming R-parity conservation (sec. 1.3.1), the lightest superparticle (LSP) is stable. Hence, on cosmological grounds, it must be electrically neutral [22]. Thus, there are excluded regions of MSSM parameter space where the LSP is charged.

1.3 Extensions Of The MSSM

1.3.1 R-parity Violation

The MSSM is often claimed to include all possible supersymmetric interactions and soft supersymmetry breaking terms given the particle content of the MSSM and the Standard Model symmetries.

In fact, the "R-parity violating (RPV) terms" eq. (1.19), which, if unconstrained, allow proton decay and flavour changing neutral currents, are also possible, but conventionally excluded. Note, this is in contrast to the Standard Model, where lepton and baryon number conservation and the absence of flavour changing neutral currents arise as an accidental consequence of other symmetries.

$$W_{\mathrm{RPV}} = \frac{1}{2}(\lambda^{ijk}\tilde{L}_{Li}\tilde{L}_{Lj}\overline{\tilde{e}_{Rk}} + \lambda'^{ijk}\tilde{L}_{Li}\tilde{Q}_{Lj}\overline{\tilde{d}_{Rk}} + \lambda''^{ijk}\overline{\tilde{u}_{Ri}}\,\overline{\tilde{d}_{Rj}}\,\overline{\tilde{d}_{Rk}}) + \mu'^{i}\tilde{L}_{Li}H_1 \quad (1.19)$$

where i, j, k are family indices. In addition, RPV soft supersymmetry breaking terms $\mathcal{L}_{\text{SOFT BREAKING, RPV}}$ also exist.

Thus, an additional discrete Z_2 symmetry, called R-parity, is often added to the MSSM to forbid such terms. The known particles and scalar Higgs particles are assigned an R-parity quantum number +1, and the "superparticles" R-parity -1. Conservation of this quantum number means that superparticles are created and destroyed only in pairs, giving rise to the usual SUSY phenomenology, where the lightest supersymmetric particle is stable.

If the R-parity violating terms are allowed to take any value, proton decay, and flavour changing neutral currents result in violation of known bounds. However, provided they are not too large [23], R-parity violating supersymmetry is not ruled out. In particular, if lepton number violating RPV terms are permitted, but baryon number violating RPV terms are forbidden, or vice-versa, proton decay cannot occur.

Without R-parity, the H_1 and L_L SU(2) doublets have the same quantum numbers, and can mix. The sneutrino fields possibly can get VEVs. Now, the model can then be seen to possess certain reparameterisation symmetries, rotations in the vector space of Higgs/Leptons. Thus, it is important to study R-parity violating models in the context of combinations of parameters which are invariants in this space [24].

1.3.2 Non-Standard Supersymmetry Breaking

In addition to the R-parity violating terms, there exists a further set of possible additional R-parity conserving "non-standard" soft supersymmetry breaking (NSSB) terms allowed by the symmetries, as remarked upon in [5,25–27]: a non-analytic scalar trilinear coupling, and a Higgsino bilinear coupling:

$$\mathcal{L}^{NSSB} = C^u_{ij} H_1^* \tilde{Q}_i \tilde{\bar{u}}_j + C^d_{ij} H_2^* \tilde{Q}_i \tilde{\bar{d}}_j + C^e_{ij} H_2^* \tilde{L}_i \tilde{\bar{e}}_j + \tilde{\mu} \tilde{H}_1 \tilde{H}_2 + c.c., \tag{1.20}$$

where i, j are family indices, and weak isospin, spinor, and gauge indices are suppressed. C^f_{ij} and $\tilde{\mu}$ are the new couplings. RPV-NSSB terms are also possible.

In [25] the C terms are written down and then taken as zero. In [26] Feynman rules and mass matrices for these terms are presented. The non-standard terms are written down in [5], and including them in SUSY studies is advocated there.

In [27] 1-loop β-functions are obtained for a SUSY model with NSSB terms, and a general particle content and gauge group. These are then specialised to a one-family MSSM. The region of $m_0, \tan\beta$ parameter space where an acceptable electroweak vacuum results is obtained, for a given value of $\tilde{\mu}(M_X)$ and with $\mu = 0$. $C_0 = C^u/Y^u = C^d/Y^d = C^e/Y^e$ is allowed to vary in order to obtain an acceptable vacuum (sec. 4.3).

When $C_0 = \tilde{\mu}$ the theory is supersymmetric (C and $\tilde{\mu}$ can be removed by a reparameterisation (sec. 4.2).) This is a fixed point of the RGEs (sec. 1.4), and its stability is discussed in [27]. In [28] the same authors present 2-loop NSSB β-functions for general particle content and gauge group, and further discuss the fixed-point properties of the NSSB RGEs.

In [29] and [30] the NSSB terms are used to generate flavour mass hierarchies through radiative corrections.

In [31] the impact of NSSB terms on flavour-changing neutral currents in the MSSM is considered. In [32] the NSSB terms are included together with dimensionless higher-order scalar couplings to examine the origin of intermediate scale physics. In [33,34] the NSSB terms are used in models of neutrino masses and rare processes in top decays. In [35] the NSSB terms are used to fix the correct mass of the b-quark in a model where the decay $b \to s\gamma$ is generated radiatively.

The terms of eq. (1.20) have traditionally been neglected because they are thought to lead to large radiative corrections when there are scalar fields present which are uncharged under the entire gauge group.

This argument cannot be used in the context of the MSSM, which contains no singlets at the SUSY scale. In a model with some higher mass singlet field of mass m_s, together with a very massive field of mass m_X, the correction, (see fig. 1.1) to the relation between the Higgs pole $m_{h,p}$ and running $m_{h,r}$ masses is:

$$m_{h,p}^2 = m_{h,r}^2(m_{h,p}) + C_s C_X S_4 \frac{m_X^2}{m_s^2} \ln(\frac{m_X^2}{m_{h,p}^2}) + ..., \tag{1.21}$$

where C_s is the coupling between the Higgs and the singlet, and C_X is the coupling between the singlet and the heavy field. S_4 is a collection of dimensionless constants. If the singlet field has a mass significantly below the high scale, the theory is thus unstable.

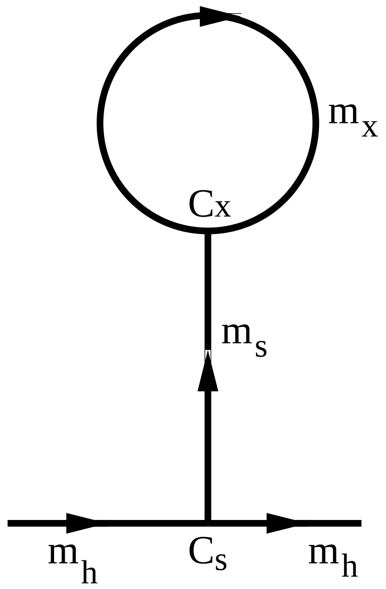

Figure 1.1: The NSSB scalar singlet tadpole correction to the Higgs propagator.

However, if any singlet fields have masses of order M_X, such as in SUSY desert scenarios, then there is no problem with including NSSB terms.

1.3.3 The MSSM With Explicit CP Violation

The MSSM as described above is a CP-conserving theory. However, in nature we observe CP-violating processes. In the standard model, this is accounted for using the Cabibbo-Kobayashi-Maskawa(CKM) mechanism [36]: with 3 or more families of quarks and leptons, CP-violating terms can occur in the Yukawa matrices. One might imagine that CP-violation could be added by including complex parameters in even the simplest models, but these can be rotated away using a reparameterisation invariance. This is an important point for the study of CP-violation: many apparently CP violating quantities are illusory, and can be removed by some redefinitions. Thus, it is important either to calculate genuinely CP-violating observables, for a given reparameterisation choice, or to describe the model using CP-violating reparameterisation invariant combinations of parameters.

In the MSSM, spontaneous CP violation is impossible: by judicious redefinitions, we can remove any CP-violating VEV generated by extremising the Higgs potential, if no explicitly CP-violating parameters are present [5]. However, in the presence of explicit CP violating parameters, the observed CP-violating effects can be accommodated– indeed there may be no CKM type CP violation at all [37]. However, if the superparticles are light, this can result in too much CP violation, in violation of present experimental bounds [38], such as those on electric dipole moments(EDMs). These bounds are sometimes avoided by making the fine-tuning assumption that CP-violating contributions from different superparticles cancel.

1.3.4 Next-to-Minimal SSM

The R-parity violating (sec. 1.3.1) and nonstandard supersymmetry breaking (sec. 1.3.2) extensions of the MSSM merely add extra terms to the Lagrangian of the MSSM for the same particle content. By contrast, the Next-To-Minimal Supersymmetric Standard Model (NMSSM) adds to the particle content of the MSSM an additional neutral chiral supermultiplet. This includes an $SU(3)_C \otimes SU(2)_W \otimes U(1)_Y$-neutral scalar S - precisely the addition which forbids the inclusion of NSSB.

The superpotential of the model is then incremented by:

$$W_{\rm NMSSM} = \lambda_{\rm NMSSM} S H_1 H_2 + W(S) \tag{1.22}$$

Thus, a vacuum expectation value for the S term introduces a μ term to the model through a symmetry breaking mechanism, solving the μ-problem (sec. 1.2.2) [39]. $W(S)$ represents some symmetry-breaking potential, an analytic function of S. Symmetries may be chosen to allow or forbid the terms in $W(S)$.

It is then necessary to forbid the μ-term of the MSSM, so that the new origin for the

μ-term is not swamped by some explicit large μ term. This is often done by imposing a Z(3) symmetry on the model, so that the Lagrangian is only symmetric under this symmetry when the total number of fields in each term is a multiple of 3, counting conjugated fields negative. Thus, the Yukawa terms and mass terms, and A-trilinears are allowed, but the μ term and B terms are forbidden. The B term is replaced by an equivalent term involving the VEV of S, and a mass term for S is included:

$$\mathcal{L}_{\text{NMSSM, SOFT BREAKING}} = a_{\text{NMSSM}} S H_1 H_2 + c.c. - V(S) \tag{1.23}$$

Where $V(S)$ is again a potential for S allowed by the symmetries and (if desired) renormalisability constraints.

By contrast with the MSSM, spontaneous CP violation in the NMSSM is possible. In one reparameterisation, this can be seen as a CP violating VEV in the S-scalar giving rise to the equivalent of explicit CP-violating μ or B terms [40].

1.4 SUSY RGE Theory

The deduction of the parameters of a SUSY model at the experimental scale, and hence the masses and interactions of the particles we hope to discover, depends upon the use of the Renormalisation Group (RG). The parameters of the model are considered to be "running" parameters, whose value depends upon the scale at which the properties of the system is to be probed. For a good discussion of the renormalisation group in high-energy physics, see [36].

1.4.1 The Running Of Parameters

The parameters running in the MSSM are the soft supersymmetry breaking parameters, $m_{\phi_i}, M_a, A^k_{ij}, B$, the supersymmetry conserving parameters μ, Y^k_{ij} and the gauge couplings g_1, g_2, g_3. In addition, the vacuum expectation values of the theory are also scale dependent, and may need to be run between the scale where, for example, M_Z is measured, and the scale where they are to be imposed using the constraints eq. (1.15) and eq. (1.16). Thus either v_1 and v_2 or $\tan\beta$ and v should be added to the list of running objects.

1.4.2 The Renormalisation Group Equations

For each of these parameters, then, one can deduce an equation showing how they run with the scale. These are given as "β-functions". For a general parameter x, running with a renormalisation scale Q, we define:

$$\beta_x = \frac{dx}{d(\ln Q)}, \tag{1.24}$$

(It should be noted that this is the common definition for SUSY work, but confusion can occur, as in other fields the differential with respect to Q^2 is often used, and Q is often called μ. Also, sometimes the definition $t \equiv \ln Q$ or $t \equiv \ln Q^2$ is used.)

The β-functions may be deduced by explicitly considering the scale dependence of certain Green's functions, or by differentiating the effective action (sec. 1.5). The β-functions for the SUSY-conserving parameters are found to effectively decouple from the SUSY-breaking parameters. (The β-functions for the Yukawa couplings, μ, and the gauge couplings are independent of the soft masses, B, and the A-trilinear terms. The β-functions for the SUSY-breaking parameters *do* depend on the SUSY conserving parameters.)

1.4.3 Boundary Conditions

The Yukawa and gauge couplings are fixed at the experimental scales where they are measured, usually at zero momentum or at the scale of the pole mass of the particle being investigated. The Z-boson mass fixes $v(M_Z)$, while $\tan\beta$ is unknown, but is usually imposed at M_Z. The supersymmetry breaking terms are fixed at some high scale, M_X, often the string or GUT scale [5], according to a scheme such as mSUGRA, except that B is not usually so fixed (sec. 1.4.5).

1.4.4 Threshold Corrections

The β-functions are calculated assuming that all of the running masses are small compared to the renormalisation scale. The particles much heavier than Q are ignored: their contributions to the β-functions are actually suppressed by powers of $\frac{Q}{m}$ [41]. However, as we run particle masses while Q varies from experimental scales to M_X, we pass through regimes where $Q \sim m$. The term "threshold corrections" refers to ways of dealing with this issue. The simplest solution is to use one set of β-functions above $Q = m(Q)$ and another below. The β-function for the mass in question is considered to be zero below $Q = m$. The parameters can then be taken as continuous at the matching point, or a finite correction can be used, a discontinuity in the parameter at the matching point, based on calculating the effect of the mass in the full theory.

An alternative approach [42], is to use the β-functions assuming all the masses are small, over the whole regime, and then apply a correction afterwards, when calculating the pole masses from the running masses.

1.4.5 RGE and REWSB

Values for μ and B are *not* imposed at M_X, but rather, deduced from the constraints given by analytical minimisation of the Higgs effective potential (sec. 1.2.6) (sec. 1.4).

Thus, the values of $\tan\beta$ and v must be run from M_Z to M_S, the scale where the constraint equations are imposed (sec. 1.4). Above M_S the values of $\tan\beta$ and v are irrelevant, since μ and B carry the equivalent information. μ and B are still run all the way down to M_Z, since they are necessary to deduce the particle masses at that scale.

1.4.6 The RGE Boundary Value Problem

The high- and low- scale boundary constraints, together with the renormalisation group equations, and the intermediate scale radiative electroweak symmetry breaking (REWSB) constraint (sec. 1.2.6), form a system of differential equations, that is, a "boundary value problem".

The numerical methods used to solve this problem are discussed in section 2.1.1 and appendix A.2.

1.5 The Effective Potential

When the effective action of a quantum field theory is considered as a function of constant values of the scalar fields, it can be called the effective potential, and treated as the function whose minimum gives the vacuum state of the theory [36]. In this section, we shall consider how the effective potential can be found, and some of its applications. Chapter 5 of this thesis describes a program capable of automatic calculation of the effective potential of any SUSY theory to next-to-leading order, from its particle content, gauge symmetries, and any superpotential or supersymmetry breaking terms.

1.5.1 The Supertrace Formula

At tree level, the effective potential is just (up to a $-$ve sign), the part of the Lagrangian which looks like a potential term for constant fields: i.e.:

$$V_{\text{Tree}} = -\mathcal{L}(\phi_i(x) = <\phi_i>) \tag{1.25}$$

In general, the loop contributions to the effective potential then come from 1-Particle irreducible (i.e. cutting one propagator won't separate the diagram) Feynman diagrams, with no external legs.

In reference [43], for example, we have the 1-loop contribution from each propagating scalar, Weyl spinor, or Lorentz vector:

$$V_{\text{1-loop, 1973, per d.o.f.}} = \frac{1}{64\pi^2}(2s+1)(-1)^s M^4 \ln M^2 \tag{1.26}$$

where s is the spin of the degree of freedom, and M its mass. This is shown separately to hold for spin $0, \frac{1}{2}$ and 1 particles, and the result is given in the renormalisation scheme of [43].

This can be compared with the general result for the 1-loop contribution to the effective action for scalar fields of [36]

$$\begin{aligned} \Gamma_{\text{1-loop}} &= \frac{i}{2} \ln \det \frac{\delta^2 \mathcal{L}}{\delta\phi\delta\phi} && (1.27) \\ &= \frac{i}{2} \text{Tr} \int \ln(\partial^2 + m^2) && (1.28) \\ &\propto \text{Tr} m^4 (\ln m^2 + C) && (1.29) \end{aligned}$$

for a Lagrangian of the Klein-Gordon form, and where C is cutoff- and scheme- dependent.

Thus, we define the "Supertrace":

$$\mathrm{STr}f(X) = \Sigma_i(2s_i + 1)(-1)^{s_i} f(X_i) \tag{1.30}$$

where $X_i =< \phi_i|X|\phi_i >$ is some function of the quantum numbers of some particle, ϕ_i, ψ_i^s or A_i^μ.

Using the $\overline{\mathrm{DR}}$ renormalisation scheme of modern supersymmetry, we thus have the "Supertrace Formula" for the 1-loop effective potential:

$$V_{\text{1-loop}} = \frac{1}{64\pi^2}\mathrm{STr}[M^4(\ln\frac{M^2}{Q^2} - \frac{3}{2})] \tag{1.31}$$

Note that at the next order, the couplings come into the diagrams for the effective potential, and so there is no equivalent model-independent supertrace formula at two loops.

Since the parameters on which the effective potential depends are running parameters in the renormalisation group, there is implicit renormalisation-scale dependence of the effective potential, even at tree level. In order to work with the effective potential, one must therefore choose a scale at which to work. A common choice is $(M_S = \sqrt{(m_{\tilde{t}_1} m_{\tilde{t}_2})})$ where 1-loop radiative corrections to the renormalisation group improved scalar potential have the smallest scale dependence. It is believed that at this scale the contribution from higher loops is smallest. This is motivated by ref. [44], which shows that for the MSSM Higgs potential, the tree-level and 1-loop results are closest at this scale. However, in [45] this relationship has been shown not to work as well for other potentials, such as MSSM charge-and-color-breaking potentials. An alternative is to use the parameters renormalised to a scale equal to the classical values of the fields for which the effective potential is being evaluated: to do this, one must extend the renormalisation group so that the parameters are functions of many renormalisation scales, one for each field in the model.

1.5.2 Uses Of The Effective Potential

The most common use of the effective potential is to obtain the expectation values of scalar fields in the model (sec. 1.2.6). These can be obtained by minimising the effective potential:

$$\frac{\partial V}{\partial \phi} = \frac{\partial V_{\mathrm{Tree}}}{\partial \phi} + \frac{1}{32\pi^2}\mathrm{STr}[M^2\frac{\partial M^2}{\partial \phi}(\ln\frac{M^2}{Q^2} - 1)] = 0 \tag{1.32}$$

Note that the supertrace of the expression involving the derivative of M^2 is defined in terms of the same function involving the derivatives of the eigenvalues of M^2, not the trace over the diagonal elements of the matrix product, which would be the more obvious meaning of eq. (1.32). These are not necessarily equal because the derivative of M^2 is not necessarily simultaneously diagonalisable with M^2. For this particular expression, the two definitions, however, are equivalent, as can be proved using certain identities involving the trace of matrix logarithms. The diagonal elements of the first derivative of the mass matrix when rotated into the eigenbasis of M^2, are the same as the derivatives of the eigenvalues. Thus, the supertrace expression is equivalent to the sum of tadpole diagrams [46], with the derivative of the field-dependent mass matrix (i.e. field-dependent two-point coupling) as the three-point coupling.

Thus, one can study electroweak symmetry breaking by considering the Higgs potential. One can examine the possibility of VEVs of charged or coloured fields, leading to the breaking of the charge and colour symmetries (CCB). In addition, one can study the possibility that the potential is unbounded from below (UFB), i.e. that the VEVs are infinite. (Or at least very large and stabilised by higher loop contributions not taken into account.) Sometimes, one finds metastable local minima, and then cosmological arguments must be applied to examine the dynamics of this situation [47].

The second derivative matrix of the effective potential around its minimum can be used to obtain the masses and mixings of the particles. If the 1-loop correction eq. (1.31) is used, one can obtain the one-loop mass matrices, where the external momentum for the self energy diagrams is zero. Normally, however, we want to obtain the on-shell masses, where the external energy used for the self-energy is the same as the mass in question. The second derivative of the one-loop effective potential is an approximation to the full on-shell one loop mass. The supertrace expression over mass matrices is *not* equivalent to the supertrace expression over masses for this quantity:

$$\begin{aligned}
\frac{\partial^2 V}{\partial\phi\partial\psi} &= 2\sum \frac{\partial m_i^2}{\partial\phi}\frac{\partial m_i^2}{\partial\psi}(\ln(m_i^2/Q^2)-1) \\
&\quad +2\sum \frac{\partial^2 m_i^2}{\partial\phi\partial\psi} m_i^2 \ln(m^2/Q^2) \\
&\neq 2\mathrm{STr}\frac{\partial M}{\partial\phi}\frac{\partial M}{\partial\psi}(\ln(M/Q^2)-1) \\
&\quad +2\mathrm{STr}\frac{\partial^2 M}{\partial\phi\partial\psi} M \ln(M)
\end{aligned} \tag{1.33}$$

The naive matrix expression, as well as involving M and its derivatives, the gauge-eigenstate couplings, involves derivatives of the orthogonal diagonalising matrix for M. However, an expression, just involving masses and couplings, and not involving derivatives of the diagonalising matrix, *can* be obtained for this quantity: it is the result of evaluating the appropriate Feynman diagram, and can be written in terms of the Passarino-Veltman function B_0 [48, 49].

The effective potential can also be used to obtain the β-functions for the model (sec. 1.4.2) [50], by differentiating eq. (1.31) with respect to the renormalisation scale Q: the explicit Q dependence of eq. (1.31) gives the right hand side of eq. (1.34), while the implicit Q dependence of the parameters and fields gives the β-functions or anomalous dimensions. As usual, the total Q dependence must be zero, since Q is not physical. The β-functions must then be extracted by comparing coefficients of various combinations of fields, since the equation is true for all classical expectation values of the fields.

$$\beta_I \frac{\partial V_{\text{Tree}}}{\partial \lambda_I} - (\gamma^i_{Lj} \phi_i \frac{\partial V_{\text{Tree}}}{\partial \phi^j} + \text{h.c.}) = \frac{1}{32\pi^2} \text{STr} M^4 \tag{1.34}$$

where I is an index which (implied-sum) runs over all the parameters in the model and γ^i_{Lj} is the Landau anomalous dimension of the field ϕ_i.

Chapter 2

Software Introduction

2.1 RGE Calculations

In this section, we will consider some computer implementations of the SUSY RGE boundary value problem (sec. 1.4). First, however, we will discuss the numerical algorithms which can be applied to the boundary value problem.

2.1.1 Solving The RGE Boundary-Value Problem

There are three methods for solving the boundary value problem resulting from the mSUGRA conditions and the RGEs 1.4. These are considered in detail in appendix A.2. The first is the formal "shooting method" where the constraint equation at one boundary is solved for those parameters which are unconstrained at the other boundary. This method cannot be used for the MSSM, because of the complicated form of the boundary conditions at the low scale.

The second method, which may be called the "drift method" involves alternate imposition of each set of boundary conditions. This constitutes a recurrence relation for successive values of those parameters unconstrained at one of the boundaries. The solution consistent with both sets of boundary conditions is a fixed point of the recurrence relation, but this point is not guaranteed to be stable or unique. If we assume the point is both stable and unique, however, simple repeated imposition of the boundary conditions, alternately at M_Z and M_X, will result in convergence toward the required solution. This is the method used in ISASUGRA [51] 2.1.2, and in SOFTSUSY [52] 2.1.3,

Because the drift method becomes unstable for certain values of the NSSB parameters, I have developed a third approach, a "single-ended" shooting method, where the fixed point of the recurrence relation is solved for, using a Newton-Raphson method. This is further discussed in appendix A.2. This was done by modifying the SOFTSUSY program.

2.1.2 ISASUGRA

ISASUGRA [51] is an implementation of the "drift method" solution of the SUSY RGE problem, provided as part of the ISAJET Monte-Carlo Event Generator package. It uses $\tan\beta(M_Z)$ as an input, rather than $\mu(M_X)$ or $B(M_X)$ (sec. 1.4.5).

As discussed in section 1.2.8, the regions of parameter space excluded due to lack of electroweak symmetry breaking show strong version dependence, as the sophistication of certain aspects of the calculation improve. Version 7.14 of ISASUGRA was used in [11, 21] to obtain the REWSB excluded region, where minimisation of the scalar potential takes place at scale M_Z [53].

Between 7.14 and more recent versions [51] such as 7.42, the region shifts to very high m_0. (Around 6 TeV for an input pole top mass of 174 GeV, as shown in figure 2.1.) In these and subsequent versions of ISASUGRA, the REWSB calculation takes place at M_S (sec. 1.5.1) [53]. (The calculation uses a renormalisation group improved effective

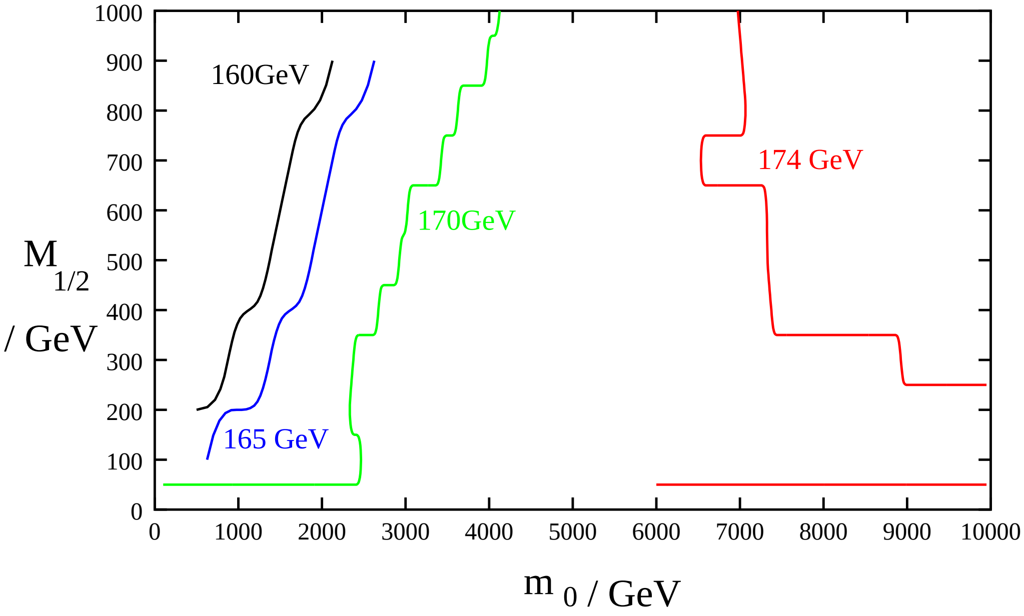

Figure 2.1: Dependence of the radiative electroweak symmetry breaking excluded region on top mass, where the top mass labels the curves, according to ISASUGRA version 7.42, for $\tan\beta = 10$, $\mu > 0$ and $A_0 = 0$. The excluded region lies to the right of the curves shown.

potential, and the renormalisation scale is chosen to minimise unincluded corrections.) This excluded region therefore no longer provides a useful limit on the values of m_0 which should be investigated. In a still more recent version of ISASUGRA, 7.51, the region returned once again to low values of m_0, see figure 2.2. Here, the change is the addition of 2-loop corrections to many aspects of the model [53].

2.1.3 SOFTSUSY

SOFTSUSY [52] is a C++ implementation of the solution of the SUSY RGE problem by the drift method. The effective potential is minimised at M_S, and the corrections, including threshold corrections and pole-mass-from-running-mass corrections of [42] are used, as are the corrections relating $\overline{\rm MS}$ to $\overline{\rm DR}$ quantities. The one-loop correction terms for the effective potential are included, as is the scale dependence of $\tan\beta$ and v and the scale dependence of the fermion masses at low scales is taken into account when

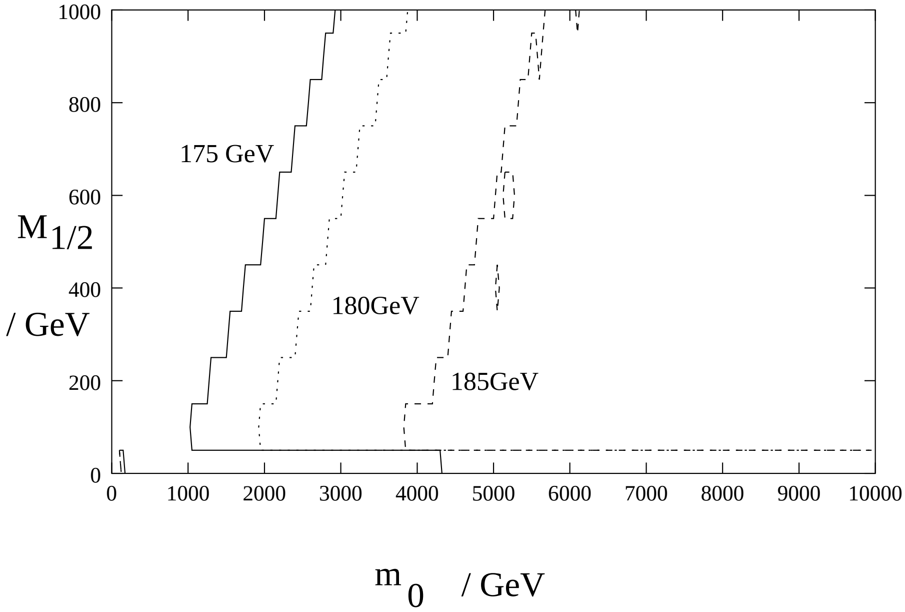

Figure 2.2: Dependence of the radiative electroweak symmetry breaking excluded region on top mass, where the top mass labels the curves, according to ISASUGRA version 7.51, for the same parameters as in figure 2.1. The excluded region lies to the right of each curve.

calculating the Yukawa couplings. The full 2-loop β-functions are used for the SUSY-conserving terms and gaugino masses, and one-loop β-functions are used elsewhere.

The REWSB exclusion region again depends sensitively upon various aspects of the physics included in the calculation and is shown in figure 2.3. Again there is a strong dependence on the top mass, and on the treatment of the running mass and strong coupling.

In the course of my PhD research, I have been the first user of SOFTSUSY other than its author, see the Acknowledgments. I have been in consultation over many aspects of its development, helped to debug it, and made many suggestions which have been adopted. In addition, I have been responsible for programming some improvements to it, such as improving the C++ class structure and the fine-tuning and drift-method routines to allow for easier extension to other models than just the MSSM, and providing error-handling code.

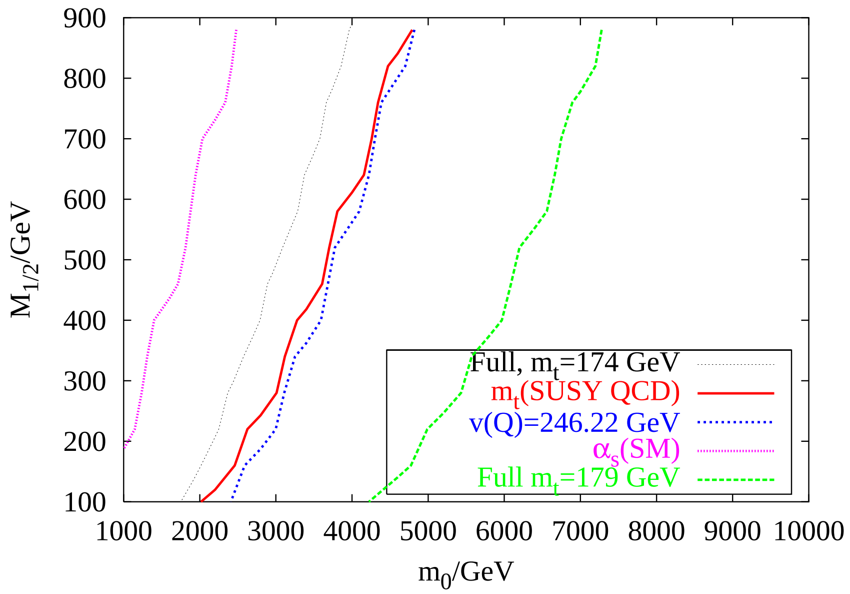

Figure 2.3: The dependence of the REWSB excluded region in SOFTSUSY on various approximations for $m_t = 174$ GeV, except for the curve marked $m_t = 179$ GeV. The curves shown are: the full calculations ('$m_t = 174$ GeV', '$m_t = 179$ GeV') and calculations leaving out chargino and neutralino corrections to the running top mass ('m_t(SUSY QCD)'), using only a constant value of the Higgs VEV ('v(Q)=246.22 GeV'), and using only Standard Model corrections to the $\overline{\text{DR}}$ value of $\alpha_S(M_Z)$ ('α_s(SM)'). Regions to the right of the curves are ruled out by the REWSB constraint.

I implemented the “single-ended” shooting method of solving the SUSY RGE problem within SOFTSUSY, see chapter 4.

2.2 Monte-Carlo Event Generators

“Event generators” are programs which purport to simulate the fundamental processes going on in a collision event at some particle physics experiment. In combination with a “detector simulation” (sec. 2.3) they allow one to predict the outcome of a particle physics experiment given a model. The parameters, i.e. masses and coupling constants, of a model, must be fed into the event generator before it can be used. Thus, SUSY analyses often consist of three software processes: RGE calculations to calculate the properties of a model, event generation, and detector simulation.

Event generators are based upon the Monte-Carlo method: random numbers are used to pick an outcome from the quantum possibilities considered at each stage of the problem. To set up a distribution based on the quantum amplitude for all the possible processes, and then draw the numbers from that distribution, is impossible. Instead, after an outcome is picked, its probability is calculated *a posteriori*, and then the outcome is *thrown away* based on that probability. Thus, to generate a valid event would take a long time if the numbers were drawn from a uniform distribution. Instead, a distribution is used which, it is hoped, approximates the required distribution, but which can be calculated beforehand. This distribution can be written down and normalised, while the true distribution can only be calculated point-by-point in its parameter space. A number of different Monte-Carlo event generators exist, the most important for new physics simulations for the LHC being ISAJET [51], PYTHIA [54] and HERWIG [55,56]. The primary difference between these programs is their approach to the hadronisation of quarks and gluons.

HERWIG is used for chapter 3. The physics content of HERWIG, the cluster model, angular ordering and colour connection, are explained in [55, 56]. HERWIG can generate 2-2 hard sub-processes for both R-Parity conserving and R-Parity violating MSSM models, as well as R-Parity violating decays.

2.3 Detector Simulations

Since a particle physics experiment cannot perfectly learn all there is to know about each event that takes place, the output from event generators must be fed to some kind of "detector simulation", which can simulate the ways in which the experiment records the event that takes place. This should attempt to reproduce statistically and systematically any "errors" in the measurements made.

Full simulations of experiments include detailed models of the experiment, describing the location of each detector element and obstacle. However, for simulations of hypothetical models at unconstructed experiments, one normally uses a "fast simulation", where one parameterises one's ignorance, simulating errors by, for example changing each particle's energy by a random value based on the experiment's known or estimated errors. For the ATLAS [11] experiment, for example, the ATLFAST program [57] fills this role.

2.3.1 GETJET

GETJET [53] is an extremely simple FORTRAN program which, in the role of a fast detector simulation, can be used to simulate the errors in the calorimeters of an experiment, and to apply the cone jet-finding algorithm (sec. 2.4) [58] to the simulated events.

The values of the error parameters chosen for the analysis of chapter 3 are given in sec. 3.4. For this research, I substantially rewrote the GETJET code in a more modern programming style to make it easier to read and modify.

2.4 Use Of The Software To Analyse Future Experiments

With a combination of event generator and detector simulation one can make an estimate of the data which real experimenters might have to work with when trying to measure some property or determine the validity of some theory. This is, in general, done by noting some class of event which would take place much more frequently if the theory being tested is true, than in the null-hypothesis case, usually the Standard Model. This category is described by a set of "cuts": properties that an event must have not to be thrown out of the candidate "signal" for the theory. It is, of course, necessary to simulate the null-hypothesis theory as well, so that the expected statistical significance of the number of observed events if the theory is true, relative to the expected number of events in the "background".

Although sophisticated statistical measures of this significance exist, taking into account estimated errors in the estimated signal and background samples, the simple measure eq. (2.1) is usually used, which is roughly the Poisson statistics condition that the observed excess of events over the expected number of background events is significant at the level of five standard deviations.

It is formally assumed that an experiment will be able to claim proof of a theory if

$$\frac{S}{\sqrt{B}} > 5 \qquad \text{AND} \qquad S > 10 \tag{2.1}$$

Where $S+B$ is the number of events expected to pass the cuts if the theory is true, and B is the number of events expected to pass the cuts if the theory is false, based on the null-hypothesis model.

Some typical variables used when constructing experimental cuts are explained below:

- Missing transverse momentum $\not{p}_T$. Since in SUSY models we expect the lightest supersymmetric particle to be stable and only weakly interacting, we expect it to carry off momentum undetected by the experiment. Since, in hadron colliders, only the transverse component of the total momentum can be measured (since the detectors do not extend to small angles to the beam), we consider only the transverse component of the missing momentum.

- Pseudo-rapidity η. The pseudo-rapidity of an object in the event is used to measure its longitudinal angle with respect to the beam, in a conveniently measurable way. Differences in η are approximately Lorentz invariant. The pseudo-rapidity is $\ln \tan \frac{\theta}{2}$ where θ is the angle to the beam. This is approximately the genuinely Lorentz-invariant-differences true rapidity $y = \frac{1}{2}\ln(\frac{E+p_z}{E-p_z})$ for relativistic particles (the z axis is the beam axis), but is easier to measure.

- Azimuthal angle ϕ, the principal-valued angle, measured in radians, around the detector, relative to some reference direction.

- Transverse momentum p_T. The transverse momentum of some track or energy deposition in the event is often considered.

- Jet multiplicity N_{JET}. As is well known, the result of the hadronisation process confining the colour of high-energy coloured particles into mesons and baryons is "jets", closely bunched sets of tracks, with a total momentum approximating that of the parent particle. The number and momenta of jets can be reconstructed from the energy deposition measured by the experiment using "jet algorithms" [41]. GETJET (sec. 2.3.1) uses a "cone algorithm", where the size of the cone can be defined using the separation measure of eq. (2.2). N_{JET} is defined with respect to jets of some minimum transverse momentum and maximum rapidity, reflecting the capabilities of the detector.

- Track isolation. We can require an object in the event to be further by some distance from other tracks in the event, using the measure of separation eq. (2.2):

$$\Delta_{ij}^{\eta\phi} = (\eta_i - \eta_j)^2 + (\phi_i - \phi_j)^2, \tag{2.2}$$

using the principal value of $|(\phi_i - \phi_j)| < \pi$. An appropriate, infrared-safe definition of "other tracks" must be given. Typically one constrains the total energy deposition in a cone of some $\Delta^{\eta\phi}$ around the particle in question to be less than some value. One can also require all tracks or jets above some appropriate momentum scale to be further away than some $\Delta^{\eta\phi}$ from the track in question. An example choice is given below (sec. 3.4).

- $N_{\text{ISOLATED LEPTONS}}$, the number of isolated leptons in the event, of some minimum momentum and maximum rapidity. Observable leptons are final state (μ or e) leptons of either sign.

- Transverse mass M_T:

$$M_{Ti} = \sqrt{2(|\mathbf{p_i}||\not{\mathbf{p}}_\mathbf{T}| - \mathbf{p_i} \cdot \not{\mathbf{p}}_\mathbf{i})} \tag{2.3}$$

where $\mathbf{p_i}, \not{\mathbf{p}}_\mathbf{T}$ are transverse two-component momenta, for some object in the event indexed by i and the missing transverse momentum respectively.

- The transverse circularity (or transverse sphericity) S_T:

$$S_T = \frac{2\lambda_2}{\lambda_1 + \lambda_2} \tag{2.4}$$

where λ_i are the eigenvalues of the matrix $S_{ij} = \Sigma_{mn} p_i^m p_j^n$, the sum being taken over all detectable final state particles, and p_i being the two-component transverse momentum of the particle.

Chapter 3

Naturalness Reach Of The LHC In mSUGRA

3.1 Introduction

The RGE evolution of minimal supergravity 1.4 shows a 'focus point' behaviour [20,59]. A relatively large region of GUT scale parameters exists for which the RGE trajectories converge towards a small range of measurable properties. Specifically, the renormalisation group trajectories of the mass squared of a Higgs doublet ($m^2_{H_2}$), for different values at M_X, cross each other close to the electroweak scale.

As a result, the electroweak symmetry breaking is insensitive to the GUT scale SUSY breaking parameters [59], and fine-tuning is smaller than expected. This focus point corresponds to a region in which the scalar SUSY breaking masses, governed by the mSUGRA parameter m_0, are large.

Previous predictions of the discovery reach of the LHC in mSUGRA parameter space, using ISASUGRA 2.1.2 [51], went only as far as $m_0 < 2$ TeV [11]. The purpose of the investigation of this chapter was to extend this reach to higher m_0 and to present it in terms of a naturalness measure. We seek to determine how the standard SUSY search channels perform in this region, where charginos and neutralinos would be the dominant SUSY particles. For large m_0, squarks, sleptons, and the heavy Higgs particle could avoid detection at the LHC, and the determination of the m_0 reach of searches for these particles would be an interesting further study.

Section 3.2 explains how the fine-tuning was determined in our investigation. In section 3.3 I discuss the issue of the bounds on which regions of the $(m_0, M_{1/2})$ plane need to be investigated. In section 3.4 I discuss the SUSY search channels considered for use at the LHC, and my simulation of the discovery reach using the HERWIG [55,56] (sec. 2.2) event generator. I present in section 3.5 the fine-tuning reach in each channel, and the overall fine-tuning reach of the LHC.

3.2 Fine-tuning

In order to use the fine-tuning measure discussed above (sec. 1.2.7), one must decide upon the way the model is parameterised.

For this investigation, our choice follows ref. [20]:

$$\{a_i\} = \{m_0, M_{1/2}, \mu(M_{\rm GUT}), A_0, B(M_{\rm GUT})\} \tag{3.1}$$

where $M_{\rm GUT} \sim 10^{16}$ GeV is the GUT scale (sec. 1.4.3). It is this selection which gives rise to low fine-tuning for large m_0.

We also considered the case where the top Yukawa coupling $h_t(M_{GUT})$ is added to the list of fundamental parameters in eq.(3.1). In refs. [20, 59, 60], it is shown that the focus point scenario with heavy scalars has a large fine-tuning if h_t is included. The inclusion of $h_t(M_{GUT})$ into the definition of fine tuning thus increases the naturalness reach of the LHC, as the results in section 3.5 will show.

The values of fine-tuning for this research were determined using SOFTSUSY (sec. 2.1.3) [52].

3.3 Constraints

The regions of parameter space considered in this chapter are limited as discussed above (sec. 1.2.8) using SOFTSUSY. The current lower bound on the light Higgs mass does not further exclude any of the parameter space shown in the figures, for the large value of $\tan\beta$ used here, ($\tan\beta = 10$), according to both ISASUGRA and SOFTSUSY.

Since the REWSB constraint is so heavily dependent upon the precise values of input parameters and details of the calculation (sec. 2.1.2), there is no reason to suppose that the exclusion region will remain stable under further refinements. Hence we believe it should not be taken as a limit upon the regions of mSUGRA parameter space to be investigated experimentally. Both SOFTSUSY and ISASUGRA could be subject to further large corrections. ISASUGRA7.42 was therefore used to compute the discovery reach, since the allowed region then extends up to values of $m_0 = 10$ TeV (fig. 2.1). Experimental scale masses and couplings suitable for input into HERWIG cannot be generated by RGE calculations which find the point in question to be invalid, but the dominant aspects of the reach calculation are robust to the same changes that shift the REWSB region so much (fig. 3.7).

3.4 Monte Carlo Simulation Of The LHC Discovery Reach

In this study, as in [21], the results of which were used in [11], the SUSY discovery reach in the $(m_0,\ M_{1/2})$ plane was found through a variety of signals involving hard isolated leptons, jets and missing transverse momentum. The cuts used here (sec. 2.4) can be applied with a range of cut energies E_{cut}, and are listed below. The cuts represent typical SUSY discovery cuts that might be used at a general-purpose LHC experiment, such as ATLAS [11] or CMS [12].

- $\not{p}_T > E_{cut}$.
- $N_{\text{JET}} \geq 2$, with pseudo-rapidity $|\eta| < 3.2$, and $p_T > E_{cut}$, using a cone algorithm with cone-size $\Delta^{\eta\phi} = 0.7$. Or: $N_{\text{JET}} = 0$, including all jets with $p_T > 25$ GeV.
- $N_{\text{ISOLATED LEPTONS}} = 0,\ 1,\ 2$ or 3, with $|\eta| < 2.0$ and $p_T > 20$ GeV. Defining isolation with $\Delta^{\eta\phi} > 0.4$ with respect to any 15 GeV jet with cone-size $\Delta^{\eta\phi} = 0.4$, and with less than 5 GeV of energy within a cone within $\Delta^{\eta\phi} < 0.3$ with respect to the lepton. Channels with two leptons of opposite or the same sign were considered separately.
- In the one-lepton channel, an extra cut was imposed to reduce the background due to Standard Model W decay, involving the transverse mass of the lepton $M_T > 100$ GeV.
- $S_T > 0.2$ (See eq. (2.4)).

The search channels used are shown with assigned labels in table 3.1.

A typical SUSY event passing the cuts in a leptonic channel is shown in fig. 3.1, where the decay of the chargino to W and neutralino results in a final-state high momentum

N_{JET}	$N_{\text{ISOLATED LEPTONS}}$	Label
> 1	0	j0
	1	j1
	2 (Opposite sign)	jos
	2 (Same sign)	jss
	3	j3
0	2	v2
	3	v3

Table 3.1: Channels in which the SUSY discovery reach has been investigated.

lepton and large missing transverse momentum. These cuts are selected to look for general properties of supersymmetry, and are not designed to seek out one particular decay mode. Processes of the type shown do, however, dominate in the j1 channels. It might be worth seeing what happens to the search reach when the coupling allowing such decays is reduced, in order to determine how model independent this search strategy is.

The events were simulated using ISASUGRA 7.42 (sec. 2.1.2) to calculate sparticle masses and branching ratios, and HERWIG6.1 (sec. 2.2) to simulate the events themselves. The expected SUSY signal was generated, together with the backgrounds due to Standard Model top anti-top and W plus jet events. The W background was generated using events with one of the jets produced in the hard subprocess, and the rest in QCD parton cascades. This produces an underestimate of the W background as discussed in [61], and I used the figures from that paper (in this thesis, figure fig. 3.2) to rescale the results accordingly.

The above cuts were implemented using original FORTRAN code (see (fig. 3.3)) and a rewritten version of GETJET (sec. 2.3.1) to implement the above cuts for use with HERWIG. The approach taken was to work as closely as possible with the direct output of the Monte Carlo, rather than to use a particular experiment simulator. The parameters of the cuts and GETJET settings were selected to simulate a general-purpose experiment at the LHC.

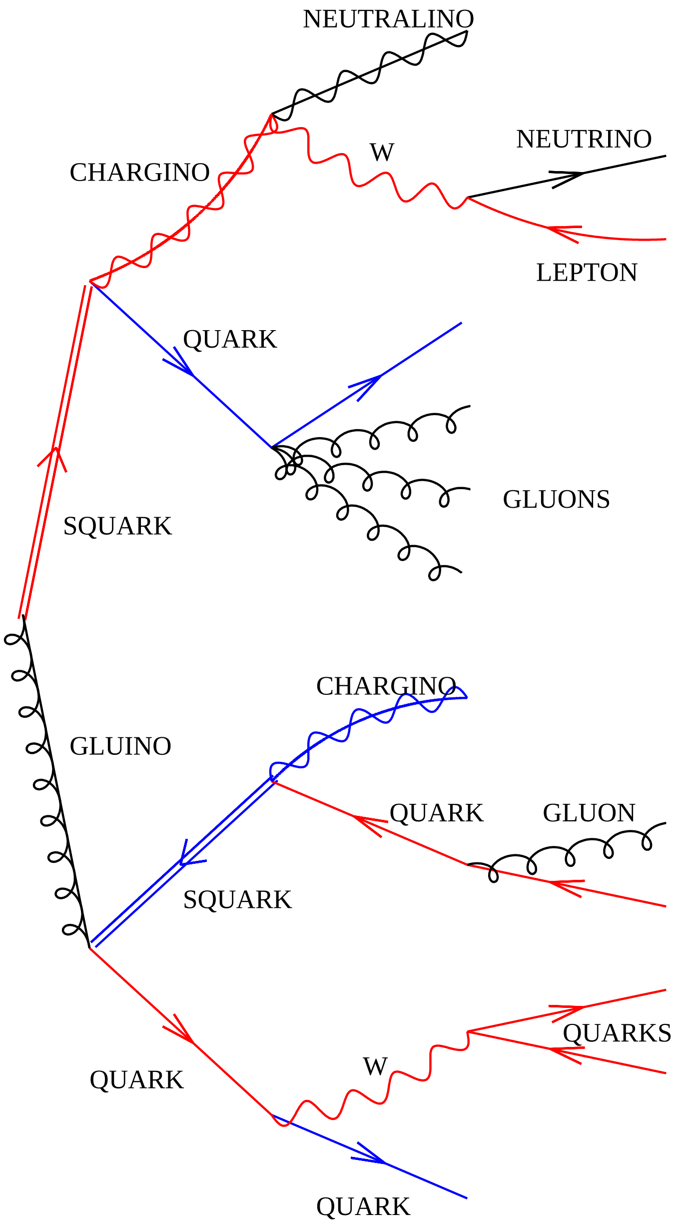

Figure 3.1: A typical SUSY process passing the cuts in the monoleptonic discovery channel j1 described in the text. The perturbative particle cascade shown should be considered to be the decay of an s-channel quark arriving at the leftmost vertex, and to be followed by further perturbative decay of some particles, followed by hadronisation of the coloured decay products into jets.

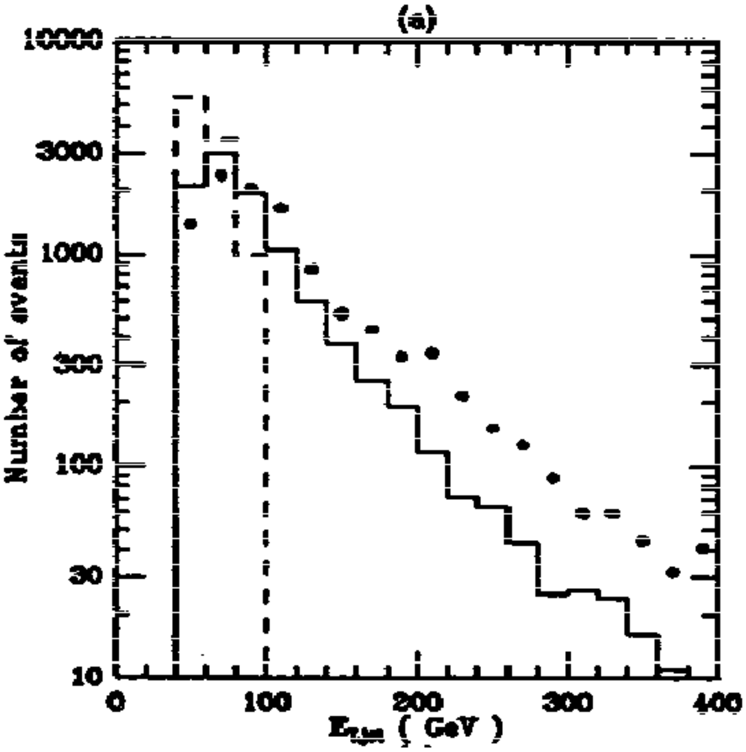

Figure 3.2: Number of W+2 jet events calculated from the HERWIG event generator with one jet coming from evolution and one from the hard subprocess, (solid line), and a tree-level three-body-final-state matrix element, (dots). The dashed line is not relevant to this analysis of this thesis, but shows the result for HERWIG when both jets are produced from the Monte-Carlo evolution.

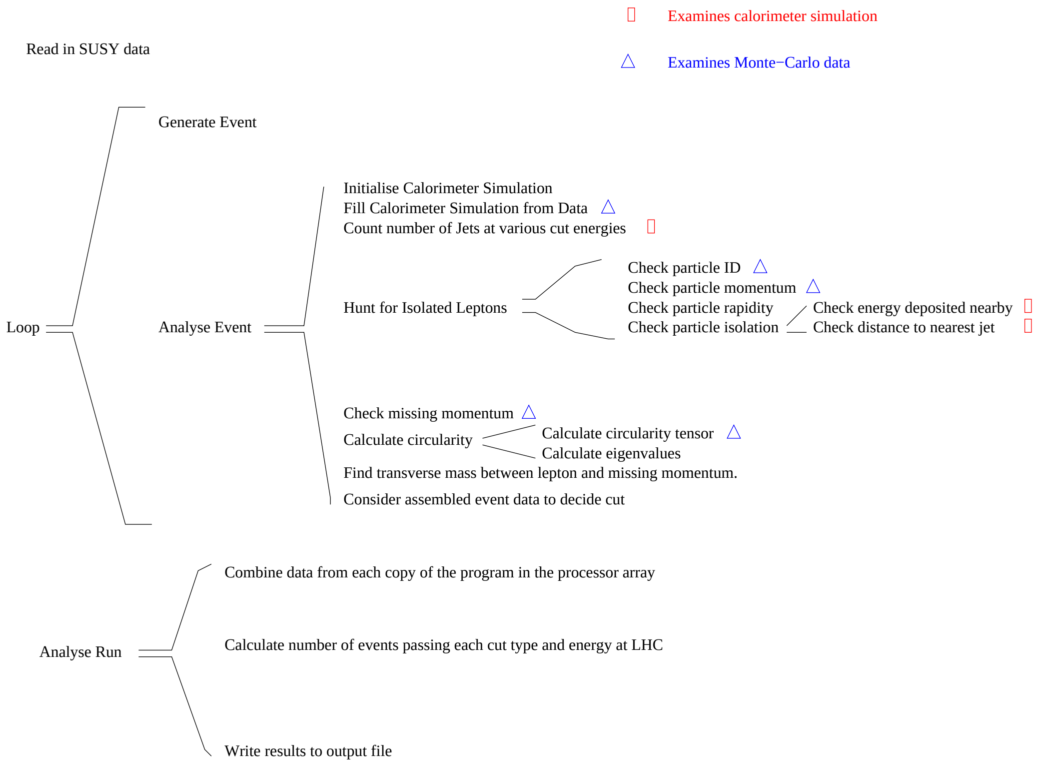

Figure 3.3: The structure of the FORTRAN program used to generate and analyse HERWIG events for the discovery reach analysis.

In order to find the hard leptons, and to determine $\not{\mathbf{p}}_{\mathbf{T}}$, and S_T, the HERWIG output was examined directly, particles with $|\eta| > 5.0$ being ignored. For the jet count and lepton isolation check, my modified version of GETJET was used (sec. 2.3.1), with hadronic resolution of $70\%/\sqrt{E}$, electromagnetic resolution of $10\%/\sqrt{E}$ and extending to pseudo-rapidities up to 5.0.

The discovery limit was set at values of m_0 and $M_{1/2}$ where $S/\sqrt{B} > 5$ and $S > 10$ where S and B are the expected number of events in the the SUSY signal and total background (sec. 2.4).

For each value of E_{cut}, the minimum final state transverse momentum in the hard subprocess was selected so as to obtain some events passing the cuts, within realistic computer time constraints. Where the minimum transverse momentum had to be increased above E_{cut}, results from the j0 channel were used to obtain linear correction factors to compensate for the resulting underestimate of the background.

In [62], preliminary results for the j1 channel were presented, where only one value of E_{cut}, 400GeV, was investigated. The program was then extended in order to obtain the discovery limit in all the channels in table 3.1, for several values of E_{cut}. This work was conducted on a parallel computer cluster, part of the Cambridge High Performance Computing Facility (sec. 2.2). I wrote C++ programs to analyse the large and complicated data-files which were produced by the program, and to analyse the SOFTSUSY fine-tuning data.

The search reach was obtained for mSUGRA with $A_0 = 0$, $\tan\beta = 10$, pole top mass 174 GeV, $\mu > 0$ and $\mathcal{L} = 10$ fb^{-1} of integrated luminosity. The integrated luminosity chosen is equivalent to one year of running in the low luminosity mode, 10^{33} cm^{-2} s^{-1}. The LHC experiments expect to collect around 300 fb^{-1} of data. A low-statistics calculation of the discovery reach with a top mass of 179 GeV was also made, to determine whether the reach is independent of the top mass. It is known that the background is largely independent of the top mass [41]. There is a small decrease in the production cross section for $t\bar{t}$ background with increasing top mass, and a compensating increase in the energy of the resulting leptons and jets, which causes a greater proportion to pass the selection cuts. Thus for this study the background could safely be assumed to be independent of the top mass. A calculation using ISAJET 7.51 was also carried out, with lower statistics, to determine whether the changes which shifted the REWSB exclusion, as discussed in section 3.3, also alter the discovery reach, see 3.5

3.5 Results

I present here the discovery limit in all the channels of table 3.1, for several values of E_{cut}, and with both definitions of fine-tuning (with/without the top Yukawa coupling).

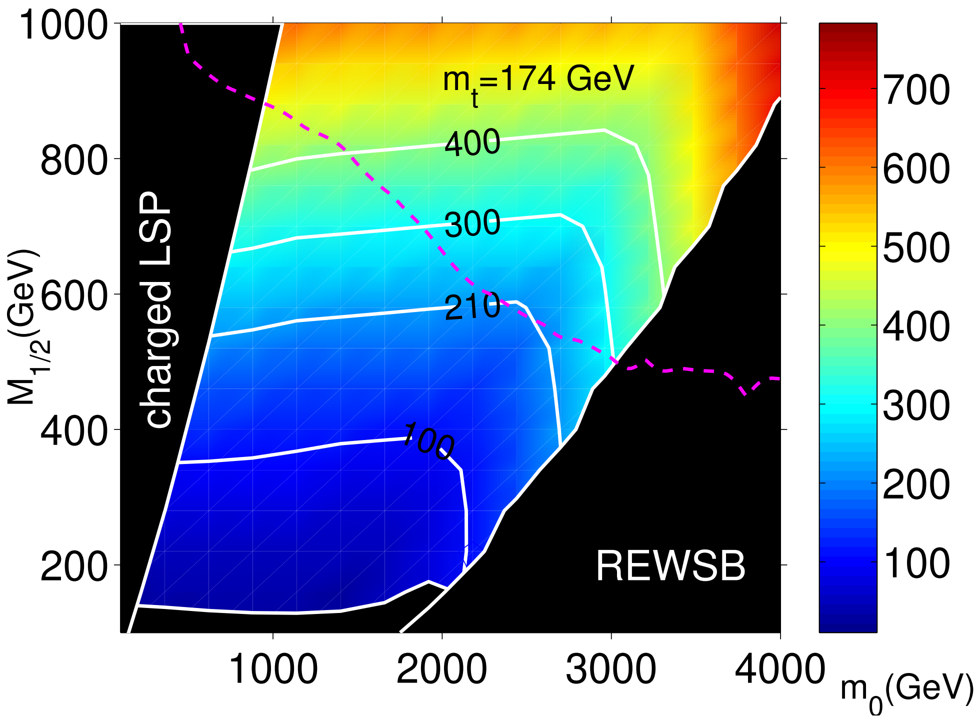

Figure 3.4: Naturalness reach at the LHC for $A_0 = 0$, $\tan\beta = 10$, $\mu > 0$, $m_t = 174$ GeV in minimal SUGRA. The fine-tuning is represented by the background density, as measured by the bar on the right. White contours of fine-tuning are also presented. Fine tuning with respect to the top Yukawa coupling is neglected. The dashed line is the LHC expectation SUSY discovery contour in the j1 channel described in the text for a luminosity of $\mathcal{L} = 10\ \text{fb}^{-1}$, and with $E_{cut} = 400$ GeV. The excluded regions are discussed in sec. 1.2.8.

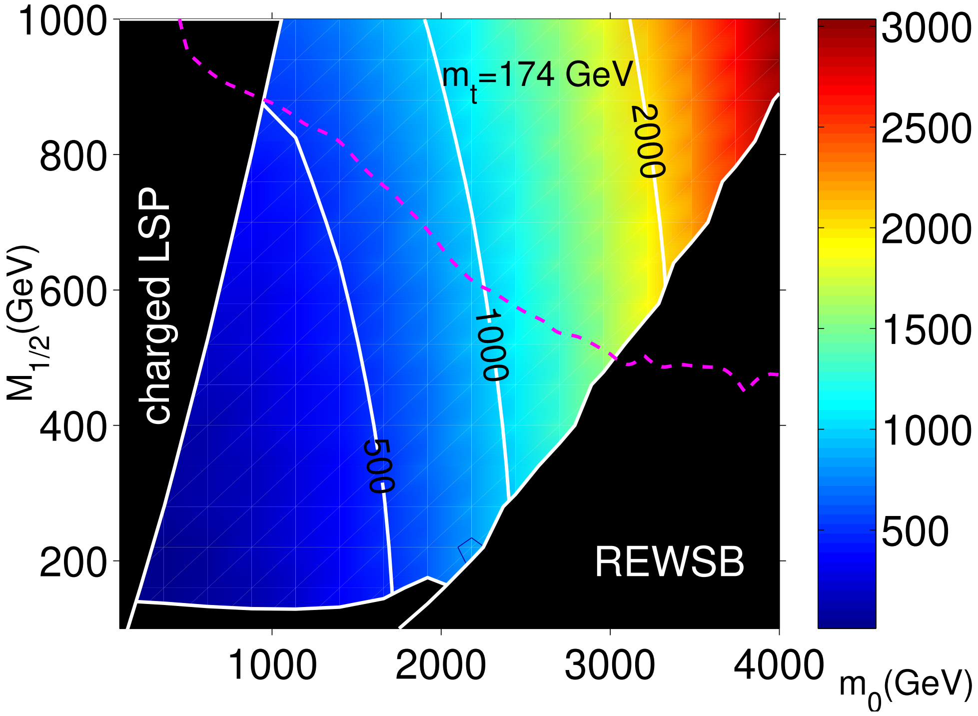

Figure 3.5: As in figure 3.4, but with fine tuning with respect to the top Yukawa coupling included.

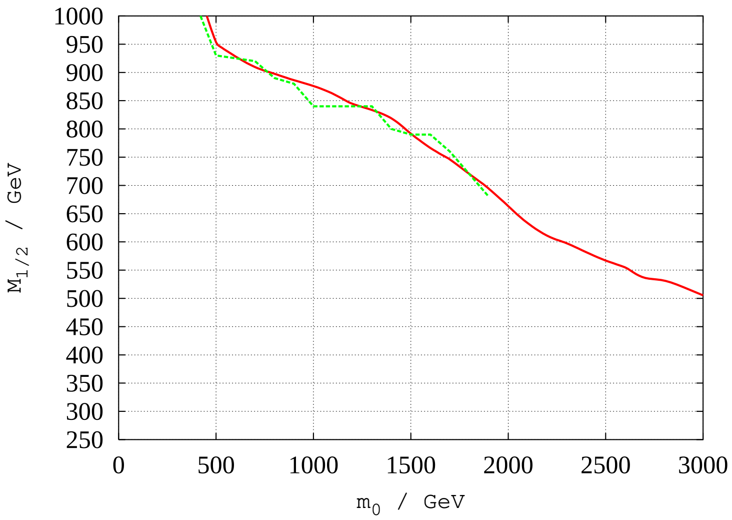

Figure 3.6: Reach at the LHC for $A_0 = 0$, $\tan\beta = 10$, $\mu > 0$, in minimal supergravity. The plot shows our HERWIG results (with m_t =174 GeV) as a solid line and the ISAJET results of [21] (with m_t = 170 GeV) as a dashed line.

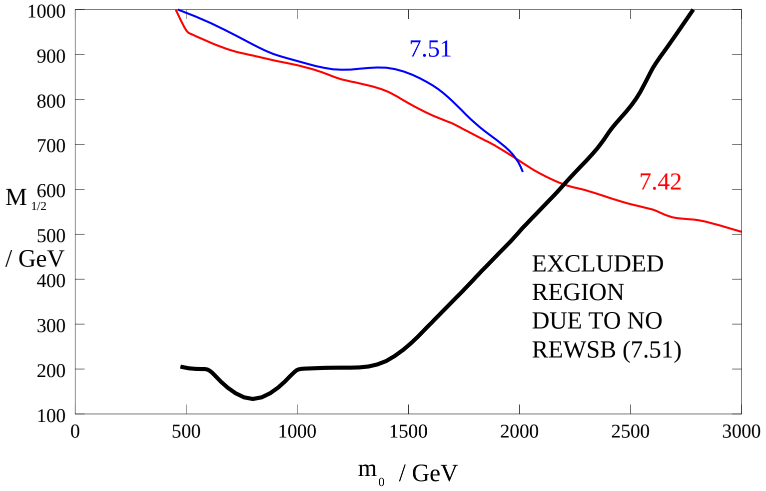

Figure 3.7: Reach at the LHC for $A_0 = 0$, $\tan\beta = 10$, $\mu > 0$, m_t =174 GeV in minimal supergravity. The plot shows our HERWIG results, using two different ISASUGRA versions to generate the SUSY spectrum and decays as shown.

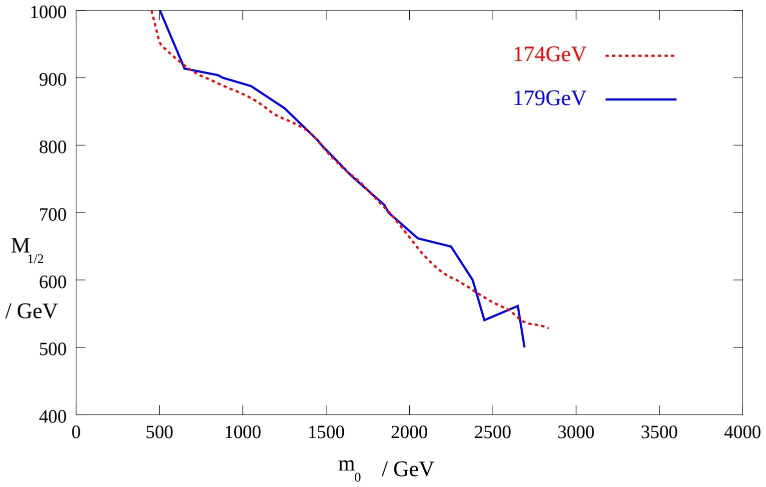

Figure 3.8: Reach at the LHC for $A_0 = 0$, $\tan\beta = 10$, $\mu > 0$, in minimal supergravity. The plot shows our results using two different top masses as shown.

Table 3.2 shows the background due to each generated channel, the total background, and the resulting expected number of supersymmetry events required to fulfill the discovery criteria detailed above. No discernible background in the jet veto channels (v2,v3) was obtained.

For each of the channels, and each value of E_{cut}, a plot was used to determine the fine-tuning reach with both definitions of fine-tuning. The fine-tuning reach is the largest fine-tuning where the fine-tuning contour is completely within the discovery limit, for $m_0 < 4000$ GeV. The values of E_{cut} giving the best fine-tuning reach, and the fine-tuning reach, for top masses of 174 GeV and 179 GeV, are shown in table 3.3. E_{cut} =100, 200, 300, 400 and 500 GeV were investigated. No results can be presented for the jet veto channels, as the number of events in these channels is too small. The reach in these channels could be obtained by considering specific SUSY processes, but is expected to be very limited.

Figures 3.4 and 3.5 show, as an example, the best obtainable discovery limit using the channel providing the best reach, the $E_{cut} = 400$ GeV j1 channel, as a dashed line in the $(m_0, M_{1/2})$ plane, and the naturalness density without and with the top Yukawa coupling included, respectively. The resulting fine-tuning limits, as defined below, are 210 and 500 units.

Figure 3.6 shows consistency of my results for $m_0 < 2$ TeV in the j1 channel with those obtained using ISASUGRA 7.14 in [63], while figure 3.7 shows the consistency between my ISASUGRA 7.42 and ISASUGRA 7.51 results, and figure 3.8 shows that the discovery reach is not altered by small changes in the top mass, unlike the REWSB exclusion region. Because of this last result, we can use our high-statistics $m_t = 174$ GeV search reach to calculate the fine-tuning reaches for $m_t = 179$ GeV, the j1 channel again being used as an example in figure 3.9.

For $m_0 > 4000$ GeV the discovery reach in $M_{1/2}$ becomes roughly independent of m_0.

Channel	E_{cut} / GeV	Total no of background events	Required no of SUSY Signal events
j0	100	5.3×10^5	3.6×10^3
j0	200	5.2×10^4	1.4×10^3
j0	300	7.4×10^3	431
j0	400	1.6×10^3	201
j0	500	451	107
j1	100	1.3×10^4	579
j1	200	394	102
j1	300	35 *	29
j1	400	4	10
j1	500	1	10
j3	100	36*	30
j3	200	20*	22
j3	300	< 1*	10
j3	400	< 1	10
j3	500	< 1	10
jss	100	115*	54
jss	200	7*	13
jss	300	4*	10
jss	400	4	10
jss	500	2	10
jos	100	7.4×10^3 *	431
jos	200	173 *	65
jos	300	12 *	17
jos	400	5	11
jos	500	2	10

Table 3.2: Total background for SUSY discovery channels. The channels are described in table 3.1. Also shown is the expected number of SUSY events required for discovery. Backgrounds marked with an asterisk $(*)$ have been corrected for the use of a minimum subprocess p_T greater than E_{cut}, as described in section 3.4.

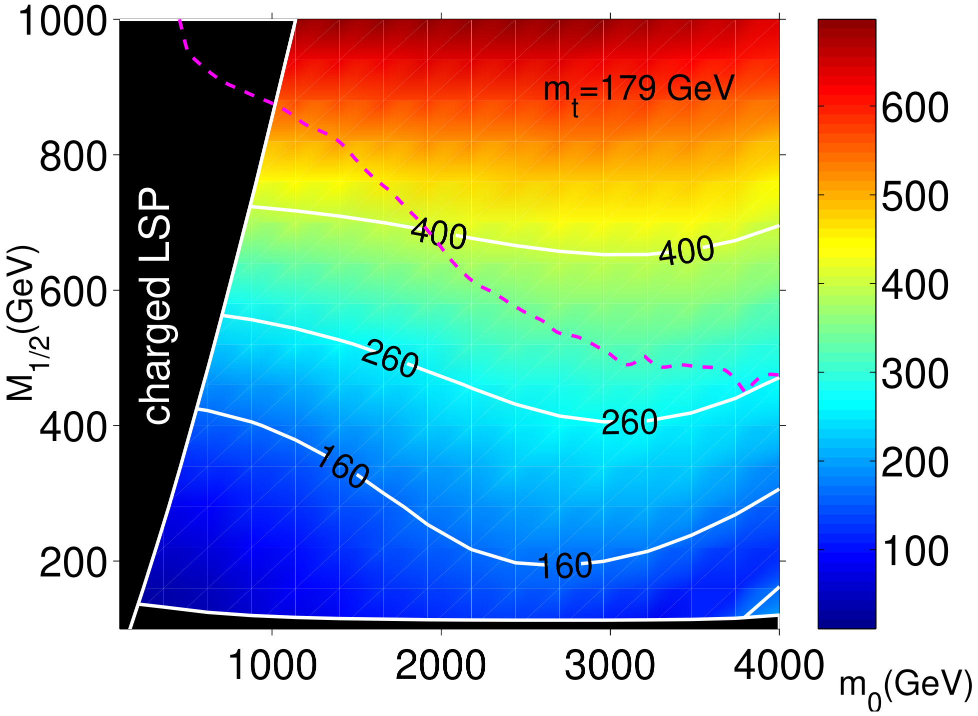

Figure 3.9: As in figure 3.4, but with a top mass of 179 GeV used to calculate the fine-tuning and REWSB excluded region.

Cut Type	E_{cut}	c	E_{cut}	c'	E_{cut}	c_{h_t}	E_{cut}	c'_{h_t}	E_{cut}	$M_{1/2}$ limit
j0	300	120	300	230	400	375	400	375	200	350
j1	400	210	400	260	400	500	400	550	300	460
jos	300	85	300	190	300	240	300	270	200	300
jss	200	110	200	215	200	240	200	270	200	350
j3	100	70	100	130	100	150	100	155	100	280

Table 3.3: For each of the supersymmetry discovery channels, this table shows the values of the cut on missing momentum and jet energy which give the best fine-tuning limits c and c_{ht}, and the $M_{1/2}$ reach for large $m_0 > 4000$ GeV. c is the fine-tuning limit as defined in the text, and c_{h_t} is the same with the fine-tuning with respect to the top Yukawa coupling included, using a top mass of 174 GeV to calculate the REWSB excluded region and fine-tuning. c' refers to the same quantities for a top mass of 179 GeV. E_{cut} and $M_{1/2}$ are given in GeV.

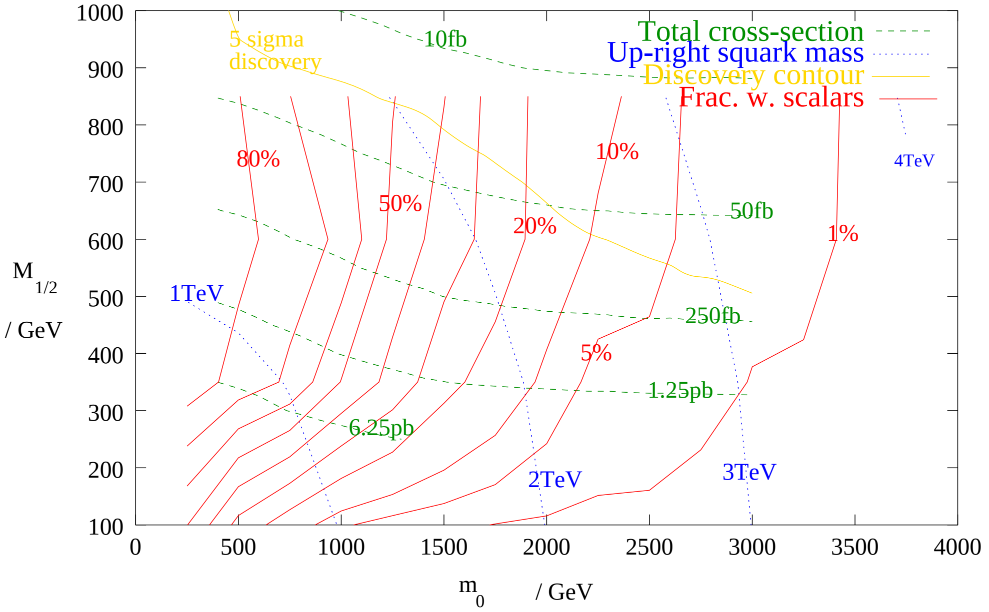

Figure 3.10: Scalar production in mSUGRA. The contours represent the total SUSY cross-section, the mass of a typical squark, (the up-right), the overall SUSY discovery contour, and the fraction of SUSY processes involving a squark or slepton.

Here, the SUSY processes involved are dominated by the gauginos, the squark masses being very high (larger than 3 TeV), as illustrated in figure 3.10. This figures also shows that scalar production, as a fraction of total SUSY processes, decreases at high m_0, being typically around one percent for $m_0 \sim 3$ TeV. However at values of $M_{1/2}$ lower than the SUSY discovery contour but at $m_0 > 2$ TeV, it is possible to produce scalar SUSY particles at the LHC. A discussion of how to attempt to obtain a limit on the region of mSUGRA parameter space where the squarks in particular (rather than SUSY in general) can be discovered is beyond the scope of this dissertation.

The calculation of the fine-tuning and search-reach is therefore terminated at $m_0 = 4000$ GeV, since for higher values of m_0 the $M_{1/2}$ discovery reach gives a representation of the overall SUSY discovery power in the channel. Note then, that only fermionic superparticles, the neutralinos and charginos, are active in this region. The scalar superparticles, the squarks and sleptons, being much heavier, are hardly ever produced, as illustrated in fig.3.10.

3.6 Conclusions

In this investigation, the discovery reach of the LHC into mSUGRA parameter space was determined, using the then new supersymmetry routines in HERWIG. Where this work repeats the calculation of [63], it provides a useful check on the consistency of the two event generators. In addition, use of the latest SUSY RGE calculations, both ISASUGRA and SOFTSUSY, updates the old results, and allows us to move into the region of high scalar masses, where it has been suggested that a focus point gives this region reduced fine tuning. Even for arbitrarily high m_0, the LHC can discover supersymmetry provided the gauginos are not too heavy ($M_{1/2} < 460$).

The possibility of using fine-tuning as a quantitative way to compare the discovery reach of various channels has been introduced. Fine-tuning can provide physicists with a quantitative measure of discomfort with a theory, which increases as the experimental bounds are improved. Since it is this disquiet which leads, in the end, to the abandonment of a theory such as low-energy supersymmetry, the fine-tuning reach represents the potential of these discovery channels for removing mSUGRA from the list of candidate theories for physics beyond the Standard Model. The work could be repeated using some different high-energy unification assumptions, instead of mSUGRA. The mSUGRA reach into A_0 and $\tan\beta$ could also be investigated.

The best fine-tuning reach is obtained in a mono-leptonic channel, where for $\mu > 0, A_0 = 0$ and $\tan\beta = 10$ (corresponding to the focus point), and a top mass of 174 GeV, all points in the $(m_0, M_{1/2})$ plane with $m_0 < 4000$ GeV and a fine tuning measure up to 210 (500) are covered by the search, where the definition of fine-tuning excludes (includes) the contribution from the top Yukawa coupling. For $m_0 > 4000$, all values of $M_{1/2} < 460$ GeV are covered by the search.

Chapter 4

Non-Standard Supersymmetry Breaking

4.1 Introduction

Previous works on NSSB (sec. 1.3.2) have not emphasised the importance of a reparameterisation invariance the model possesses, considered how the mSUGRA assumptions can be adapted to be used with NSSB, determined the size of the valid NSSB parameter space for fixed values of the standard MSSM parameters, presented mass-spectra for the NSSB MSSM, or calculated the fine-tuning of the model. These issues are examined in the present work.

In the following sections my new work regarding the MSSM with NSSB is considered in detail. This work was carried out by modification of SOFTSUSY (sec. 2.1.3) to produce a program capable of solving the SUSY RGE problem in the presence of NSSB. In section 4.2 a reparameterisation invariance is introduced, which the inclusion of these terms gives to the MSSM. In section 4.3 we develop a version of the "constrained MSSM" or "minimal supergravity" (mSUGRA) high-scale boundary conditions (secs. 1.2.5 and 1.4.3) consistent with the reparameterisation symmetry. In section 4.4 the calculation of the 3-family renormalisation group equations (RGEs) for this model is considered. These are presented in appendix A.1. The impact of these terms upon electroweak symmetry breaking is discussed in section 4.5. In section 4.6 an interesting subset of the particle masses for a standard mSUGRA point but with non-standard breakings is presented. In section 4.7 the reasons for the limits on the magnitudes of the non-standard couplings are explored. In section 4.8 numerical measures of the fine-tuning of the model (sec. 1.2.7) are considered, and results for the fine-tuning presented and discussed. Appendix A.1 lists the NSSB contribution to the 1-loop renormalisation group equations for the model.

4.2 The NSSB Lagrangian And μ-Reparameterisation

The non-standard SUSY breaking terms to be added to the MSSM Lagrangian are given in eq. (1.20). Using the usual formula [64] for extracting the full Lagrangian from the superpotential, the following terms are those involving $m^2_{H_{1/2}}$, the Higgs soft masses, μ, the Higgs bilinear superpotential term, and the NSSB couplings:

$$\begin{aligned}\mathcal{L} \; = \ldots \; & +(\tilde{\mu}-\mu)H_1H_2+(\mu^2+m^2_{H_1})|H_1|^2+(\mu^2+m^2_{H_2})|H_2|^2 \\ & +(C^u_{ij}-Y^u_{ij}\mu)H_2^*\tilde{Q}_i\tilde{\overline{u}}_j+(C^d_{ij}-Y^d_{ij}\mu)H_2^*\tilde{Q}_i\tilde{\overline{d}}_j+(C^e_{ij}-Y^e_{ij}\mu)H_2^*\tilde{L}_i\tilde{\overline{e}}_j \\ & +c.c., \end{aligned} \tag{4.1}$$

where $Y^{u/d/e}_{ij}$ are the Yukawa couplings.

Therefore, the Lagrangian is invariant under the following reparameterisation:

$$\mu \;\; \rightarrow \;\; \mu+\delta;$$

$$
\begin{aligned}
\tilde{\mu} &\rightarrow \tilde{\mu} + \delta; \\
m_H^2 &\rightarrow m_H^2 - 2\mu\delta - \delta^2; \\
C_{ij}^f &\rightarrow C_{ij}^f + Y_{ij}^f \delta.
\end{aligned}
\tag{4.2}
$$

This was partially pointed out in [27] where it was noted that one could write an MSSM Lagrangian ($\tilde{\mu} = 0, C_{ij}^f = 0, \mu \neq 0$) in terms of an NSSB model with zero μ but non-zero C_{ij}^f and $\tilde{\mu}$. Here a different emphasis is used: the Lagrangian contains all terms allowed by the symmetries, and the reparameterisation is used like a gauge freedom, to allow calculations to be made in the most convenient "gauge".

The above Lagrangian contains all terms involving μ, provided the Higgs bilinear breaking term is written as

$$\mathcal{L} = ... + m_3^2 H_1 H_2 \tag{4.3}$$

and not

$$\mathcal{L} = ... - B\mu H_1 H_2 \tag{4.4}$$

as is sometimes used (sec. 1.2.4), factoring out the μ. In the latter case, B would become a μ-reparameterisation dependent quantity. In order that this work can easily make contact with MSSM work conducted using B, we instead have the freedom to define B using the Lagrangian term:

$$\mathcal{L} = ... - B(\mu - \tilde{\mu}) H_1 H_2. \tag{4.5}$$

On the MSSM subspace of parameter space, where $\tilde{\mu}$ and C_{ij}^f are zero, this definition is consistent with eq. (4.4), but B remains μ-reparameterisation invariant.

4.3 The High-Scale Boundary Conditions

While the approach to dealing with μ in RGE calculations of (sec. 1.4.5) is the conventional one for the MSSM, in [27] the authors chose to use the reparameterisation freedom to take $\mu = 0$, solving the SUSY μ-problem. Instead of leaving μ and B at M_X unconstrained, so that they can vary to fit M_Z and $\tan\beta$, in this approach C and B are left unconstrained at M_X, (with C^e, C^d, C^u taken as equal at M_X and $\tilde{\mu}$ at M_X given as an extra boundary condition.)

In this investigation, we want to impose values for both C and $\tilde{\mu}$ as boundary conditions at M_X, with the same kind of universality assumptions as in mSUGRA, i.e. $C^f_{ij} = Y^f_{ij} C_0$. The parameter μ will remain in the model, and will, together with B, be varied to fit $\tan\beta$ and v. Since we do not choose $\mu = 0$ the model retains its reparameterisation symmetry.

This approach is perhaps preferable because it implements non-standard supersymmetry breaking with *minimal* changes to mSUGRA. However, there is a subtle difficulty, because we wish to use the mSUGRA assumption of universal high-scale soft scalar masses: the mass term for each of the sleptons, squarks and Higgs bosons should be the same at M_X. This assumption is inconsistent with the reparameterisation invariance. A reparameterisation changes the Higgs soft masses but not the squark and slepton masses, breaking the equality. To make the boundary condition well defined, we must therefore select the reparameterisation in which we want the scalars to be universal.

As will be seen in section 4.4, the renormalisation group running will take place in $\mu = 0$ reparameterisation. If we simply impose the mSUGRA boundary conditions in that reparameterisation, including a value for $\tilde{\mu}$, we cannot have μ as an unconstrained parameter at high scale.

Consider a model with m_0, $M_{1/2}$, C_0 and $\tilde{\mu}$ at M_X given as constraints, and values for μ (μ_S) and B (B_S) and for the other parameters unconstrained at high scale, but which are consistent with the low energy constraints. (This discussion is illustrated in table 4.3). On changing to the $\mu = 0$ reparameterisation used to run the RGEs, or the $\tilde{\mu} = 0$ reparameterisation used for some parts of the calculation, the values of μ and $\tilde{\mu}$ are mixed up, and only $(\tilde{\mu} - \mu)$ is known. In addition, the Higgs soft mass-squareds become different from those of the squarks and sleptons.

If we then run the RGEs, do the rest of one cycle of the calculation, and then return to M_X, we do not know how to separate μ and $\tilde{\mu}$. It seems we cannot return to the reparameterisation used to impose the constraints. However, the difference between the Higgs scalar masses and the squark and slepton masses must be that caused by the reparameterisation. Thus, the reparameterisation which makes the squark/slepton soft masses equal to the Higgs soft masses must be that which returns us to the initial state. This can be called the "universality reparameterisation". Re-imposition of the high-scale boundary conditions then leaves the model unchanged.

As the calculation converges toward a solution consistent with both sets of boundary conditions, we need an estimator for the difference between the Higgs and squark/slepton soft mass-squareds at M_X. Until convergence is reached, $m_{H_1} \neq m_{H_2}$, $m_{\tilde{u}} \neq m_{\tilde{d}}$ etc. The choice used here is the difference between the average Higgs mass-squared and the average squark mass-squared.

Unlike the $\mu = 0$ approach this approach allows us, for any point in the MSSM, to model the same point, by using the NSSB with $C_0 = \tilde{\mu} = 0$. The resulting solution is identical to that obtained using SOFTSUSY normally, and the high-scale value of μ which the model selects to fit $\tan\beta$ is the same as in the MSSM. It is possible to gradually turn on $\tilde{\mu}$ and C_0 and move away from any MSSM point. The MSSM is a $D - 2$ dimensional subset of the D dimensional NSSB parameter space.

$\overline{m_{\tilde{q}}}$	$\overline{m_h^2}$	$\tilde{\mu}$	μ	C^f	Action
MSSM as MSSM					
m_0	m_0^2	N/A	μ_c	N/A	Arrive at high scale
m_0	m_0^2	N/A	μ_c	N/A	Impose b.c.: at convergence this does nothing.
True NSSB					
m_0	$m_0^2 + \mu_c^2$	$-\mu_c + \tilde{\mu}_c$	0	$(C_0 - \mu_c)Y^f$	Arrive at high scale in $\mu = 0$ reparameterisation
m_0	m_0^2	$\tilde{\mu}_c$	μ_c	$C_0 Y^f$	Reparameterise $\delta = \sqrt{\overline{m_h^2} - \overline{m_{\tilde{q}}^2}} = \mu_c$
m_0	m_0^2	$\tilde{\mu}_c$	μ_c	$C_0 Y^f$	Apply b.c.
m_0	$m_0^2 + \mu_c^2$	$-\mu_c + \tilde{\mu}_c$	0	$(C_0 - \mu_c)Y^f$	Reparameterise $\delta = -\mu_c$
MSSM as NSSB					
m_0	$m_0^2 + \mu_c^2$	$-\mu_c$	0	$-\mu_c Y^f$	Arrive at high scale in $\mu = 0$ reparameterisation
m_0	m_0^2	0	μ_c	0	Reparameterise $\delta = \sqrt{\overline{m_h^2} - \overline{m_{\tilde{q}}^2}} = \mu_c$
m_0	m_0^2	0	μ_c	0	Apply b.c.
m_0	$m_0^2 + \mu_c^2$	$-\mu_c$	0	$-\mu_c Y^f$	Reparameterise $\delta = -\mu_c$

Table 4.1: The high-scale boundary condition(b.c.) part of the iterative procedure for determining the model parameters consistent with the chosen input parameters. The state of the model after convergence is achieved is shown, i.e., once the model has become invariant under the iterative numerical procedure used. Thus, the imposition of the high-scale boundary conditions leaves the parameters unchanged, as shown in the table. $\overline{m_{\tilde{q}}^2}$ is the average squark mass-squared, $\overline{m_h^2}$ is the average Higgs mass-squared. X_c is used to denote a particular value of the parameter named X.

4.4 NSSB β-functions

Ref. [27] presents general one-loop beta functions for a general SUSY model with arbitrary particle content and gauge group, allowing NSSB terms. The two-loop results are presented in [28]. Reference [27] also gives the RGEs specialised to the NSSB MSSM with one family and with the Yukawa couplings factored out of the parameters. For example, the Lagrangian "A" soft breaking term is written as $m_{10} Y^t H_2 Q \bar{t}$.

An alternative presentation of the beta functions, better suited to numerical implementation, is the 3-family matrix form for the MSSM without NSSB used in [46], with the Yukawa matrices not factored out of the soft breakings. This version of the beta-functions has been calculated.

A subtle question is the impact of the μ-reparameterisation on the beta functions. The results of [27] are in $\mu = 0$ reparameterisation. The MSSM results of [46] have non-zero μ. We do not wish to re-calculate all of the MSSM part of the beta functions for the $\mu = 0$ reparameterisation. We wish to use part of the results of [46], modified according to the general results of [27], which are for $\mu = 0$. By considering the μ-reparameterisation behaviour of each quantity, and representing the beta functions as pieces with different reparameterisation behaviours, and with dependence on each parameter, it is possible to obtain for the soft masses:

$$\beta^{NSSB}_{m_i^2} = \beta^{MSSM}_{m_i^2} + \beta^{C,\tilde{\mu}}_{m_i^2}, \tag{4.6}$$

where the left hand side of each equation is the NSSB beta function for $\mu = 0$, β^{MSSM} is the MSSM $\mu \neq 0$ beta-function *with μ set to zero*, and $\beta^{C,\tilde{\mu}}$ is the piece from the general result of [27] which has $\tilde{\mu}$ or C dependence. A similar equation can be obtained for β_B, but it is simpler just to calculate it afresh. The beta functions for C and $\tilde{\mu}$ can be obtained from the general expression of [27].

The renormalisation group equations are presented in appendix A.1.

4.5 Radiative Electroweak Symmetry Breaking And Low-Scale Considerations

The form of the tree-level radiative electroweak symmetry breaking (REWSB) constraint equation for μ eq. (1.15) suggests that the resulting value of μ will be correct in any reparameterisation, because of the way in which the reparameterisation keeps $m_H^2 + \mu^2$ constant. This equation finds the μ value consistent with given Higgs soft masses. However, in the $\mu = 0$ reparameterisation, numerical implementation of this equation fails, because the resulting μ^2 value close to convergence toward zero is sometimes negative.

The values of the model parameters obtained after imposing the REWSB constraints, if compared in the same reparameterisation, must be the same whatever reparameterisation we impose eq. (1.15) in. This is a consequence of the invariance of the Lagrangian, and can be verified by considering the application of a reparameterisation to the tree-level result eq. (1.15). In order that the REWSB routine be convergent around a positive value of μ^2, we can thus choose to impose the REWSB constraint after reparameterising so that $\tilde{\mu} = 0$.

The physical mass matrices for those particles affected by $\tilde{\mu}$ and C in $\mu = 0$ reparameterisation are given in [27]. The unaffected mass matrices can be used as originally implemented in SOFTSUSY.

The NSSB contributions to the mass matrices given in [27] are the leading, tree-level, NSSB corrections to the relationship between the physical particle mass and the running model parameters. SOFTSUSY includes some MSSM loop corrections in the mass matrices, but such corrections involving the NSSB couplings have not been added.

The one-loop corrections to the effective potential are included, with the leading top/stop contributions from the NSSB couplings, and the calculation is performed at the renormalisation scale where the scale dependence of the 1-loop corrections is smallest, approximately $\sqrt{m_{\tilde{t}_1} m_{\tilde{t}_2}}$. This scale, M_S is approximately 760 GeV for the mSUGRA parameters used here, and is intermediate between M_Z and M_X.

4.6 Results On The Particle Spectrum

As an example of the superparticle spectrum in NSSB, figures 4.1 and 4.2 show some of the masses on lines through NSSB parameter space passing through mSUGRA standard point II (defined using the sign conventions of [11]):

$$\begin{aligned} m_0 &= 400\mathrm{GeV}; \\ M_{1/2} &= 400\mathrm{GeV}; \\ \tan\beta &= 10; \\ A_0 &= 0; \\ \mu &> 0. \end{aligned} \tag{4.7}$$

The same point with the opposite sign of μ, has been investigated and shows very similar results, except with $C_0 \mapsto -C_0$ and $\tilde{\mu} \mapsto -\tilde{\mu}$.

Note that there is nothing special about the spectrum at the zero values of C_0 or $\tilde{\mu}$. The MSSM point already has broken supersymmetry. The NSSB terms break a few remaining equalities between SUSY breaking terms, but this has no sudden qualitative effect on the superparticle spectrum.

The masses and soft breakings for non-zero C_0 near mSUGRA point II show an

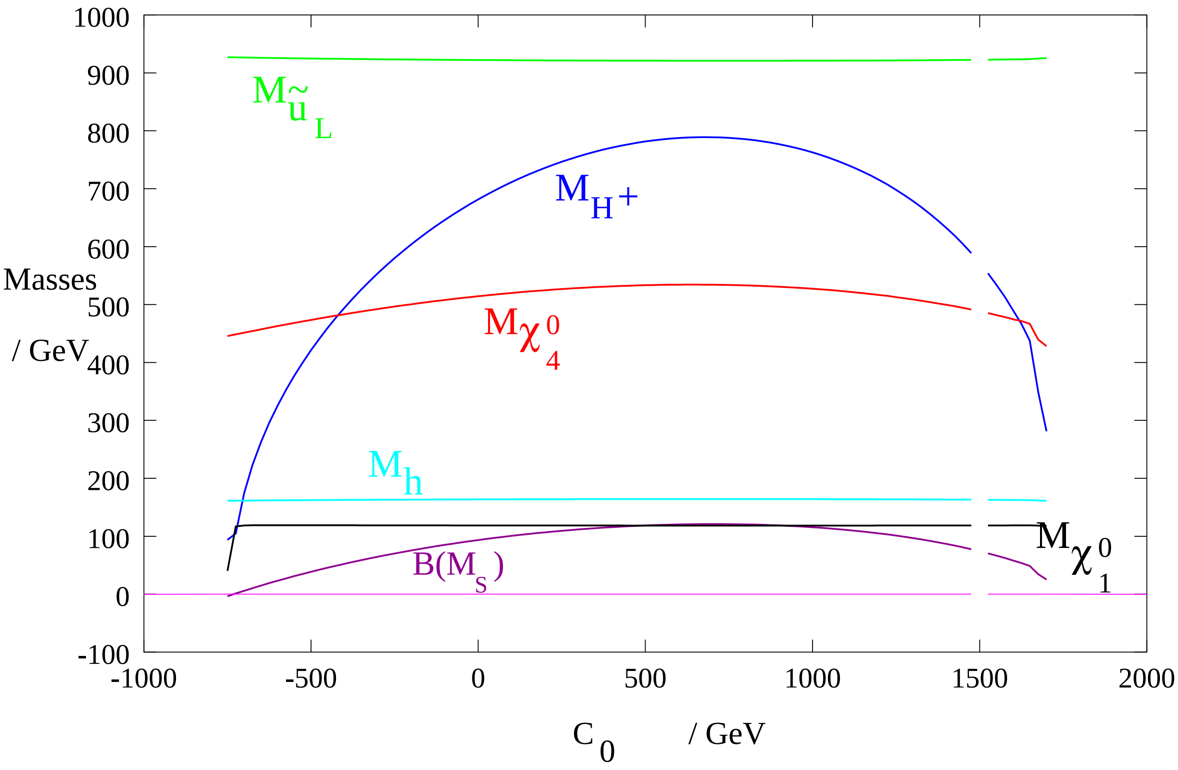

Figure 4.1: Some of the MSSM particle masses, and the B parameter at the REWSB scale, for non-zero values of the non-standard supersymmetry breaking parameter C_0. $C_0 = 0$ here is the mSUGRA point II: eq. (4.7). At the missing point, and the final point, the numerical method failed to converge correctly. Detail of this region can be seen in figure 4.6. The masses and parameters shown are those referred to in section 4.7, or those masses which vary significantly across the range. Those masses shown which do not change significantly have been chosen to indicate this fact.

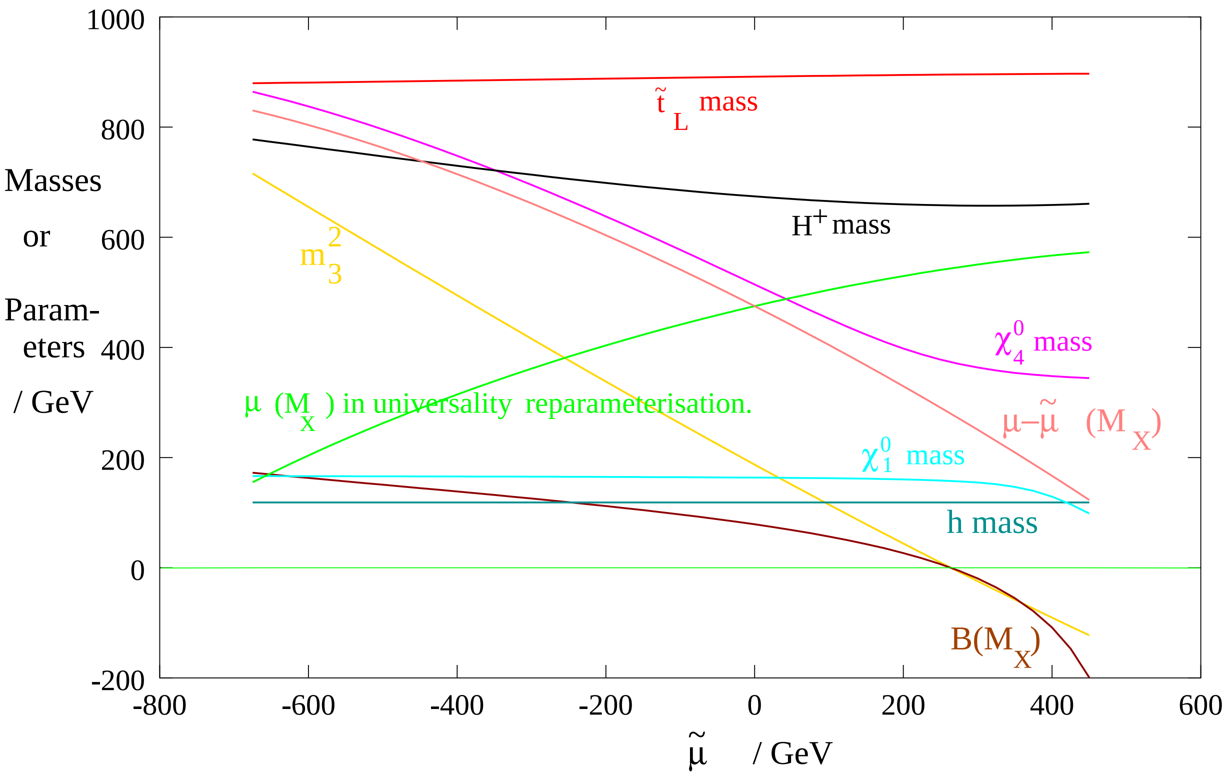

Figure 4.2: Some of the MSSM parameters and particle masses for non-zero values of the non-standard supersymmetry breaking parameter $\tilde{\mu}$. $\tilde{\mu} = 0$ here is the mSUGRA point II: eq. (4.7).

extremum in fig. 4.1. This occurs where the B parameter is equal at M_S and M_Z. This behaviour is a property of the RGEs for the system.

The very low masses of the normally heavier Higgs bosons $(A, H^{\pm}, H^0)$ for large negative values of C_0, as shown in fig. 4.1, and the removal of all but the lightest neutralinos and charginos from the lower mass part of the spectrum (fig. 4.2) for large negative values of $\tilde{\mu}$, might show interestingly different phenomenology. This may be worth investigating with ISAJET [51] or HERWIG [55, 56].

4.7 Parameter Space Constraints

What determines the largest positive and negative values of C_0 and $\tilde{\mu}$ allowed? For very large negative C_0 both the eigenvalues of the second differential matrix of the Higgs 1-loop effective potential at M_S become negative at $\langle H_1 \rangle = \langle H_2 \rangle = 0$. This is in contrast with the usual MSSM case where only one of the eigenvalues is negative – a phase transition has occurred. In this region, the REWSB constraint (eq. (1.15)) fails to correctly place the minimum of the Higgs effective potential at the required values of v and $\tan\beta$, placing a saddle point there instead. See fig. 4.1, where the Higgs masses become small as we approach the transition at $C_0 \sim -750$ GeV. The shape of the surface below the transition is shown in fig. 4.3. Note that eq. (1.15) assumes that the point found does correspond to the physical minimum, so we do *not* have a correct determination of the superspectrum in the unusual phase.

In order to obtain the above understanding, and obtain fig. 4.3, code was written to obtain the full shape of the Higgs effective potential away from the minimum, including the dominant 1-loop corrections (sec. 5.2).

We should next attempt to resolve the question: is there a point in the parameter space where this new phase yields physical values of the particle masses? For the pa-

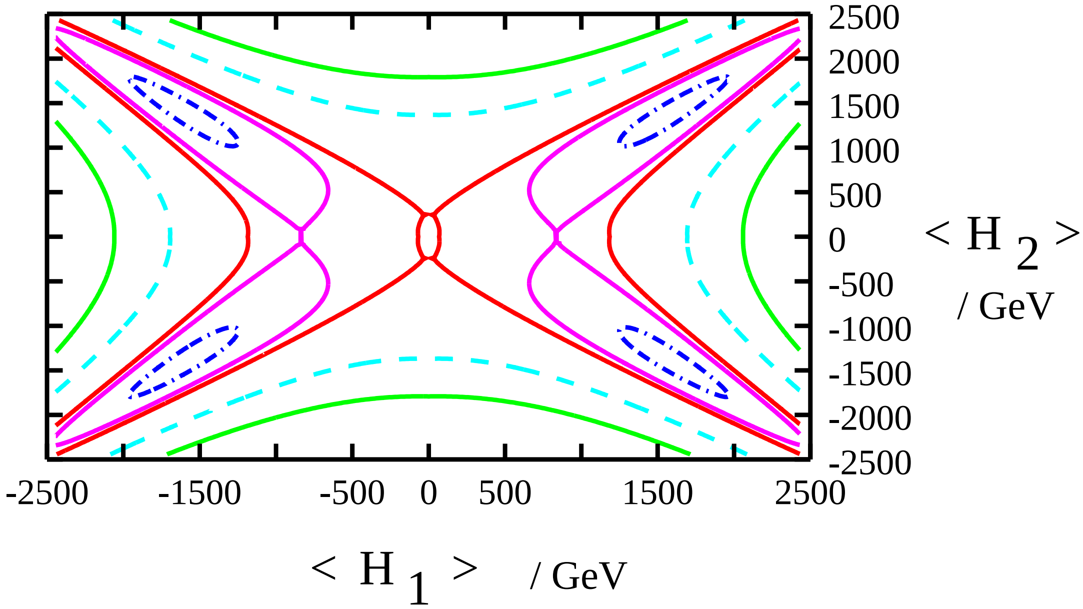

Figure 4.3: The Higgs effective potential surface for large values of C_0 near mSUGRA point II. (This plot was made with $C_0 = -800$ GeV.) Note the saddle point at $\tan\beta = 10, \langle v \rangle = 243$ GeV, i.e. at $\langle H_2 \rangle \sim 240, \langle H_1 \rangle \sim 0$. The central (red, solid) contour is -1×10^8 GeV^4, the next contour (magenta, solid) is at -8.5×10^9 GeV^4, the small elliptical contours (blue, dot-dashed) are at -2×10^{10} GeV^4, the blue, dashed contour is 10^{11} GeV^4, and the outermost (green, solid) contours are at 2×10^{11} GeV^4.

rameter set shown in fig. 4.3 the Higgs VEV is much too large, resulting in a value of M_Z which is too large. Perhaps, for a given pair of $\tan\beta$ and $|\langle H\rangle|$, more than one set of values for the soft breakings is possible, corresponding to each of the two phases. Although, at tree level, eq. (1.15) suggests a unique value of the parameters for a given $\tan\beta$ and $|\langle H\rangle|$, it must actually be solved iteratively when the loop corrections are taken into account, because these corrections depend on the soft SUSY breakings. It is therefore possible that this iterative procedure possesses more than one solution. However, after an extensive search of parameter space (sec. 5.2), nowhere was the new phase found to be relevant to real physics. One of the ways in which this search was carried was to ask the question: for a given set of parameters chosen using SOFTSUSY to put an extremum at a specified $\tan\beta$ and M_Z, does there exist an alternative choice of μ and B which also puts an extremum at the same location? Plots showing the location of the Higgs minimum versus μ and B never showed two points with the minimum at the same location, where that location was the correct value of v consistent with M_Z. An attempt to embed the effective potential minimisation into SOFTSUSY, replacing eq. (1.15), failed due to numerical instabilities and speed problems.

There exist points in parameter space where the "universality reparameterisation" discussed in section 4.2 does not exist after imposing the low-energy constraints and running up to the high scale: the required value of μ^2 in the universality reparameterisation at high scale becomes negative. At such points the Higgs soft masses cannot, for positive μ^2, be made equal to the sfermion soft masses, while maintaining consistency with the electroweak symmetry breaking conditions. If this equality is forced, there is no positive value of μ^2 for which electroweak symmetry breaking occurs. This provides the limit on large negative values of $\tilde{\mu}$ at mSUGRA point II.

It is for these large negative values of $\tilde{\mu}$ at mSUGRA point II that the recurrence relation approach becomes unstable. As shown in figure 4.4, the convergence toward the

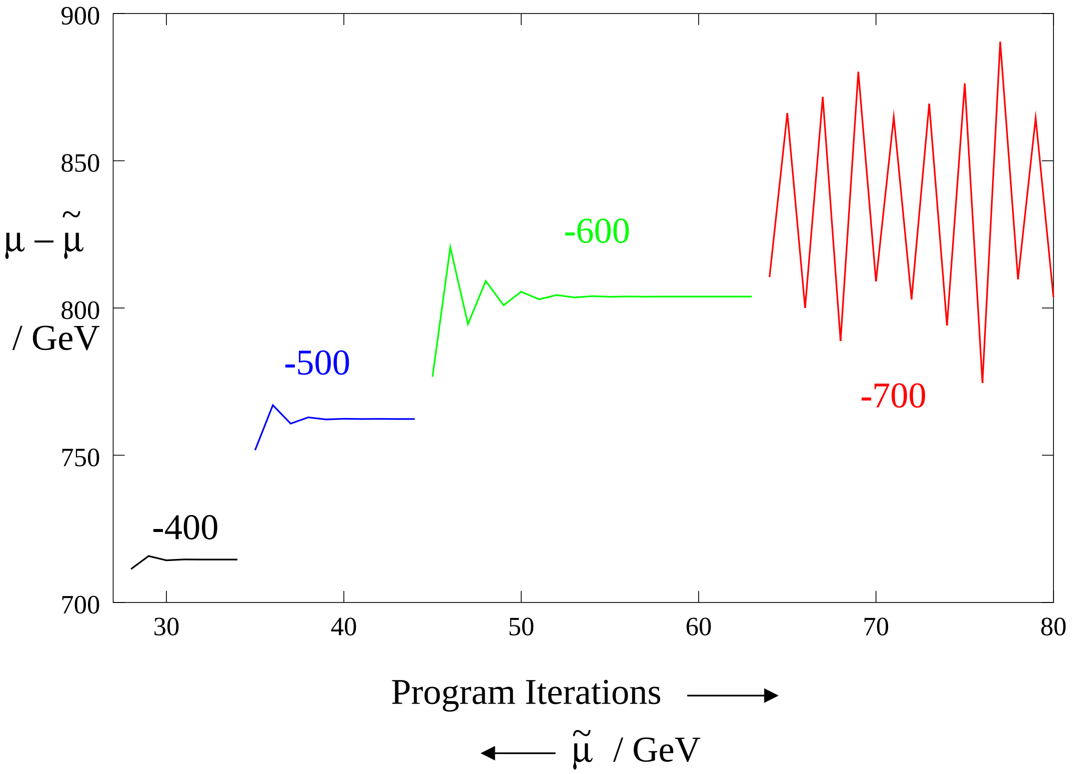

Figure 4.4: At mSUGRA point II, the recurrence relation solution to the SUSY RGEs converges more and more slowly for increasingly negative values of $\tilde{\mu}$. Each separate convergence in the plot is for a different value of $\tilde{\mu}$, with $\tilde{\mu}$ becoming more negative to the right. Note that for sufficiently large negative values of $\tilde{\mu}$, the method fails to converge at all. The numbers near the lines show the value of $\tilde{\mu}$ used for that point, in GeV.

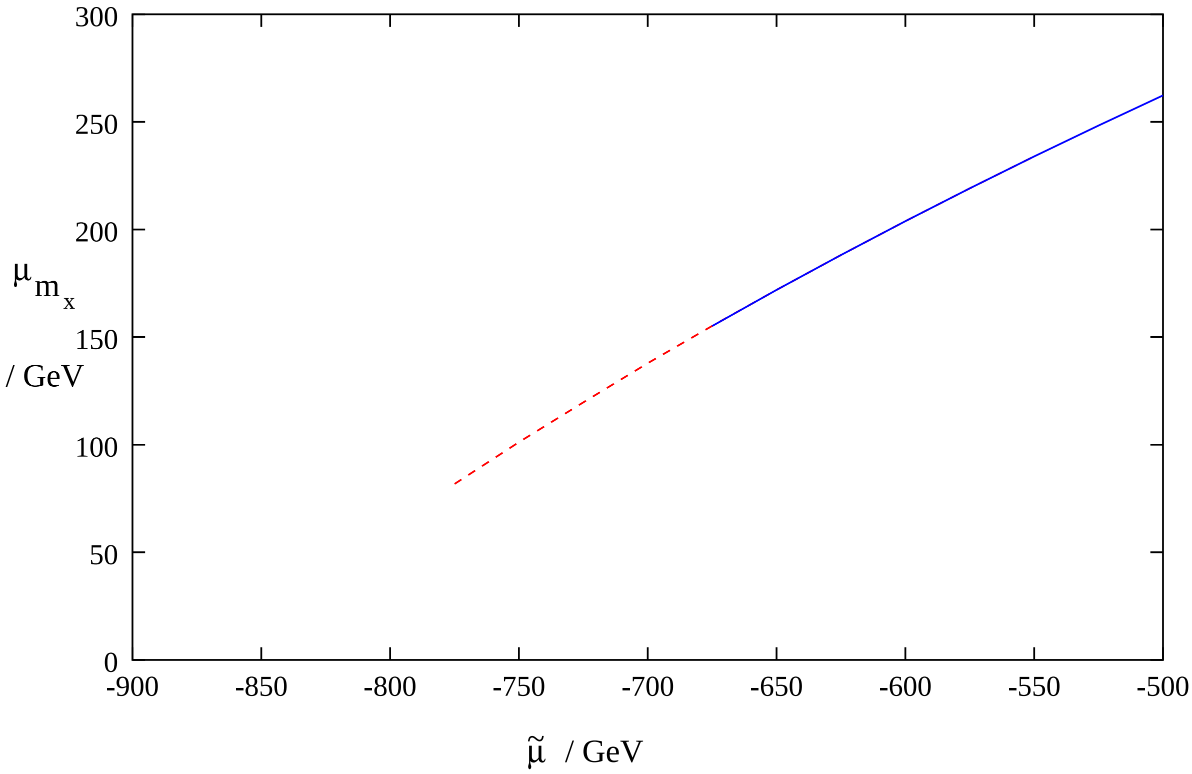

Figure 4.5: The value of μ in universality reparameterisation at M_X for non-zero $\tilde{\mu}$ near mSUGRA point II. The dotted part of the line shows the extra reach provided by the single-ended drift method.

fixed point becomes steadily slower, before it finally becomes unstable. A naive belief in the recurrence relation approach would result in an underestimate of the size of the valid parameter space. The recurrence relation approach becomes unstable at $\tilde{\mu} \sim -675$ GeV, while the single-ended drift method explained in appendix A.2 extends the region which can be explored as far as $\tilde{\mu} \sim -775$ GeV. Even that method cannot reach the physical limit, due to numerical instabilities caused by early iterations entering the unphysical region. This is illustrated in fig. 4.5.

For large positive $\tilde{\mu}$ at mSUGRA point II, the bound on $\tilde{\mu}$ due to the value of B runs to extremely large negative values at high scale, making the calculation unstable. This is an artificial consequence of using B rather than m_3^2. As shown in fig. 4.2, $m_3^2 = B(\mu - \tilde{\mu})$ is finite, but $\mu - \tilde{\mu}$ is becoming small, so B is singular. The calculation becomes unstable here due to the large value of B, but the upper bound on the value of $\tilde{\mu}$ comes from the

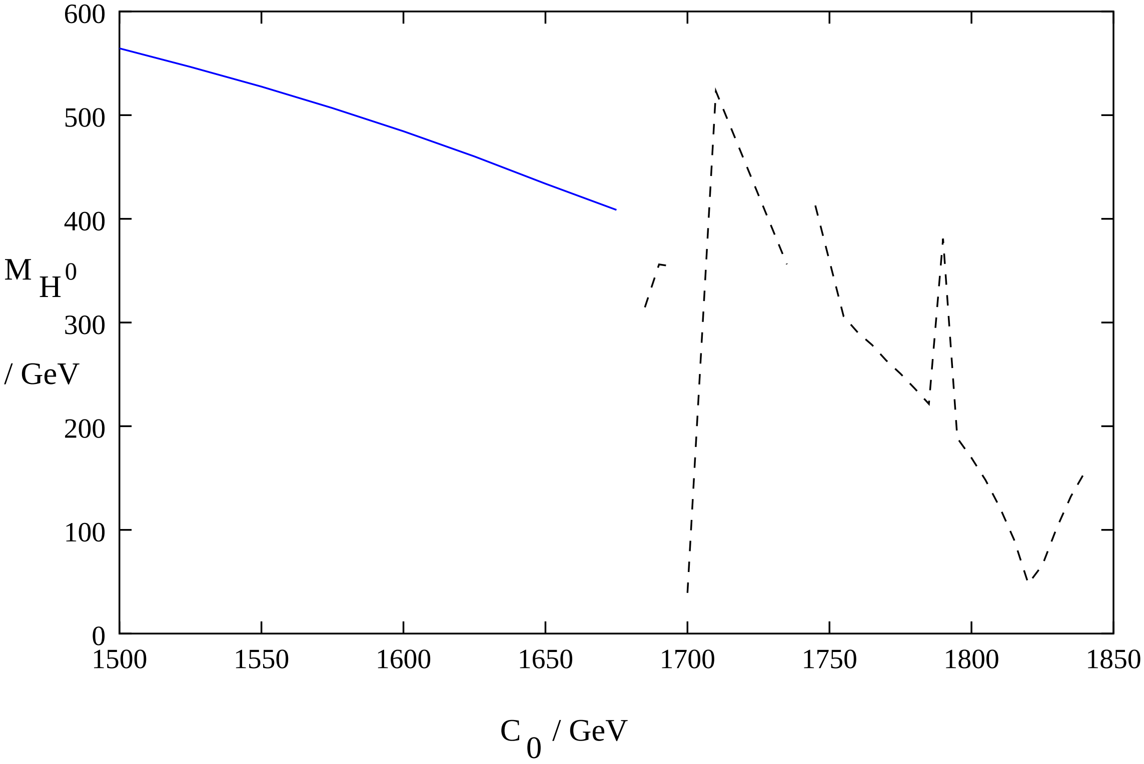

Figure 4.6: The mass of the heavy neutral Higgs particle, for non-zero C_0 near mSUGRA point II. All the data was produced using the single-ended shooting method. The dashed part of the line is the region near the physical limit where transients spoil the stability of the method. The figure shows the outcome of the method, whether or not it has formally converged.

lightest neutralino mass, which is becoming small as $(\mu - \tilde{\mu})$ does.

For large positive values of C_0, above around $C_0 \sim 1500$ GeV, the drift method becomes non-convergent. The single-ended shooting method discussed in section 2.1 and appendix A.2 takes us further, and is used to produce figure 4.1, which takes us up to $C_0 \sim 1675$ GeV. Extrapolating, it appears that the physical limit occurs for the same reason as for large negative C_0, i.e. the Higgs masses become small. However, the physical limit cannot be reached even with the single-ended shooting method, for the reason discussed above. With care, some useful data can be teased out of this region (see fig. 4.6), showing that the physical limit is around $C_0 \sim 1675$ GeV.

4.8 Fine-tuning

Here, there is a subtlety, again caused by the presence of the reparameterisation invariance: the same Lagrangian may be described by a different choice of parameters (sec. 1.2.7). For example, one could choose, instead of C_0 and $\tilde{\mu}$, to reparameterise so that $C_0 = 0$, and use $(\overline{m_{\tilde{q},\tilde{l}}} - \overline{m_h})$ as the other parameter. Then, one would get different fine tuning values for the same Lagrangian, depending on one's choice of parameter set. If this situation is thought to be unsatisfactory, the solution is to take the fine tuning with respect to the reparameterisation-invariant combinations of parameters appearing in the Lagrangian, for example, $(\tilde{\mu} - \mu)$.

On the other hand, one may view it as acceptable that the fine-tuning depends upon the choice of reparameterisation, given that the fine-tuning measure is supposed to be a measure of one's satisfaction with the deeper model lying beyond the Lagrangian being studied. A parameterisation choice reveals something of one's assumptions about the beyond-the-MSSM physics giving rise to the MSSM-type Lagrangian.

Fig. 4.7 shows fine-tuning contours near mSUGRA point II with respect to invariant combinations of parameters, and fig. 4.8 for the parameter set chosen here.

These results show that, in both cases, there is significant fine-tuning with respect to negative $\tilde{\mu}$. There is no significant fine-tuning with respect to C_0, and for positive $\tilde{\mu}$ the dominant fine-tuning is that with respect to the standard supersymmetry breakings. These effects are consistent with the behaviour explained in section 4.7. The absolute magnitude of the fine tuning is smaller when considered with respect to the invariant combinations of parameters.

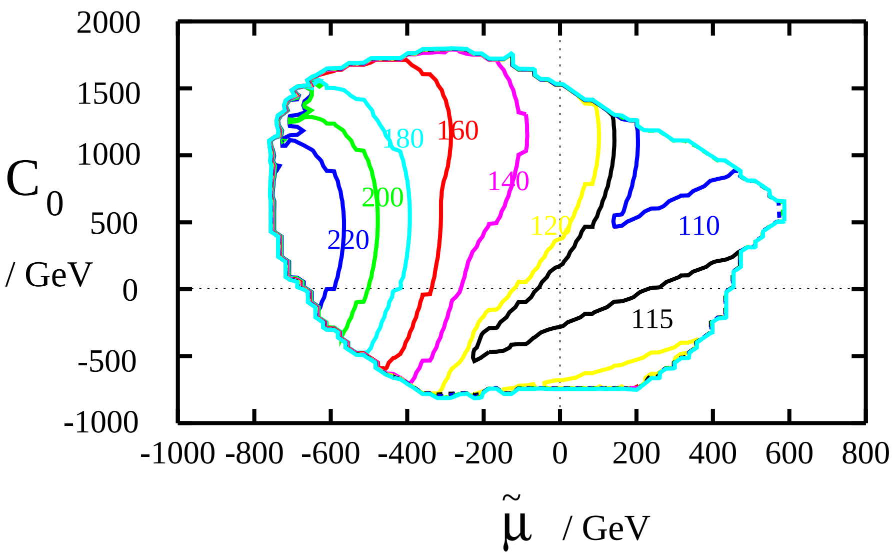

Figure 4.7: Fine tuning contours for non-standard supersymmetry breaking, with fine-tuning differentials taken with respect to invariant combinations of parameters. The plane is shown parameterised in terms of C_0 and $\tilde{\mu}$. The outermost line shows the edge of the valid parameter space, according to the drift method.

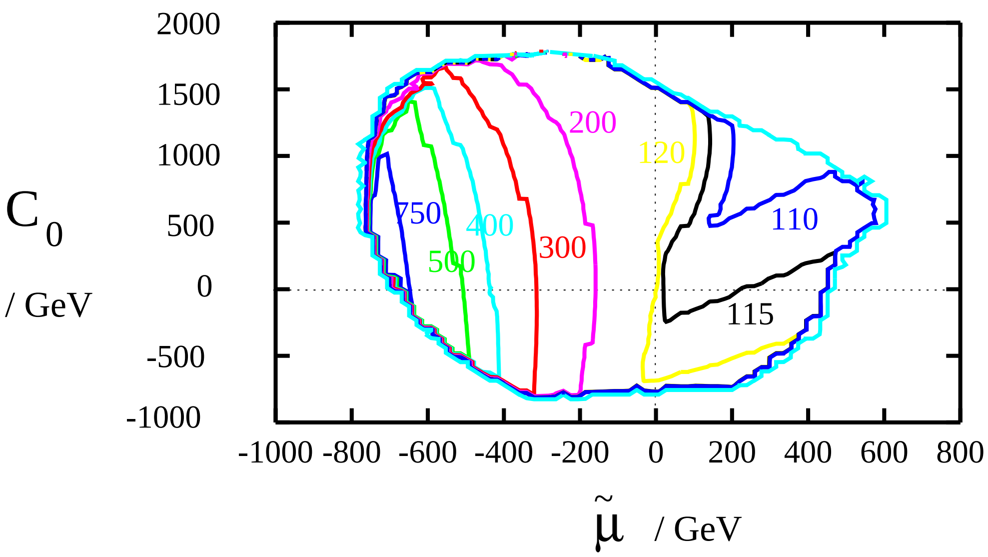

Figure 4.8: Fine tuning contours for non-standard supersymmetry breaking, with fine-tuning differentials taken with respect to the usual mSUGRA parameters, C_0 and $\tilde{\mu}$.

4.9 Conclusions

The 3-family beta functions have been obtained for the MSSM with the NSSB terms, in a form suitable for numerical implementation, and in an economical way making use of the reparameterisation invariance.

The mSUGRA boundary conditions have been adapted for use in the context of the NSSB reparameterisation invariance, by choosing to impose the boundary conditions in the reparameterisation where they are most nearly satisfied. These boundary conditions allow the conventional mSUGRA (or CMSSM) model to be seen as a subspace of the full parameter space including NSSB terms, and the calculation of the superspectrum can be made in the conventional way.

The superparticle spectrum and a fine-tuning measure have been calculated for non-standard SUSY breaking near mSUGRA point II, where it is found that there is no significant experimental signature indicating the new terms, except where they approach their maximum allowed values.

The conventional MSSM methods are, however, found to be inadequate in this extreme region, due to the instability of the numerical method used. A more stable numerical method has been developed which solves this problem.

The phase transition in the Higgs potential occurring for large negative C_0 at mSUGRA point II suggests that this model potentially has a rich phase structure, although this appears to be of only theoretical significance, since in this phase, the Higgs VEVs are very large.

In conclusion, we see that the numerical approach used to calculate the MSSM superspectrum can be applied to this model, but there are subtle complexities which must be dealt with. As supersymmetric models continue to be developed, given the need to calculate their properties sufficiently accurately for comparison with experiment, such subtleties must be treated carefully.

Chapter 5

Automating The Analysis Of Supersymmetric Models

5.1 Introduction

The analysis of a candidate model of particle physics consists of a number of tasks, each of which must be performed so that an understanding of the properties of the model can be obtained, and its investigation at some experiment considered. These include:

- The deduction of the Lagrangian of the model, for example, from its particle content and gauge symmetries, its superpotential, and the inclusion of soft supersymmetry breaking terms.
- The examination of the interaction terms of the Lagrangian, to deduce the couplings between the fields and the Feynman rules for vertices.
- The construction of the effective potential for scalar fields, and its minimisation to find the expectation values of the scalar fields. This tells us which symmetries of

the Lagrangian are spontaneously broken, and whether the potential is bounded from below.

- The deduction of the "mixing-groups" for the model: the sets of fields which mix so that their gauge, or "interaction" and mass eigenstates are not the same.
- Calculation of the mixing matrices for each model, so that the masses of the mass eigenstates and the mixing angles can be deduced. If these results are required at one-loop accuracy, then self-energy diagrams must be evaluated.
- Construction of renormalisation-group $\beta-$functions for the model, so that input parameters can be defined at a variety of scales, and the possibility of unification and contact with high-scale theories may be considered. Threshold corrections should be taken into account.
- The deduction of a variety of observable properties of the model, so that they can be compared with the expected reach of future experiments and with existing experimental bounds.

This chapter describes an attempt to implement a computer program capable of automating the above procedure. The goal: to be able to describe simply a model in terms of its particle content and symmetries, and the values of its parameters, and obtain automatically the information needed to investigate the model. This eliminates the usual need to carry out manually certain symbolic analyses, and the separate implementation of these analyses in a new computer program for each model.

The goal has been partially achieved: the program, EFFECTIVE, can automatically produce a Lagrangian from a model specification in terms of the gauge symmetries present, its matter content specified as representations of those gauge symmetries, the superpotential, and any additional soft supersymmetry breaking terms (SSBT). The superpotential and SSBT are defined in terms of the natural "multiplets"- family triplets, gauge representation multiplets and so on. The Lagrangian is converted to a simple computer representation, by expanding the Lagrangian symbolically in terms of the components of fields. A database of couplings between these component fields is generated from this simplified Lagrangian. This is used to deduce the tree-level mass matrices and mixing-groups.

Structures are defined to enable Feynman diagrams to be defined in terms of a "loop-function" of the masses of the particles involved in each propagator and the couplings at each vertex. Such diagrams can automatically be evaluated for the identification of each propagator in the diagram with a field in the model, with the coupling for each vertex and mass for each propagator being looked up automatically in the programme's databases. The diagram structures are used to evaluate the self-energy diagrams for the fields to obtain one-loop masses, and the one-loop effective potential. Routines exist to allow the one-loop potential to be minimised numerically. The diagram structures are also used to obtain the total tadpole diagrams for each scalar field, so the effective potential may instead be extremised by solving numerically over a desired subspace of parameter space for the tadpoles to be zero.

An input file format exists so that values of parameters can be specified, including support for scans or the random sampling of parameter space. An output file format is specified for the recording of the masses and parameter values calculated. Structures exist to facilitate the inclusion of additional variables in the output file, and alteration of the potential-minimisation calculation, as the user may desire.

What aspects of the goal have not been achieved? The primary unsolved problem is the automatic construction of the renormalisation-group $\beta-$functions. If this were completed, then EFFECTIVE could become a fully automatic program for the investigation of BSM physics: the SOFTSUSY-style task of reconciling high- and low-scale inputs could be included. I believe I understand how this could be done, and discuss it below (sec. 5.3.11).

Other failings of the current implementation include its inability to represent some candidate models in its model definition format: non-standard gauge kinetic functions, and Kähler potentials are not supported, nor are models defined in more than 3+1 dimensions. Gauge groups other than direct products of U(1) SU(2) and SU(3) factors are not currently supported, but could be implemented very easily merely by specifying the generators and structure constants of any new factors. (And names for the components of their multiplets to facilitate human-readable output!) Not all self-energy diagrams have been coded; currently, only those for scalar fields are included, but the full set could be added swiftly. The anticommuting nature of fermion fields is dealt with by exploiting their commuting nature when Weyl spinor doublet indices are suppressed- it is possible this technique could fail for models more complicated than those considered here, when the symbolic engine would need to be modified to take this into account.

For all of the various diagrams used by the model (effective potential, tadpole, self-energy, and any specified for other output data required, such as the electric dipole moments (sec. 6.2)), the loop-functions of the diagrams must be specified explicitly as functions of the propagator masses. (Although these need only ever be specified once for each diagram: the variation between models of the Feynman rules for the vertices is handled automatically.) The program uses a representation in which the real and imaginary parts of scalar and fermionic fields are treated as separate fields. While this representation is completely equivalent to the conventional one using complex fields, and while its use facilitates the implementation of certain aspects of the program, certain results must be translated from the conventional representation in terms of complex fields when implementing them in the program. This last point is not a failing of the program to achieve something, since the two representations are completely equivalent, but a change of this design choice might be preferred by some users. Finally, the program does not automatically deduce which fields will be mixed by loop corrections, when those fields do not mix due to the tree-level mass matrices.

The software has been tested in a variety of ways. The tadpole diagrams and tree level and one-loop masses have been compared with those hard-coded for the MSSM in SOFTSUSY (sec. 5.3.5). The tadpoles and self-energy diagrams have also been tested by ensuring that the results are consistent with those obtained (for zero external momentum) by numerical differentiation of the effective potential (sec. 5.3.8). Results for the standard, CP-violating, and R-parity violating versions of the MSSM have been compared with those in the literature (Chapter 6).

Before discussing the development of this program, we first discuss some of the physics associated with a very early version, created for use during the NSSB research (sec. 4.7).

5.2 An Early Effective Potential Generator

While investigating the mysterious phase transition of the Higgs potential for large values of the non-standard SUSY breaking parameters, I wanted to be able to plot the shape of the Higgs potential surface, so as to examine its structure away from the extrema, and characterise those extrema. The minimisation conditions eq. (1.15) and eq. (1.16) can be used to determine the values of μ and B which place an extremum at a desired location, but cannot guarantee that this extremum is a minimum.

I quickly discovered that the tree-level Higgs potential is not sufficient for such investigations: using parameter values imported from SOFTSUSY, the extremum for a well-understood point far from the phase transition was determined to be far from the location obtained using SOFTSUSY (fig. 5.1). In fact, for much of parameter space, the electroweak symmetry is unbroken at tree level. However, when the 1-loop effects were included using the supertrace formula, the results were consistent with those of SOFT-

SUSY (fig. 5.2). In this program, the mass matrices were inserted manually, taken from [50] with values of the parameters imported from SOFTSUSY. The logarithms of matrices were taken by the diagonalise-and-then-log-the-eigenvalues approach. Note that an easy mistake is to take literally the two-by-two chargino mixing matrices given in most of the literature. In the natural representation the chargino mixing matrix is four-by-four and two-by-two-block off diagonal. The two-by-two matrix approach is fine, but the contribution to the effective potential must then be doubled. For a general approach, useful for automation, we will see later that the four-by-four approach can be used, but with structures to exploit the symmetry properties of a matrix for speed purposes (sec. 5.3.5). It is interesting that the tree potential was so wrong: the requirement of sec. 1.5.1 that the 1-loop result have the smallest scale dependence is NOT the same as the requirement that the 1-loop contribution to the location of the minimum be smallest.

Note also that the effective potential plots are not symmetrical with respect to a change of sign of one of the Higgs fields. This sign change in one of the Higgs VEVs can be re-absorbed into a change of sign for the B parameter, but then one must remember that the minimisation of the Higgs potential explores both positive and negative B regimes simultaneously.

In principle, this code could be inserted in a SUSY RGE calculation and used instead of eq. (1.15), avoiding the danger of the program finding a saddle point or maximum instead of a minimum, if an appropriate numerical method such as Powell's [65] is used. However, since the use of $\tan\beta$ and M_Z as inputs requires one to solve for μ and B to put the minimum in a desired place, one must insert the minimisation algorithm in an equation-solving algorithm. This was tried, but proved unstable and slow. This will be discussed in more detail below (sec. 5.3.9).

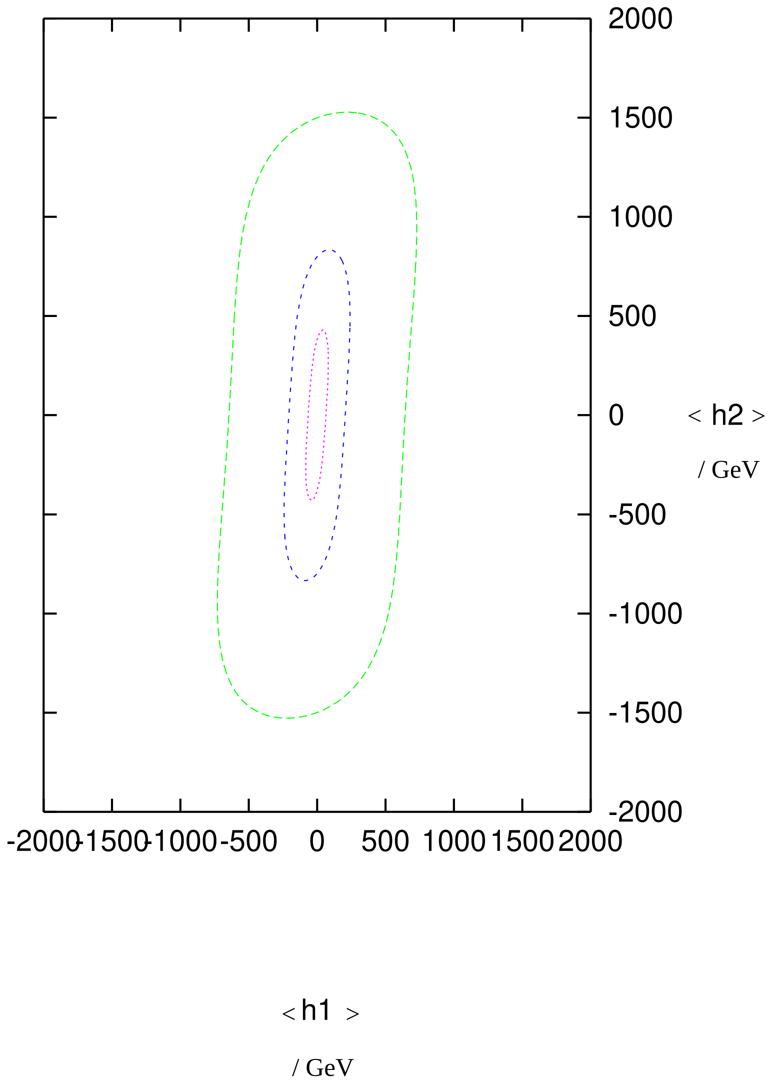

Figure 5.1: Tree level effective potential for mSUGRA point II eq. (4.7). Lines are contours of equal potential, relative to the origin, at 1×10^9, 1×10^{10} and 1×10^{11} GeV^2. Note that at tree level the symmetry remains unbroken.

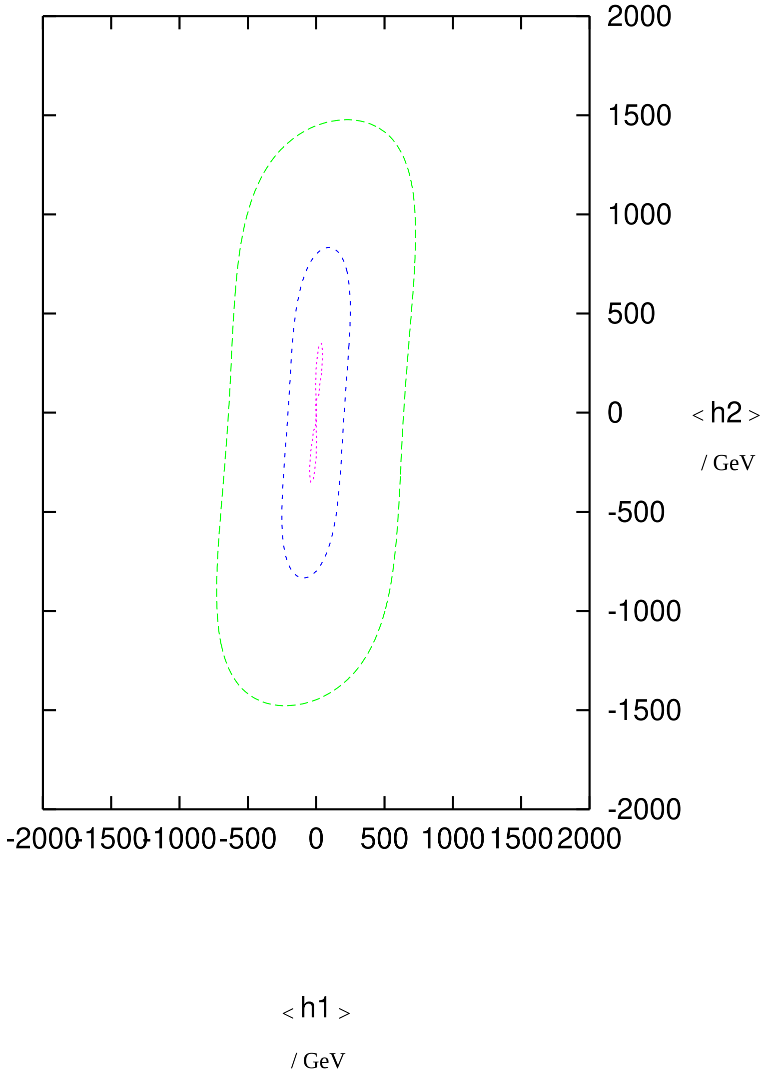

Figure 5.2: One loop effective potential for mSUGRA point II eq. (4.7). Lines are contours of equal potential, relative to the origin, at 0.0, 1×10^{10} and 1×10^{11} GeV^2. Note that the electroweak symmetry is broken, with a minimum at $v = 243$ GeV, $\tan\beta = 10$.

5.3 The Main EFFECTIVE Program

The development of EFFECTIVE has involved building C++ routines and class structures capable of handling issues such as:

- Symbolic expansion of contractions of physical multiplets into expressions involving their component fields.
- The complex nature of physical fields, facilitating the study of CP violation.
- Compound physical multiplets with gauge, Lorentz and family indices, their raising and lowering and contraction rules, and with component elements which may be parameters, constants or fields with or without VEVs.
- Symbolic expressions which can easily be searched for coefficients of groups of fields. This allows the couplings between sets of fields, including the elements of tree-level mass matrices and vertex Feynman rules to be obtained.
- Storing mass-mixing-matrices, allowing for tree-level and one loop matrices, and the block diagonalisation of the all-fields by all-fields mixing matrix.
- Supermultiplets, and the deduction of the Lagrangian from the superpotential.
- Gauge factors and matter gauge representations, including fields charged under more than one gauge factor.
- Automatic generation of the gauge coupling contribution to the Lagrangian.
- An input format suitable for interfacing with SOFTSUSY to set the values of the model parameters, and allowing for parameters to be scanned over or sampled randomly.
- Presentation of results in a form suitable for data visualisation.

- A format for storing the couplings between specified interaction eigenstate fields, and routines for obtaining couplings between mass eigenstates from these.
- Using numerical algorithms to find the extrema of the effective potential.
- Representing Feynman diagrams in terms of the masses and couplings generated by the program.
- Automatically obtaining the tree-level and one-loop effective potential, and the total tadpole diagram.
- Automatically evaluating the self-energy diagrams to obtain the one-loop masses.

We now turn to the discussion of each of these development issues in turn. Figure 5.3 shows the class structure of EFFECTIVE. A discussion, with examples, of how to use EFFECTIVE to build up and study a new model is given in an appendix (sec. A.3).

5.3.1 The Tree-And-Leaf Structure For Physical Multiplets

The core of EFFECTIVE is a structure for representing, manipulating, and simplifying expressions involving physical multiplets, such as gauge multiplets, Lorentz vectors and Weyl spinors, and family triplets. This structure keeps track of contraction rules, conjugation rules, and the raising-and-lowering of indices. The C++ inheritance structure handles the degrees of specialisation and implementation as shown in (fig. 5.3).

The individual components of multiplets, or "leaves" may be either "volatile", in that new storage is allocated when a multiplet is copied, or "nonvolatile", in that the new multiplet points to the same leaf as the old one. The use of nonvolatile leaves allows, for example, fully expanded expressions to be searched for the coefficients of particular fields. Leaves include fields with or without VEVs, constants, and parameters. A "parameter" object represents one of the variable parameters of the model at hand, such as the value

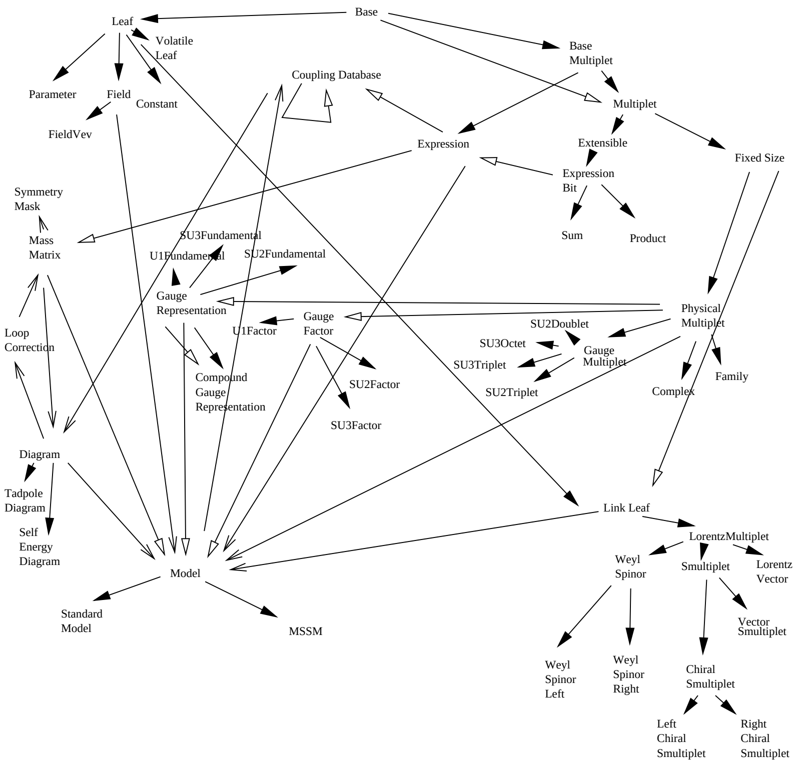

Figure 5.3: The class structure of the EFFECTIVE program. Solid arrows show C++ class public inheritance (Read as "...becomes..." or "...is a...".) Triangular open arrows show ownership relationships including memory allocation (Read as "...is controlled by...".) V-arrows show classes which contain a pointer to objects, but without control over memory allocation and deallocation (Read as "...uses..." or "...is pointed to by...".) Note that both ownership relationships are manifested via pointers, and the object owned is usually a derived class of the class of the pointer. Note the places where recursive structures are possible: where a derived class controls or points to itself or a base class thereof.

of $\tan\beta$. When a parameter's value is changed, it changes in all the expressions and multiplets of which it is a part.

Compound multiplets, (for example Vector-Supermultiplet SU(3)-octet SU(2)-triplet Complex-doublet fields), are dealt with by allowing the components of a multiplet to be multiplets themselves, using a polymorphic base class, a common ancestor of both multiplets and leaves. Complex numbers are defined as a special derived class of multiplet. The structure allows for subtle relationships between derived classes of multiplets, such as the conjugate of a left-handed Weyl spinor being a right-handed Weyl spinor.

This tree-and-leaf structure is built using the C++ standard container types "vector" and "list". Classes wrapping these containers templated for containing pointers to the common base tree-and-leaf type are used, to take control of memory management for the manipulation of volatile and nonvolatile components.

The program keeps track of the Lorentz and Weyl spinor indices using a structure called a "link field" (sec. 5.3.4): the components of spacetime multiplets (Weyl spinors or Lorentz vectors) are not treated as separate fields. There exist a finite set of Lorentz invariant contractions of Weyl spinors and Lorentz vectors. These are represented in the program using dummy objects: a *parameter* called "Sigma" is used to represent the Pauli matrices when used in invariants involving Weyl spinors, while objects called Inner-Product-Signals (IPS) are used to keep track of which spacetime indices are contracted, so that, for example $(\psi^\alpha\chi_\alpha)(a^\beta b_\beta)$ can be distinguished from $(\psi^\alpha\chi_\beta a^\beta b_\alpha)$. A dummy field called "partial" is used to keep track of terms in the Lagrangian (other than kinetic terms) involving a derivative, i.e. couplings with a momentum on one of the legs. An IPS keeps track of which field is being differentiated. These dummy objects are used when calling the routine which generates symbolically the expression representing the coupling between a set of interaction eigenstate fields, so that the coupling involving a particular structure of spacetime indices can be obtained. Suppression of the Weyl spinor indices within expressions means spinor fields can be treated as commuting objects, rendering the symbolic simplification of the Lagrangian significantly faster and easier to code. An alternative setup where the components of Lorentz and Weyl spinor multiplets are considered as separate fields was tried, but proved to be extremely slow. (Multiplication of the number of quark fields by two represents a much greater increase in the number of terms in the Lagrangian). This approach would, however, prove useful if EFFECTIVE is ever extended to apply to extra-dimension models, where, for example, VEVs can break 5-D Lorentz symmetry.

In EFFECTIVE, the real and imaginary components of scalar and spinor fields are everywhere treated as separate fields. Consider, for example, a fermion mass term of the form $\overline{\psi}_a M^{ab} \psi_b + c.c.$ where a, b are family indices, and M is complex, possibly describing CP violation. In EFFECTIVE, we would instead obtain a real mass matrix linking vectors of the real and imaginary component fields, with the vector ψ having twice the number of components as in the case where the components are complex: $\psi_a^T M_R^{ab} \psi_b$. The imaginary part of M corresponds to the parts of M_R linking real and imaginary components of ψ. The Lagrangian density is a real function of the degrees of freedom of the fields of the model; complex numbers represent a method of bookkeeping describing the way the Lagrangian density is built from the real degrees of freedom of the model. Note that a consistent set of Feynman rules for treating these real fields exists - conversion of results between these two equivalent representations must involve careful examination of possible factors of two, for example, when deducing the Lagrangian from the superpotential (sec. 5.3.4).

5.3.2 The Symbolic Engine

The multiplet structure discussed above allows an expression defined in terms of multiplets of fields or parameters to be expanded as a sum of products of components. This allows for efficient representation of the Lagrangian: a sum of terms, each of which is a product of fields, parameters and constants. The structures describing sums and products are economically defined, using the same base class as that for multiplet fields or parameters. An expression can have as its components other expressions, multiplets, or leaves. When debugging, expressions are validated by checking, for example, that no sum can add multiplets of different indices. Symbolic manipulation of component fields is accelerated by allowing them to be sorted based on an arbitrary order, speeding up the recognition of identical products for factorisation. This means that the components of multiplets ("leaves") must be commuting objects: hence the speed gain by suppressing Weyl spinor indices. The anticommuting nature of products of SU(2) doublets is retained. (Remember the metric of SU(2) space is totally antisymmetric.) Sorting these products would not give a speed increase, since we do not need to factorise them. Thus, it is easier to leave the algebra anticommuting, and suppress the metric tensor. Inclusion of the metric to create commuting objects would increase the complexity of the expressions and reduce the speed.

5.3.3 Gauge Factors, Gauge Representations, And Gauge Coupling Lagrangian Terms

In order to build software capable of automatically generating the gauge interaction terms of the Lagrangian, several sections of program are required. First, and relatively trivially, the multiplets describing the representations of the gauge groups in the model have been defined, describing the way they are contracted and conjugated.

Next, a "gauge factor" class has been developed, capable of being derived from (using the terminology of object oriented programming) in order to define different gauge factors. The gauge group of a given model is defined using a list of these factors. These objects can construct the gauge field they represent, add it to the list of fields in the model, and add to the Lagrangian the terms involving their interactions. Similarly, a "gauge representation" class can construct each matter field in the model and add its interaction terms to the Lagrangian: the matter content of a model is defined as a list of gauge representation objects. These objects can be queried by other routines to obtain the fields, or, in the case of supersymmetric fields, just the fermionic or bosonic parts - this is used, for example, in the definition of the soft supersymmetry breaking terms.

Compound gauge representations, such as the left-handed electron which is a representation both of $U(1)_Y$ and $SU(2)_L$, can be built using a compound gauge representation class which takes arguments of its component representations, and which can build the appropriate gauge interactions.

At the present time, only matter fields in the fundamental representations and gauge fields in the adjoint representations of $U(1)$, $SU(2)$ and $SU(3)$ are available in EFFECTIVE. A model with a gauge group consisting of a direct product of such factors can be built. Other Lie groups and representations could be added by specifying the generators and structure constants (sec. A.3.2).

The scalar quartic "D-term", required for gauge invariance and arising from integrating out the auxiliary scalar fields associated with each vector field, involves terms which link matter fields in different representations of a gauge factor. Thus, these terms are created by a separate routine, rather than by the gauge representation classes.

5.3.4 The Superpotential

Multiplet types for vector and chiral supermultiplets are defined in the program, and the component vector, spinor, and scalar fields can be extracted. EFFECTIVE works with the theory after the auxiliary components of the superfields have been integrated out, and these do not form part of the supermultiplets. Supermultiplets inherit from the base class of representations of the Lorentz group, the same base class as for scalars, Weyl spinors, and Lorentz vectors.

If the full superfield were used when constructing the superpotential, the component bosonic and fermionic fields would be contracted out. Instead, we want the superpotential to expand to an expression containing superfields. A structure (called a "Link-leaf") can be defined, preventing certain indices of the multiplets in an expression from being contracted.

Another issue here is correctly fixing the factors of two obtained when the sums over components of superfields are taken when treating real and imaginary components of scalar and spinor fields separately. It can be shown that an extra factor of $1/2$ is needed in the D-term but not in the F-term.

5.3.5 Mass Matrix Generation and Block-Diagonalisation

By examining the coefficient of each possible bilinear in the Lagrangian the tree-level masses can be extracted, and one can discover which fields mix. We assume rotational symmetry, so that fields with different spin do not mix, generating three separate mixing matrices, for scalar, spinor, and vector fields.

These matrices must then be block-diagonalised, so that each mixing-set of fields has its own mass matrix.(e.g. in the MSSM the $\tilde{B}$ and $\tilde{W}_3$ gauginos and the neutral parts of the higgsino fields mix to become the neutralinos (table 1.2).)

One must be careful when working out the groups of fields which mix if, for example, field A mixes with field B which in turn mixes with field C, but A does not mix directly with C. If one is not careful, one ends up building two mixing-groups for these fields instead of one.

From this calculation, we obtain symbolically the expressions describing the components of the tree-level mass matrices. These are stored in a mass-matrix class, which may be queried to obtain the mixing angles and mass eigenvalues. When it is desired to include one-loop corrections to these masses (sec. 5.3.10), the class describing such corrections is attached to the mass-matrix object, and the methods returning the masses and mixing angles can be used as normal.

Since the diagonalisation of matrices can be quite slow, the mass matrix class stores the values of its eigenvalues and diagonalising matrices. A method must be called to remind the program that these are out of date whenever parameter values are changed. This is a gain of speed at the cost of possible serious mistakes at the hands of an incompetent user, and as such is a design choice worth debating. (The methods that change the parameters could automatically notify the model of the change, but this would force all parameters to keep a copy of the pointer to the overall model, a space waste, and a failure of encapsulation. In addition, if we are changing the values of many parameters, we can save time by only notifying the matrices that the parameters have changed once, instead of after every change).

Another speed gain can be obtained through the use of a "symmetry mask" for a mass matrix. All mass matrices are symmetric matrices, but other elements may be equal, or have simple relationships: for example, they may definitely be zero, or one element may always be the negative of another. By attaching a symmetry mask to a mass matrix, such properties can be exploited for a speed increase. This must be done manually: it is probably too risky and unstable to force such properties based on the automatic inspection of the matrix at a "typical" point.

5.3.6 Input and Output

In order that values for the large population of parameters can be read into the program, an input-file-format has been defined. For each parameter, one can specify that it should be set to a particular value, scanned over to allow plots involving parameter-space-scans to be produced, or drawn from a uniform or Gaussian random distribution. A utility program exists to create an input file appropriate for the implementation of the MSSM in EFFECTIVE using SOFTSUSY.

The symbolic simplification of the Lagrangian and calculation of the mass matrices and their derivatives would have to be repeated each time EFFECTIVE were run for a different set of parameter values, were it not for the fact that EFFECTIVE allows for its multiplets and leaves to be saved to and loaded from disk. Each expression is examined recursively to build a list of pointers to things to be saved. The base type contains a virtual method for writing a multiplet or leaf to disk. As the file is read back in, a map from the old pointers to the objects to newly created ones is built up, so that the structures can be re-assembled. Hence, the symbolic part of the calculation need only be performed once for each model, no matter how many parameter space points need to be examined.

The simplified Lagrangian and symbolic tree-level mass-matrices are of interest, and indeed, for some models may be symbolic results never before obtained, and so a human-readable output format for the symbolic expressions and multiplets of EFFECTIVE has been designed, example output being demonstrated in (sec. A.3.1). In addition, for checking and debugging purposes, human-readable lists of the contributions from each field to the tadpoles and of the mass matrices may be generated.

A method exists to build an output table, suitable for input into analysis or data visualisation software, of the parameters, tree level masses, and effective potential and tadpole contributions. To make this easier to use, the method automatically generates an index, indicating, in a human-readable way, which parameter is in which column in the output file. This method is virtual, and additional outputs, such as the value of certain diagrams (sec. 5.3.7), can be added to the output file by inheriting the appropriate class (sec. A.3.5).

5.3.7 Couplings

When coefficients of products of fields are taken from the Lagrangian, i.e. it is differentiated partially with respect to one or more fields, that part of the result which is independent of any other fields gives, up to combinatoric factors, the coupling between those fields, and the Feynman rule for the corresponding vertex. Thus, an expression for the coupling between a given set of fields may be obtained symbolically using EFFECTIVE. Obtaining the nth partial derivative with respect to many fields involves taking first partial derivatives consecutively. The same differentiations of the Lagrangian would be repeated each time a coupling were required, especially when cycling over all possible couplings, such as the two-point couplings constituting the mass matrix. Thus, the results of these differentiations are stored in a "CouplingDatabase". The method used stores all the coefficients generated as each separate partial derivative is taken, favouring speed over storage space. (Although the objects representing the expressions are space-efficient anyway, using pointers almost everywhere.) By sorting the fields into an arbitrary order before obtaining a coupling, this routine is made faster.

In principle, the symbolic expressions for each coupling could be saved to disk along with the simplified Lagrangian in the saved-model file, however, the coupling database is currently re-generated whenever a model is loaded in, its calculation not taking too long.

The methods of EFFECTIVE return couplings with the extra combinatoric factor of the factorial of the number of identical fields at the vertex included, as is correct for obtaining mass matrices. (Witness the factor of 3 in one of the gauge terms in the MSSM neutral CP-even Higgs mass matrix: this comes from 4! arising from the scalar-quartic D-term.) Such factors must be divided out where necessary.

The coupling database gives analytic expressions for couplings between interaction (gauge) eigenstates. For couplings between mass eigenstates, the values of such couplings must be rotated. This can be done using the mixing angles, or, for mixing-groups of 3-or-more particles, using appropriate contractions with the orthogonal matrices which diagonalise the mass matrices. The orthogonal matrices are available automatically by interrogating the mass-matrix objects. A method exists within EFFECTIVE to perform the contractions automatically. With a simple function call, the coupling can be obtained between an arbitrary set of mass eigenstates, gauge eigenstates, or a mixture of these. Note that since we work in a system of non-complex real and imaginary field components, we do not need to distinguish between incoming and outgoing fields at these vertices.

5.3.8 Diagrams

Many of the calculations made in the program amount to the evaluation of certain classes of diagram, and the summation of these over all the possible particles flowing in the loops of the diagram. In this category are included the zero-leg diagram corresponding to the effective potential, the one-leg diagrams corresponding to the total tadpole, which must be zero at the minimum of the effective potential, and the two-leg diagrams corresponding to the self-energy corrections to particle masses. In addition, many of the extra data which one might wish to evaluate as observables for a model under consideration can be cast in this fashion: for example, electric and colour electric dipole moments.

The evaluation of the loop-integral for a diagram, and the enumeration of all the possible topologies of diagram which must be evaluated for a given process, are both nontrivial exercises, although software packages capable of these tasks do indeed exist (e.g. [66]). However, for the classes of models addressed in this chapter, these answers are *not model dependent*. The diagrams can usually be cast in terms of the product of a "loop function", (a function only of the propagator masses) and a coupling term (the product of the vertex Feynman rules for each vertex in the diagram). At worst, diagrams can be expressed as a sum of such factorised terms. The component quantities are available automatically in EFFECTIVE: The masses, at whatever level of approximation is desired, can be obtained from the mass-matrix database (sec. 5.3.5), while the couplings can be obtained from the coupling database (sec. 5.3.7). Thus, a base class for diagrams can be defined, allowing the automatic evaluation and summation of such diagrams. To specify a diagram, we derive from the base class and specify the loop-function of the masses, how many vertices there are, and which fields in the diagram meet at each vertex. When a diagram is evaluated, we then specify which actual field in the model is to be associated with which propagator in the diagram. Through the base class, the program can be instructed to sum the diagram over all mass eigenstates in a given mixing group, or over all fields of a given spin.

Now, the results of such diagrams are gauge dependent, for example the Goldstone bosons have zero mass only in the Landau gauge, where the gauge-fixing parameter ξ is zero. The gauge dependence cancels when one calculates proper observables, such as pole masses. When self-energy diagrams are not included in a mass, the answer remains gauge dependent. This is important when comparing the results of diagrams between different sources, since it is often not well explained: the tadpoles in [42], for example, are in the Feynman gauge $\xi = 1$, where the Goldstone bosons have a mass equal to that of the gauge bosons which eat them. In general, the expression for a diagram is dependent both on the gauge and the renormalisation scheme. When converting loop-functions from source-papers for use in EFFECTIVE, one may have to convert: to the Landau gauge, to the DR-bar renormalisation scheme, and to the representation where real- and imaginary- component fields are treated separately.

5.3.9 The One-Loop Effective Potential

The supertrace formula, eq. (1.31), for the effective potential arises from the simplest possible one-loop diagram: a simple single loop with no external legs. This is remarkable, in that this one-loop effect can be evaluated as a sum of functions of eigenmasses, or as a sum of functions of mass matrices, without any reference to the couplings or Feynman rules of the model.

The evaluation of the effective potential in principle allows us to obtain much knowledge of the theory at hand: its extremisation allows us to obtain any vacuum expectation values of the fields. Plotting it will allow us to characterise those extrema, and gain an insight into the structure of the potential, which can help in stabilising any numerical extremisation procedure. Numerical approximations to first derivatives (called finite-difference derivatives (FDDs)) of the effective potential can be used to obtain the tadpole diagrams, while second finite differences produce the self-energy diagrams at zero external momentum, an important contribution to the self-energy correction to particle masses. Again, these results, stemming from FDDs, are independent of any knowledge of the vertex Feynman rules of the model. As we will see, this has allowed some powerful checks on the correctness of the routines and representations used in EFFECTIVE.

Routines in EFFECTIVE allow the effective potential to be evaluated at tree-level and at one-loop, using both the eigenmass approach where we sum over all mass eigenstates in the model, and the mass-matrix approach where the sum is taken over mass mixing groups, and functions of matrices are evaluated using linear algebra libraries.

Routines to evaluate the first- and second- finite difference derivatives of the potential exist, and also of each individual mass-matrix's contribution to the potential. The minimum of the tree-level or one-loop effective potential can be obtained using Powell's method [65], although this is unstable and slow. Thus, to obtain a more useful route to numerical extremisation of the effective potential, the total tadpoles with respect to each external field must be obtained.

Now, the tadpole diagram includes a single coupling: between the mass eigenstate running in the loop, and the gauge eigenstate on the external leg. If loop-functions are specified for scalar, spinor, and vector loops, the total tadpole can be obtained using the diagram class structure. In addition, the total tadpole can also be evaluated using the matrix expression given in the theoretical introduction to this thesis, eq. (1.32). Since this expression depends on the derivative of the mass-matrix, it can be evaluated using explicit derivative-of-mass-matrices obtained symbolically from the tree-level mass matrix entries. The equivalence of these two approaches, and of the first FDD of the effective potential, has been verified for each of the models used to test EFFECTIVE: verifying the diagram and mass- and interaction- eigenstate coupling routines.

Routines are provided in EFFECTIVE to allow the extremisation of the effective potential by zeroing the tadpole, using both the classical Newton's method, and the globally convergent Newton's method of [65]. Since we may often want to solve other equations numerically while simultaneously extremising the potential, for example, when requiring a specific eigenmass to have a given value, facility is provided for this, as well.

5.3.10 One-loop Masses And Self-Energy Diagrams

The square-masses of a group of mixing particles are properly given by the solution of the propagator equation,

$$M^2_{\text{Tree}} + \Pi(p^2) - Ip^2 = 0 \tag{5.1}$$

where $\Pi(p^2)$ is the self-energy matrix, whose elements are the two-external-leg diagrams with the interaction eigenstate on each leg specified by the location in the matrix. I is the identity matrix, while p is the external momentum flowing into these diagrams. Each value of p^2 solving this equation is the square-mass of a mass eigenstate field. The mixing angle describing mixing between the mass eigenstates of m_1^2 and m_2^2 is the appropriate element of the matrix diagonalising $M^2_{\text{Tree}} + \Pi(\frac{m_1^2+m_2^2}{2})$ [67].

Now, in EFFECTIVE, we can obtain $\Pi(p^2)$ using the diagram class (sec. 5.3.8). Again, we can check this using FDDs of the effective potential, which should correspond to $\Pi(0)$, the self energy diagram at zero external momentum (sec. 1.5). This verifies the diagram and coupling routines for a more complicated problem. The diagrams, and their loop-functions, corresponding to these quantities have been obtained for use in EFFECTIVE by translating the results of [42] into the gauge of EFFECTIVE.

However, numerical solution of eq. (5.1) would probably be very slow. Therefore, the following approximate procedure is used: the tree level mass matrices M^2_{Tree} are evaluated. The masses and mixing angles thus obtained are used to evaluate $\Pi(0)$. The eigenvalues of $M^2_{\text{Tree}}+\Pi(0)$ are then used as a better approximation of the mass matrices, and the eigenmasses and mixing angles re-evaluated. Note that tree-level masses were used in the loops when evaluating these masses. This procedure can be iterated at will, so that consistent masses are used in the loops as are obtained as outputs: however, it is found that this matters little (fig. 5.4). So far, only $\Pi(0)$ has been used. How can $\Pi(p^2)$ be used without explicitly solving eq. (5.1)? Let the result of this procedure be labeled

Code	Zero-external momentum correction used?	Number of iterations correction used	Nonzero external momentum?
T	No	0	No
Z1	Yes	1	No
Z2	Yes	2	No
P	Yes	1	Yes
Code	Effective potential	Masses during effective potential minimisation	Masses at final print
TTT	Tree-level	T	T
OTT	One-loop	T	T
OT1	One-loop	T	Z1
OT2	One-loop	T	Z2
OTP	One-loop	T	P
O11	One-loop	Z1	Z1
O1P	One-loop	Z1	P

Table 5.1: The different levels of approximation possible with analyses using EFFECTIVE.

m_0. Then, the eigenvalue at the same position in the ordered string of eigenvalues of $(M^2_{\rm Tree} + \Pi(m_0))$ as m_0 was in the eigenvalues of $(M^2_{\rm Tree} + \Pi(0))$ is used as a better approximation to the true mass. If this procedure were repeated indefinitely, the true solutions of eq. (5.1) would be obtained. Again, for speed, all the mixing angles are obtained from the matrix diagonalising $M^2_{\rm Tree} + \Pi(0)$.

A list of codes for the different levels of approximation which can be used with EFFECTIVE is given in table 5.1. These are used for the figures in this chapter and the next. There are another few points worth making: the "tree-level" values often used here, are not the true tree-level values used by evaluating the tree-level matrices with the VEVs obtained from using the tree-level potential (approximation TTT). Instead, the values of the tree-level matrices obtained when the VEVs minimising the one-loop potential are used (approximation OTT). While not strictly speaking a physically well-defined quantity, these masses are usually closer to the one-loop value than the complete tree-level masses. However, the Goldstone boson masses obtained from such "sort-of-tree-level" mass matrices are *not zero*, indeed, the Goldstone boson masses obtained can

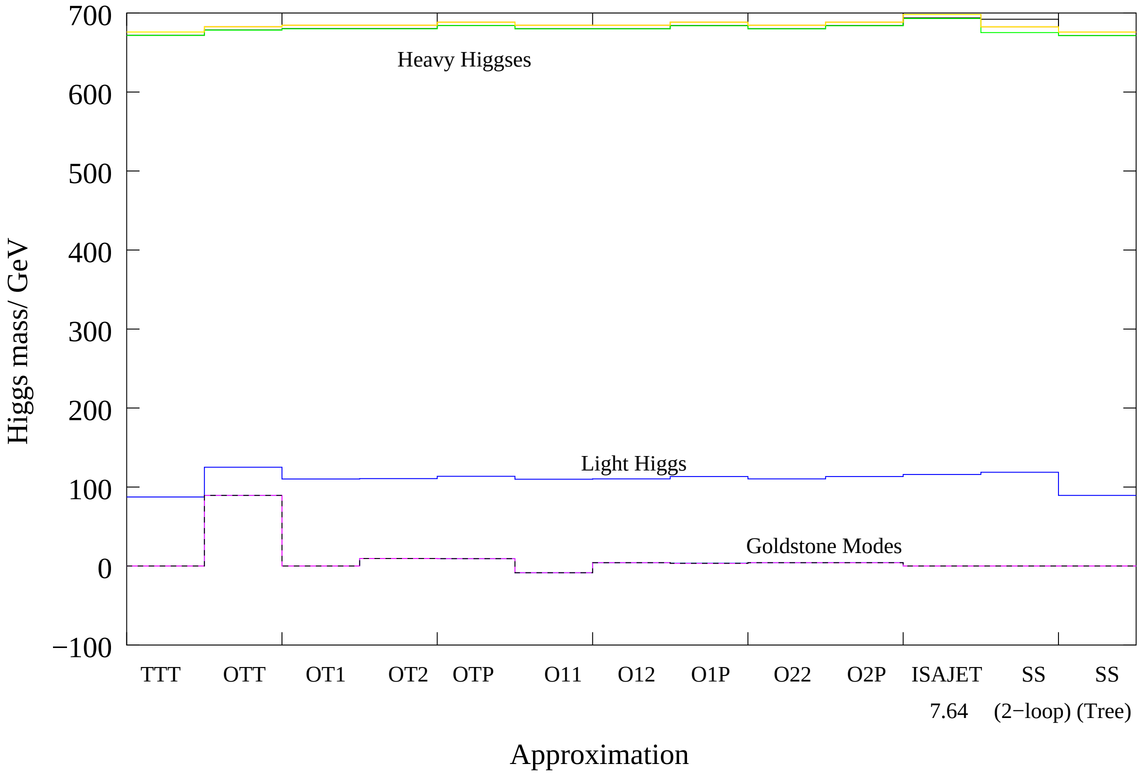

Figure 5.4: The effect of changing the approximations used when obtaining Higgs masses in the MSSM at mSUGRA point II. Negative masses are the negative square root of the absolute value of the small negative mass-squareds which sometimes arise for Goldstone boson masses. The codes indicate the approximation used according to table (table 5.1). The final two columns, marked SS, show the results according to SOFTSUSY. Results using ISAJET 7.64 are also presented.

be of order M_{SUSY}. The masses obtained after inclusion of $\Pi(0)$, however, are indeed almost zero (4.5×10^{-2} GeV at mSUGRA point II). (As they must be: this is Goldstone's theorem at its most basic, in terms of the properties of second differentials of potential surfaces.)

Note that $\Pi(0)$ has an infrared singularity- if a particle of small mass m_χ flows in the loop, the contribution is of order $\ln(m_\chi^2/Q^2)$. The Z1 and Z2 masses are thus not physical but are dependent on a cutoff: the contribution from particles whose mass is below a certain value is removed. In the OT2 approximation, the mass of the charged Higgs boson changes fractionally by 1.3×10^{-5} when the contribution from the Goldstone bosons is switched on or off by the cutoff. (This quantity should be infinity, but, the Goldstone mass does not quite cancel to zero, so the logarithm is not large.) The iterative procedure defined above would eventually produce the correct, cutoff independent masses. Just one step of this procedure, the OTP approximation, reduces the above cutoff dependence by a factor of six, to 2×10^{-6}.

5.3.11 Possible Future Extensions Of EFFECTIVE

As discussed above (sec. 5.1), the primary unsolved problem as regards the complete task of automating the analysis of BSM theories is the deduction of the renormalisation group equations and their inclusion in a numerical procedure to reconcile high-and-low scale boundary conditions. The latter is a relatively trivial programming task, and has been solved many times: for example, using the "drift" method in ISASUGRA and SOFTSUSY (sec. A.2.3), and using the "single-ended shooting method" in a modified version of SOFTSUSY by the present author (sec. A.2.4).

The automatic deduction of the β functions from a computer representation of the Lagrangian, mass matrices, and couplings, such as that of EFFECTIVE, remains to be done. In this section, I present an idea as to how this may be achieved. This has not yet been implemented in EFFECTIVE.

As pointed out in [27], the explicit first derivative of the supertrace expression for the one-loop effective potential, eq. (1.34), allows a general approach to the calculation of the β-functions to be made. Indeed, for the most general set of possible soft mass terms, including non-standard terms, a general renormalisable superpotential, and a general particle content and gauge group, the result of such a calculation, at one loop, is presented in the same reference. This could be coded for SOFTSUSY, with the relevant soft mass parameters being picked out of the Lagrangian by the coupling routine.

An alternative approach, however, would be to implement numerically the matrix equation of eq. (1.34). The various derivatives of the tree-level potential occurring as coefficients of β-functions and anomalous dimensions on the left hand side of the equation can be obtained directly from the coupling database, while the product of tree-level mass matrices on the right hand side could also be made symbolically: the routine to symbolically obtain the square of a mass matrix has already been written, for use in obtaining the symbolic tree-level mass-squared matrix for a spinor field. To obtain the β-functions, we then construct the left-hand side of the equation using symbolic dummy-fields for the β-functions and anomalous dimensions. We then compare coefficients of various groups of fields left and right, to obtain symbolically a set of simultaneous equations for the β-functions and anomalous dimensions. This part of the procedure would probably be the most complicated to code. Finally, these equations can be solved numerically by a matrix decomposition method for a given set of parameter values to obtain the β-functions. This would allow the β-functions to be obtained for a general model, independent of the choice of renormalisable, soft terms made in [27]. For most models, the method of the previous paragraph would, however, be sufficient, and the two results could be compared as a verification.

Chapter 6

Results Of Some Calculations Using EFFECTIVE

This chapter demonstrates the usefulness and accuracy of EFFECTIVE, by presenting reproductions of known calculations using the methods, assumptions, and approximations of the present chapter. We consider in turn the properties of the standard MSSM, its extension to include explicit CP violation through the trilinear A parameters, and its extension to include R-parity violating parameters and expectation values.

6.1 Comparison Of Results With SOFTSUSY and ISASUGRA

Figures (fig. 5.4) and (fig. 6.1) show how the Higgs boson masses obtained using EFFECTIVE compare with those of SOFTSUSY and ISASUGRA, again using a variety of approximations. We see that good agreement is obtained, with the inclusion of the one-loop zero-external-momentum self-energy being particularly important for obtaining the correct result for the light Higgs boson. Disagreement with SOFTSUSY is of the order a few GeV, due to the presence of full two-loop corrections in SOFTSUSY, and also due to the correct (recursive) use in SOFTSUSY of the pole masses deduced for the external momenta in the self energy diagrams. Note that the tree-level results are fully consistent, confirming EFFECTIVE's symbolic calculation of the tree-level mass matrices. Similar discrepancies are found with respect to ISAJET 7.64. SOFTSUSY shows, with loop corrections included, a large mass splitting between the heavy CP-even and CP-odd Higgs states, while ISAJET 7.64 and EFFECTIVE (and, at tree-level, SOFTSUSY) agree that this splitting is small. It is now believed, after consultation with the author of SOFTSUSY, that it is SOFTSUSY that is inaccurate in this regard. As discussed above (sec. 5.3.10), for speed, we use only the first step of the recursive procedure in defining the "P" approximation of EFFECTIVE.

6.2 Explicit CP Violation In The MSSM

In [68], the results of an analysis of the properties of the MSSM with explicit CP-violation in the form of a complex third-family trilinear term are presented: The properties of the Higgs bosons in an effective two-Higgs-doublet model at scale M_Z are calculated. In that analysis, the superparticles have a common mass scale M_{SUSY}, and CP-violating effects are transmitted to the effective theory through the renormalisation group. Along with other variables, results for the electron electric dipole moment (EDM) and for the effective CP violating parameter $g^{P/S}$ are presented:

$$\begin{aligned} g_S &= g_S(e,e,h) \\ &= g(\Re(e),\Re(e),h). \\ g_P &= g_P(e,e,h) \end{aligned}$$

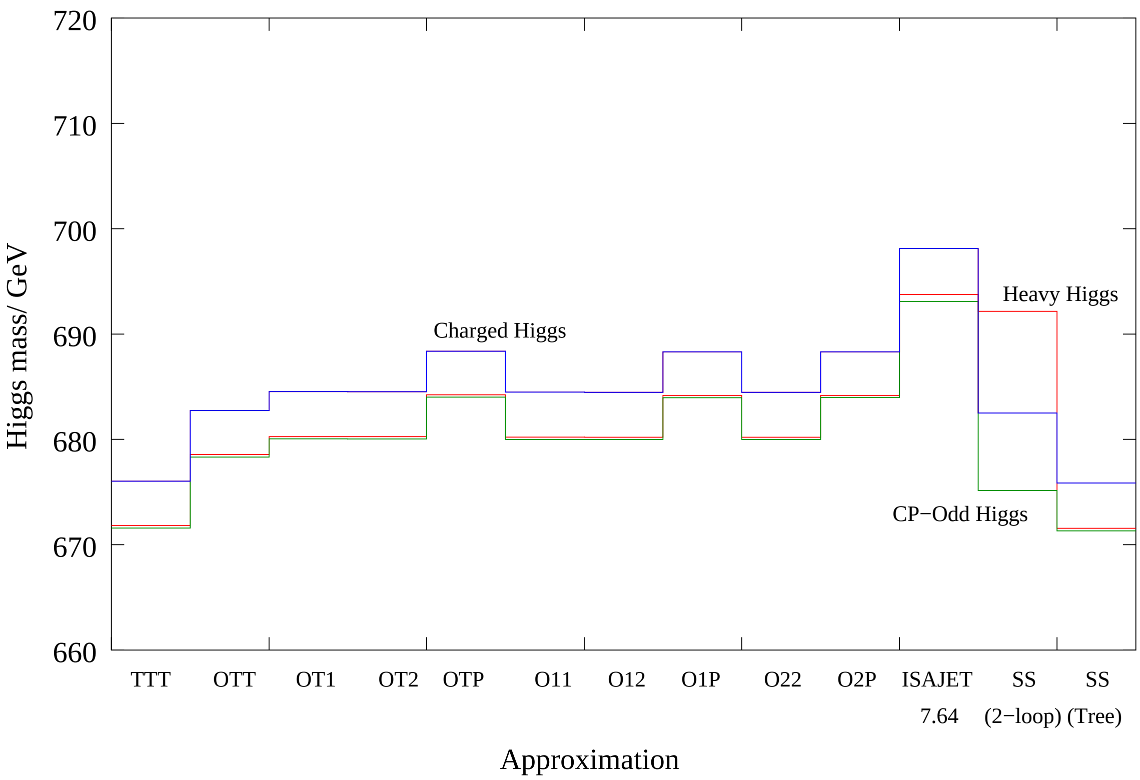

Figure 6.1: The effect of changing the approximations used when obtaining Higgs masses in the MSSM at mSUGRA point II. The codes indicate the approximation used according to table (table 5.1). Here, we zoom in on the heavy Higgs bosons, where, when the loop corrections are included, discrepancy between SOFTSUSY and EFFECTIVE at the level of a few GeV is revealed. Results using ISAJET 7.64 are also presented. The final two columns, marked SS, show the results according to SOFTSUSY.

$$
\begin{aligned}
&= g(\Re(e), \Im(e), h). \\
g^{P/S} &= 2g_S g_P/(g_S^2 + g_P^2) \\
&= g_P/g_S \text{ given } g_P \ll g_S. \qquad (6.1)
\end{aligned}
$$

Here g^S is the scalar, and g^P the pseudoscalar, coupling between the electron and the lightest (CP-mixed) Higgs boson. In the real/imaginary representation of EFFECTIVE, these correspond to the real-real, and real-imaginary couplings, respectively.

I present here the results of a calculation corresponding to, and a comparison with the results of, [68]. For the EFFECTIVE results, the entire analysis was carried out at M_{SUSY}, so the couplings are somewhat altered by the lack of renormalisation group running. The results of [68] depend on the neglect of the chargino and neutralino contributions to the tadpole, so that an accidental symmetry means any CP violating phase in the Higgs VEV induced by minimising the effective potential can be rotated into the definition of the phase of the μ-parameter. Since I make no such approximation, we should use, for comparison with [68], as the horizontal axis the total equivalent CP violating parameter of that paper: $(\arg A + \arg v + \arg \mu)$. However, the effect of this change is small.

In addition, the closed expressions used in [68] allow the authors to take the mass of the charged Higgs boson as an input parameter. With EFFECTIVE, this is done by solving for the mass to have the required value, simultaneously with the minimisation of the potential. For speed, the OTP approximation of (table 5.1) is used, with the exception that the Z1 approximation for the charged Higgs mass is used during the minimisation, as that is the mass taken as an input parameter.

The results for the EDM, calculated for EFFECTIVE by entering the dominant Barr-Zee diagram using the diagram class structure of EFFECTIVE, show that the EDM is below the experimental bound, of about 10×10^{-27} e cm except where the lightest Higgs mass drops below experimental bounds. Indeed, we note that, as in chapter 4, for large values of the parameter controlling the deviation from the usual MSSM, (without CP violation), the conventional potential minimum becomes a saddle point. The magnitude of the EDM is larger than that calculated in [68], where the result is 5.5×10^{-27} e cm at $\arg A = \pi/2$. (Results are presented there only for $\arg A = \pi/2$.) The difference is explained thus: In [68], as discussed above, there is no Higgs mixing, and the EDM is calculated using the couplings of the A Higgs, which remains a mass eigenstate. When the full set of corrections is used, it emerges that the contribution of the light Higgs boson, which now contains some CP violating character, is significant, especially as its mass becomes small. When the effect of the light Higgs is excluded, the result agrees with [68]. (Using an input M_{H^+} such that $M_{A^0} \approx 150$ GeV, consistent with the mass chosen in [68].) This last result acts as a confirmation of the correct implementation of the "diagram" structures of EFFECTIVE. The largest contribution to the EDM, expect when the light Higgs boson mass is very small, comes from the "would-be" CP-odd state, i.e. the state which becomes CP-odd in the absence of CP-violation.

The result for $g^{P/S}$ are qualitatively consistent with those of [68]. The amount of CP violation is larger in my analysis, again because the mechanism of CP violation through Higgs mixing is fully calculated. Note the existence of a zero in $g^{P/S}$ for non-zero $\arg A$. Note that full consistency between these results is not expected, as they are running quantities calculated at different scales.

6.3 R-parity Violation In The MSSM

The symbolic calculation of the tadpole for the R-parity violating MSSM is complicated: in principle, all the sneutrinos can get VEVs, and a large number of R-parity violating parameters could be nonzero. R-parity violation means the sets of mixing particles

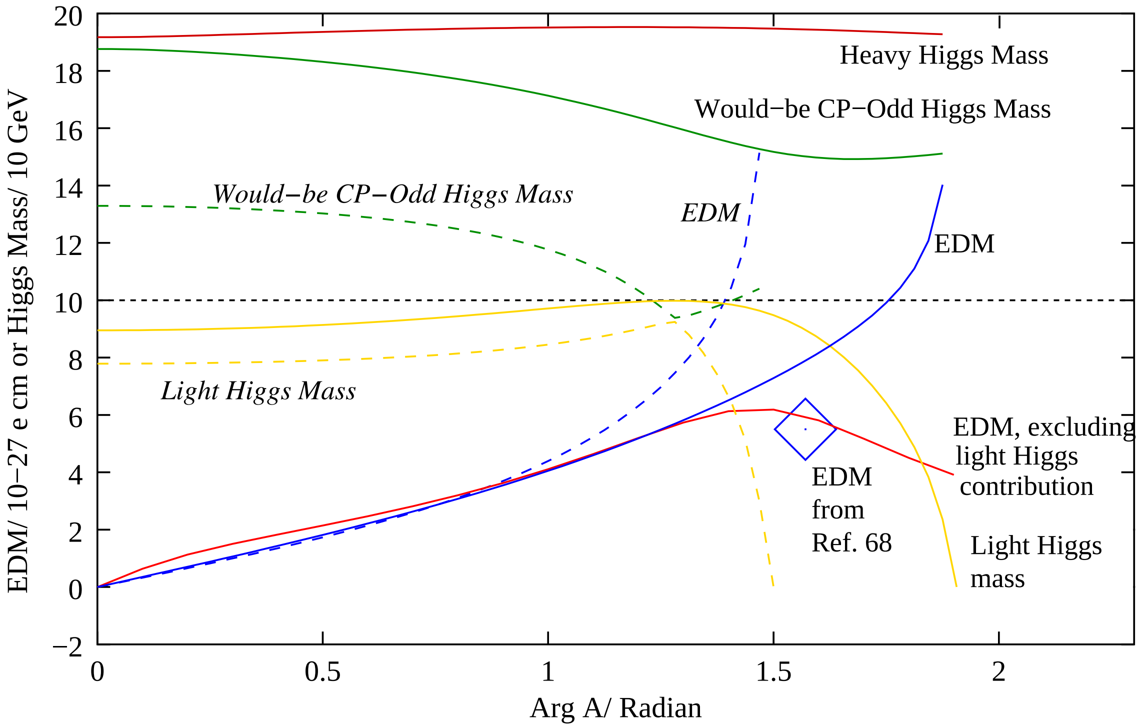

Figure 6.2: The results for the electron EDM in the CP violating MSSM calculated using EFFECTIVE, and the Higgs boson masses. These were calculated for $M_{SUSY} = 500$ GeV, $\tan\beta = 4$, and a charged Higgs boson mass of 150 GeV (dotted curves, italic labels) or 200 GeV (solid curves, roman labels). The result obtained from [68] was calculated for a fixed "would-be" CP-odd Higgs boson mass of 150 GeV, which is not a mass eigenstate in my analysis. The choice of $M_{H^+} = 200$ GeV results in $M_{A^0} \approx$ 150 GeV close to $\arg A = \pi/2$. Also shown is the approximate experimental upper bound on the EDM, at 10×10^{-27} e cm.

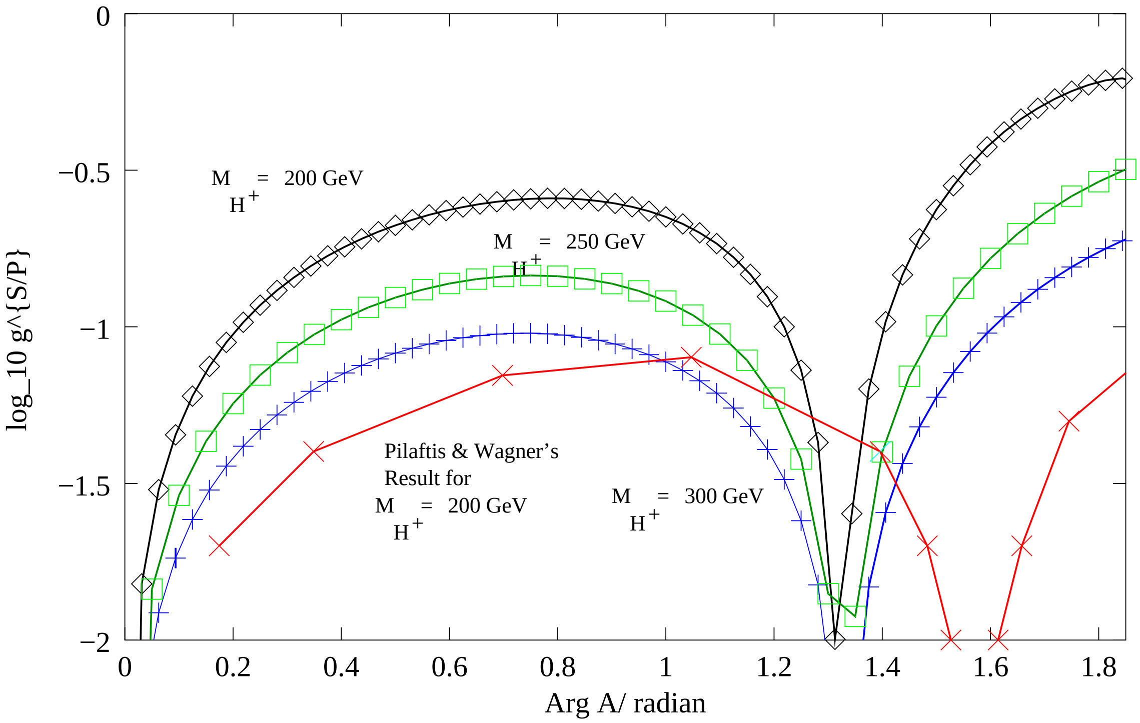

Figure 6.3: The results for $g^{P/S}$, as defined in the text, for the CP violating MSSM, calculated using EFFECTIVE, and in [68]. These were calculated for $M_{SUSY} = 500$ GeV, $\tan\beta = 4$, and a charged Higgs boson mass of 250 GeV.

become ever larger. This, however, is no problem for EFFECTIVE, which can handle arbitrarily many VEVs and arbitrarily large mixing-groups. I present here some results for the lepton-number violating R-parity violating MSSM, where the R-parity violation is, in the reparameterisation used, restricted to the third-family B parameter and third sneutrino VEV. These results are compared with those of [24], which also studies this case.

For this model, $\tan\beta$, the masses of the two CP-odd scalar bosons, (Mixtures of the A-Higgs and the imaginary part of the third family sneutrino) and the angle between the VEV and B vectors are taken as input parameters. The third-family sneutrino VEV is allowed to vary in order to zero the tadpoles, as are the third family neutrino and Higgs soft mass terms. The other soft mass terms, μ, and the trilinear terms are also taken as input parameters. The neutral CP-even Higgs mass matrix now includes the real third family sneutrino. There are thus two light Higgs bosons, which (due to the choice of input parameters) are approximately degenerate for zero R-parity violation. As the R-parity violating parameter (δ_R, which is the square of the sine function of the R-parity violating angle) is increased, the two light Higgs bosons are driven apart (fig. 6.4). δ_R is defined thus, in the conventional basis of the Higgs and τ-neutrino eigenstates:

$$\delta_R = 1 - \frac{<\nu_\tau> B_{H_2\nu_\tau} + <H_1> B_{H_1H_2}}{\sqrt{(<H_1>^2 + <\nu_\tau>^2)(B^2_{H_2\nu_\tau} + B^2_{H_1H_2})}} \tag{6.2}$$

The same result was found in [24], except that in this analysis, we obtain a greater state-repulsion effect because the unperturbed mass matrix has a smaller mass difference in our approximation. We take the Z1 approximation CP-odd masses as inputs, not the tree-level values as in [24]. Note also, that in [24] no value for the gaugino soft masses is specified, as the contribution of the particles affected by this parameter is neglected. My results show that the effect of changing these parameters is indeed small (fig. 6.4).

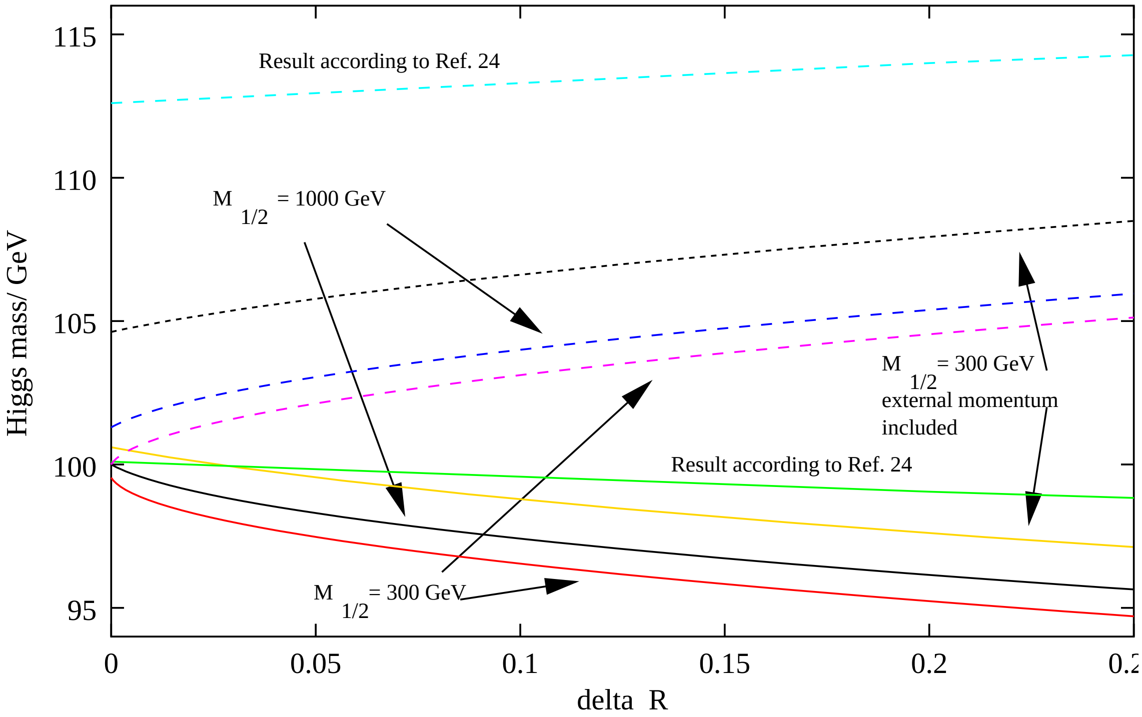

Figure 6.4: The two lightest neutral CP-even Higgs/tau sneutrino boson masses in the R-parity violating MSSM. The square of the sine of the R-parity violating angle between the VEV and B parameter vectors, δ_R is the horizontal axis. The parameters chosen were: $\tan\beta = 10$, $\mu = 200$ GeV, $m_0(\text{Left}) = 500$ GeV $m_0(\text{Right}) = M_{1/2} = 300$ GeV, $A^U_{3,3} = A^D_{3,3} = 200$ GeV, $A^E_{3,3} = 20$ GeV, and the 1-loop (Z1 approximation) masses for the CP-odd Higgs/sneutrino bosons were set at 100 GeV and 300 GeV. The results of [24] are presented for comparison. Also shown are the results for $M_{1/2} = 1.0$ TeV, and the results for $M_{1/2} = 300$ GeV in the P approximation. The solid curves are the mass of the lightest Higgs state, the dotted curves the second lightest state.

6.4 Conclusions

We have seen that it is possible to build a consistent software framework within which one can analyse particle physics models, up to the point where parameters are entered into an event simulation. This allows abstraction of the analysis into three sections: aspects which can be performed automatically (e.g. the use of the mass matrices to obtain the effective potential), calculations which need be made once (e.g. the evaluation of the loop-function for a given diagram), and aspects which must be considered once per model (e.g. the choice of input parameter set). The obvious labour-saving advantages are considerable, as witness the ability of a physicist equipped with EFFECTIVE to consider a new model with the minimum of work. However, there is a further important advantage to the approach used here. As seen in previously in chapter 4, regarding non-standard symmetry breaking there is considerable advantage to adopting a consistent methodology across different models, in order to facilitate their comparison. The use of a tool such as EFFECTIVE enforces this approach. Contrast the technique used in many of the papers cited in this thesis: for each different model, a different clever approximation is made, maximising the degree to which symbolic results can be obtained for each model, but reducing the consistency and comparability of the results obtained.

Conclusions

While the separate results and conclusions of each element of my research have each been presented in their own chapters, it is proper to sum up here how I believe consideration of the work of this thesis should affect one's view of particle physics.

Simplifying assumptions are the true core of physics. The art of simplification, the "spherical horse rolling on a frictionless racetrack", is what we do. But, we must not forget where we have simplified, and we must not be afraid to return again to analyses where results were obtained using simplifications, and try again. The parameter space of the MSSM really is as large as a hundred or so parameters. The effect of non-leading terms can be large. The universe may not lie in the subspace of tractable problems. If the art of simplification cannot solve our problems, we must turn to our other great labour-saving device: the computer. If nature sneers at the difficulty of integration, computers at least sneer at the difficulty of multiplication: some problems are enormous in size, yet simple in nature. This is how EFFECTIVE works: the Lagrangian, expressed in terms of component fields, may be a huge expression, but a computer *does not care.*

Computer calculations represent an ever-growing and increasingly important part of theoretical physics. This aspect of physics can be at least as nontrivial as analytical work: Evidence for this ranges from the version-number dependence of the REWSB exclusion region in ISASUGRA, to the difficulties of working with legacy code such as GETJET, the instabilities of the "shooting-method" in NSSB studies with SOFTSUSY, to the subtleties of implementing the structure of physical objects in EFFECTIVE. As a new period of comparison with data approaches with the building of the LHC, and with the huge amount of effort now being invested in software tools on the experimental side, we must be sure that the theoretical community is not left behind. We need to be able to obtain results as needed; quickly and comparably regarding new models as they are suggested, and accurately when necessary, so that theoretical uncertainties are comparable with the experimental errors. Robust, accurate, fast, trustworthy, consistent and full-featured software is, I believe, essential for the future of the field.

Appendix A

Appendices

A.1 Renormalisation Group Equations

The 1-loop three family β-functions for the MSSM are presented below, in the reparameterisation where $\mu = 0$, with family, colour and electroweak indices suppressed. The convention for the β-functions of ref. [46] is used, i.e.:

$$\beta_x = \frac{dx}{d(\ln Q)}, \tag{A.1}$$

where Q is the renormalisation scale.

Note that for the β-functions of the scalar masses, only the additional contribution from the non-standard terms is given. These should be added to the expressions given in [46], which is denoted as β^{MSSM}. The β^{MSSM} in SOFTSUSY include some two-loop terms. For β-functions not given below, the NSSB couplings do not contribute, and the results of [46] may be used.

$$\begin{aligned}
16\pi^2\beta_{C^u} &= 3\mathrm{Tr}(Y^dY^{d\dagger})C^u + \mathrm{Tr}(Y^eY^{e\dagger})C^u + 2C^uY^{u\dagger}Y^u + Y^uY^{u\dagger}C^u \\
&\quad +6Y^u\mathrm{Tr}(C^uY^{u\dagger}) + 3Y^dY^{d\dagger}C^u + 2C^dY^{d\dagger}Y^u, \\
&\quad -C^u(\frac{4}{9}g'^2 + \frac{16}{3}g_3^2) - 4\tilde{\mu}Y^dY^{d\dagger}Y^u - 2\tilde{\mu}Y^u(g'^2 + 3g_2^2), \qquad \text{(A.2)} \\
16\pi^2\beta_{C^d} &= 3\mathrm{Tr}(Y^uY^{u\dagger})C^d + 2C^dY^{d\dagger}Y^d + Y^dY^{d\dagger}C^d \\
&\quad +6Y^d\mathrm{Tr}(C^dY^{d\dagger}) + 3Y^uY^{u\dagger}C^d + 2C^uY^{u\dagger}Y^d + 2Y^d\mathrm{Tr}(C^eY^{e\dagger}), \\
&\quad +C^d(\frac{2}{9}g'^2 - \frac{16}{3}g_3^2) - 4\tilde{\mu}Y^uY^{u\dagger}Y^d - 2\tilde{\mu}Y^d(g'^2 + 3g_2^2), \qquad \text{(A.3)} \\
16\pi^2\beta_{C^e} &= 3\mathrm{Tr}(Y^uY^{u\dagger})C^e + 2C^eY^{e\dagger}Y^e + Y^eY^{e\dagger}C^e \\
&\quad +2Y^e\mathrm{Tr}(C^eY^{e\dagger}) + 6Y^e\mathrm{Tr}(C^dY^{d\dagger}) \\
&\quad -2C^eg'^2 - 2\tilde{\mu}Y^e(g'^2 + 3g_2^2) \qquad \text{(A.4)} \\
16\pi^2\beta_{m^2_{H_1}} &= 16\pi^2\beta^{MSSM}_{m^2_{H_1}} + 6\mathrm{Tr}(C^uC^{u\dagger}) - (6g_2^2 + 2g'^2)\tilde{\mu}^2, \qquad \text{(A.5)} \\
16\pi^2\beta_{m^2_{H_2}} &= 16\pi^2\beta^{MSSM}_{m^2_{H_2}} + 6\mathrm{Tr}(C^dC^{d\dagger}) + 2\mathrm{Tr}(C^eC^{e\dagger}) - (6g_2^2 + 2g'^2)\tilde{\mu}^2, \qquad \text{(A.6)} \\
16\pi^2\beta_{m^2_{\tilde{q}_L}} &= 16\pi^2\beta^{MSSM}_{m^2_{\tilde{q}_L}} + 2(C^uC^{u\dagger} + C^dC^{d\dagger}) - 4\tilde{\mu}^2(Y^uY^{u\dagger} + Y^dY^{d\dagger}), \qquad \text{(A.7)} \\
16\pi^2\beta_{m^2_{\tilde{l}_L}} &= 16\pi^2\beta^{MSSM}_{m^2_{\tilde{l}_L}} + 2C^eC^{e\dagger} - 4\tilde{\mu}^2Y^eY^{e\dagger}, \qquad \text{(A.8)} \\
16\pi^2\beta_{m^2_{\tilde{u}_R}} &= 16\pi^2\beta^{MSSM}_{m^2_{\tilde{u}_R}} + 4C^{u\dagger}C^u - 8\tilde{\mu}^2Y^{u\dagger}Y^u, \qquad \text{(A.9)} \\
16\pi^2\beta_{m^2_{\tilde{d}_R}} &= 16\pi^2\beta^{MSSM}_{m^2_{\tilde{d}_R}} + 4C^{d\dagger}C^d - 8\tilde{\mu}^2Y^{d\dagger}Y^d, \qquad \text{(A.10)} \\
16\pi^2\beta_{m^2_{\tilde{e}_R}} &= 16\pi^2\beta^{MSSM}_{m^2_{\tilde{e}_R}} + 4C^{e\dagger}C^e - 8\tilde{\mu}^2Y^{e\dagger}Y^e, \qquad \text{(A.11)} \\
16\pi^2\beta_B &= \frac{2}{\tilde{\mu}}\mathrm{Tr}(3C^{u\dagger}A_u + 3C^{d\dagger}A_d + C^{e\dagger}A_e) + 2g'^2M_1 + 6g_2^2M_2, \qquad \text{(A.12)} \\
16\pi^2\beta_{\tilde{\mu}} &= \tilde{\mu}\mathrm{Tr}(3Y^uY^{u\dagger} + 3Y^dY^{d\dagger} + Y^eY^{e\dagger}) - \tilde{\mu}(g'^2 + 3g_2^2). \qquad \text{(A.13)}
\end{aligned}$$

A.2 Numerical methods

A.2.1 Introduction

The numerical methods used in this paper may be formally described as follows, where for clarity we note what each general variable corresponds to in our SUSY case. Let the boundary conditions at scale $x = M_X$ be

$$f(p(x)) = 0. \tag{A.14}$$

This equation corresponds to the mSUGRA boundary conditions, e.g. $m_q^2 = m_0^2$ and $p(x)$ corresponds to m_0, $M_{1/2}$, etc. Let the boundary conditions at scale z ($= M_Z$ and/or M_S) be

$$g(q(z)) = 0. \tag{A.15}$$

This condition corresponds to the physical values of the Yukawa couplings, (h_t etc.), the gauge couplings, and the REWSB condition (which constrains μ and B). The full set of parameters for the model is $\{p(t), q(t)\}$, with $p(t)$ constrained at $t = x$ and $q(t)$ constrained at $t = z$. Let q_C be the q solving eq. (A.15) and let p_C be the p which solves eq. (A.14). The differential equations (renormalisation group equations) then relate the parameters at the two scales:

$$\begin{aligned} q(z) &= R^q(q(x), p(x)) \\ p(z) &= R^p(q(x), p(x)). \end{aligned} \tag{A.16}$$

A.2.2 The Shooting Method

For a given $q(x)$, i.e. $\mu, B, Y^f \tan\beta$, and $g_{1,2,3}$, at M_X, therefore, $g(q(z))$ can be calculated numerically through R^q. The solution of the boundary value problem therefore reduces to the numerical solution of the algebraic equation $g(R^q(q(x), p_C)) = 0$ for $q(x)$. This is the "shooting method" of [65].

The shooting method cannot, however, be used for SUSY. Firstly, we have three scales at which boundary conditions are imposed: M_Z, M_S and M_X. Secondly, the boundary conditions at M_Z and M_S cannot be conveniently expressed in the form of eq. (A.15).

A.2.3 The Drift Method

In most implementations of the shooting method for SUSY, an alternative technique, which can be called the "drift method", is used: Start with a guess, q^g, for $q(x)$, i.e. $\mu(M_X)$ etc, and determine $p(x)$ from eq. (A.14). Determine $q(z)$ and $p(z)$ from eq. (A.16), the renormalisation group equations. Impose eq. (A.15) to re-determine $q(z)$. (Set the Yukawa matrices and gauge couplings from experimental data and set μ and B from the REWSB constraints.) Use the inversion of eq. (A.16), i.e. run back up to high scale, to find new values for $q(x)$ and $p(x)$, $q'(x)$ and $p'(x)$ respectively. This corresponds to a recurrence relation $q'(x) = Q(q^g)$. Alternatively, the same procedure can be applied with a guess p^g for $p(z)$, i.e. the soft breaking parameters at M_Z, and a recurrence relation for $p(z)$.

The required values for p, q consistent with both sets of boundary conditions will be a fixed point of Q. We can hopefully determine this fixed point by making a guess for $q(x)$ and iterating the procedure until it is convergent, i.e. hoping the recurrence relation will drift to the fixed point we want. Convergence is tested for by requiring q

and p not to change over a cycle. However, note that the fixed point corresponding to the physical solution is not guaranteed to be the only fixed point, nor is it guaranteed to be stable.

A.2.4 The Single-Ended Shooting Method

When the required fixed point of Q becomes unstable, and/or the drift method drifts into a different fixed point of Q, a different approach can be used. The equation:

$$Q(q^g) - q^g = 0 \tag{A.17}$$

can be solved for q^g. In this work, the Newton-Raphson method was used to solve this equation. This has improved stability, but is not perfect, because any unrequired fixed points of Q will also correspond to roots of eq. (A.17). The method can be slow, but, if an approximate solution only is desired, one can just take initial guesses for the less important parts of q^g such as Y^e, rather than solving for them, making the method faster by reducing the parameter space to be solved.

The procedure used to generate q' also generates $p' = P(q^g)$. For q^g consistent with both sets of boundary conditions (and therefore a solution of eq. (A.17)), $p' = p_C$, and therefore $f(p') = 0$. This provides a check that one has found the desired root.

One might imagine that the boundary value problem can be reduced to the numerical solution of the algebraic equation $P(q^g) - p_C = 0$, but this turns out to be unstable: formally, it is overconstrained (there being more elements in p than in q for SUSY), but many of the constraint equations are approximately degenerate.

A.3 Examples Of How To Use EFFECTIVE

In this appendix, I give some examples of how models are built up and analyses conducted using EFFECTIVE. It is hoped that the names of the methods referred to in this section are self-explanatory with regard to their function. For more information, refer to the header files in the EFFECTIVE sourcecode (available from the author on request).

A.3.1 A Simple Example

In order to use SOFTSUSY, one must derive from the base `Model` or `LoaderModel` class to define the model you wish to work with. Derive from `Model` when creating a new model, in order to save the symbolic parts of the calculation to disk. Then, derive from `LoaderModel` to specify additional output data when making a parameter space scan. The default `LoaderModel` may be used for a standard output dataset consisting of the parameters, tadpole and effective potential contributions, and tree-level masses.

As a brief introductory example of the use of SOFTSUSY, in this section I present the user-written code necessary to build and use a simplified version of the MSSM.

First, the header file defining the class as a derived class of `Model`.

```
class SusyTestTwo : public Model
{
protected:
void AddGaugeFactors();
void AddMatterRepresentations();
void AddOtherInteractions();
Expression * Superpotential();
```

```
public:
SusyTestTwo():Model("STT.inp","STT.sav"){IndirectedConstructor();}
virtual ~SusyTestTwo();
};
```

Note the arguments passed to the Model constructor, the names of the parameter-input file and the saved-model file to be used.

Next, specification of the gauge factors and matter representations.

```
void SusyTestTwo::AddGaugeFactors()
{
VectorSmultiplet *v = new VectorSmultiplet;
AddFactor(new SU2Factor("WBoson",v));
AddFactor(new U1Factor("BBoson",v));
};
void SusyTestTwo::AddGaugeCouplings()
{
Model::AddGaugeCouplings();
};
void SusyTestTwo::AddMatterRepresentations()
{
LorentzSymmetry * w = new LeftChiralSmultiplet;
GaugeRepresentation * SU2LL =
new SU2Fundamental(GetFactor("WBoson"),w,"SU2LeptonL");
GaugeRepresentation *ERB =
new U1Fundamental(GetFactor("BBoson"),w,"ElectronRB",1);
GaugeRepresentation *U1LL =
new U1Fundamental(GetFactor("BBoson"),w,"U1LeptonL",2);
```

```
GaugeRepresentation * U1H =
new U1Fundamental(GetFactor("BBoson"),w,"U1Higgs",2);
GaugeRepresentation * SU2H =
new SU2Fundamental(GetFactor("WBoson"),w,"SU2Higgs");
GaugeRepresentation * U1H2 =
new U1Fundamental(GetFactor("BBoson"),w,"U1Higgs2",-2);
GaugeRepresentation * SU2H2 =
new SU2Fundamental(GetFactor("WBoson"),w,"SU2Higgs2");
AddRep(new CompoundGaugeRepresentation(U1H2,SU2H2,w,"Higgs2",
"Upper Scalar Real "));
AddRep(new CompoundGaugeRepresentation(U1LL,SU2LL,w,"LeptonL"));
AddRep(ERB);
AddRep(new CompoundGaugeRepresentation(U1H,SU2H,w,"Higgs",
"Lower Scalar Real "));
};
```

Note how fields charged under more than one gauge factor are specified using the `CompoundGaugeRepresentation` class, and how the `LeftChiralSmultiplet`, `w`, is used to specify that the fields being constructed are supermultiplet fields: a `WeylSpinorLeft` could be used instead to specify a non-supersymmetric field. Notice also how each representation or gauge factor is added to the list of fields in the model using `AddRep(GaugeRepresentation *)` or `AddFactor(GaugeFactor *)`. Utility functions to assist in the creation of models with a 3-family structure have been created: if an extra argument of '3' is passed as a final argument to the `GaugeRepresentation` constructor, a family multiplet field is created. The three is a mnemonic for the number of fields in a family, the parameter is not yet implemented to specify a general family size, although the RPV definition file introduces four-member families needed to express the Higgsino as part of a family of leptons (sec. 1.3.1).

The final argument `"Lower Scalar Real "` tells the program that this component field will have a vaccuum expectation value and may be a field whose classical value may be an argument of the effective potential.

The code specifying the superpotential for this model is given above (sec. 5.3.4).

In addition, one must specify the soft supersymmetry breaking terms, in `SusyTestTwo::AddOtherInteractions()` for example, the "B" term of the simple SUSY model under discussion is defined thus:

```
Expression * BTerm = new Expression(new Product());
Parameter *m3 = new Parameter;
m3->SetName("m3_or_muB");
AddParameter(m3);
BTerm->PushBack(m3->Copy());
BTerm->PushBack(GetRep("Higgs")->ShowField(DBoson));
BTerm->PushBack(GetRep("Higgs2")->ShowField(DBoson));
IncrementLagrangian(BTerm());
```

In order to generate the Saved-Model file "`STT.sav`", it is necessary to create an executable file creating the model:

```
SusyTestTwo m; // Create a SusyTestTwo model.
m.ScanParameterFile(); // Read in some parameter values:
      //  scan from ‘‘STT.inp’’ file
      //  specified in the constructor for SusyTestTwo.
m.ShowFieldsWhichBlock(opt); // Print the human-readable list of
      // mixing-groups, in this case onto the
      // output file stream defined as ‘‘opt’’.
m.Save(); // save the result of the symbolic calculation to disk.
```

When the command "`SusyTestTwo m;`" is executed, the model is assembled, and the "`Model::IndirectedConstructor()`" method called by the `SusyTestTwo` constructor symbollically simplifies the Lagrangian and builds the mass matrices and differentiated mass matrices.

The human-readable output generated by the method "`Model::ShowFieldsWhichBlock(ostream &)`" includes the following, showing that the code has correctly determined the fields contributing to the neutralino matrix:

```
Here's a bunch of fields that mix:
WBoson->Three->WeylSpinorLeft
BBoson->WeylSpinorLeft
Higgs->Upper->Real->WeylSpinorLeft
Higgs2->Lower->Real->WeylSpinorLeft
```

It also gives the mass matrices, for example, here is an element of the chargino mass matrix:

```
Mass of Higgs->Lower->Real->WeylSpinorLeft with BBoson->WeylSpinorLeft
An expression which is
{The sum [1] of the following 1 things:
[1]No.0 which is a An expression which is
[The product [1] of the following 3 things:
[1]No.0 which is a Parameter of value 1 labelled BBosonCoupling.
[1]No.1 which is a Field with a Vev of 2 labelled
                         Higgs2->Upper->Real->Scalar.
[1]No.2 which is a Constant of value -2.828.
]
}
```

The numbers in square brackets indicates the number of nested layers of sums or products, counted separately. A separate executable can then be created, to use the result of the symbolic calculation to obtain plottable data regarding the model.

```
ofstream data("Data.opt");
  ofstream index("Index.opt");
LoaderModel m("STT.sav","STT.inp");
m.AddParameterToSolveOver(m.GetParameter("m3_or_muB"));
m.AddParameterToSolveOver(m.GetParameter("Mu"));
m.GeneratePlottableOutput(data,index);
```

The method "`LoaderModel::GeneratePlottableOutput(ostream &, ostream &)`" will repeatedly, for each set of parameters specified in the parameter input file (e.g. "`STT.inp`"), extremise the potential over the specified parameters by zeroing the tadpoles. (Note that one must specify an number of parameters to vary using `Model::AddParameterToSolveOver(Parameter *)` equal to the number of fields in the model with VEVs, so that the solution is not over- or under- constrained). One can specify a different calculation to be performed for each parameter set by deriving `LoaderModel` and overloading the method `DoAnyCalculation()` (sec. A.3.6), which by default just calls the method `SolveForZeroTadpolesByVaryingParameters (ShowParametersToSolveOver(),false);` – the final `false` instructs the program to use the 1-loop, rather than the tree-level, effective potential.

The file "`Index.opt`" contains a human readable list of which column in the output file "`Data.opt`" contains which datum.

We now turn to more detail on certain aspects of using EFFECTIVE.

A.3.2 Listing The Gauge Factors And Matter Representations

The gauge factors are specified in `AddGaugeFactors()`, which is called through `IndirectedConstructor()`. The matter representations are specified in `AddMatterRepresentations`. Note that, it is possible to derive one model from another, and call the base model's `AddMatterRepresentations` from the derived class's method, if one wishes to create a model like the base model, but with a small number of additional fields. A definition file for the NMSSM might use this technique.

The available gauge factors are defined in `GaugeFactors.cpp` and `GaugeFactors.h`, and use the gauge-multiplets defined in `Physicals.cpp` and `Physicals.h`. To make available a new gauge factor, derive a class from the base `GaugeFactor` class, defining the pure virtual functions specifying the generators and structure constants. Create a new gauge multiplet type like those in `Physicals.h`, giving names to the elements of the multiplet. Specify the multiplet type in the `AddMyFactors` method of your derived class. New representation matter types may also be created in the same way.

As an illustration the following shows the construction of the generators of SU(2):

```
Constant *c = new Constant;
Complex *com = new Complex(c);
SU2Doublet *row = new SU2Doublet(com);
SU2Doublet *column = new SU2Doublet(row);
column->ChangeIndex();
SU2Triplet *ans = new SU2Triplet(column);
ans->AllocateTree();
ans->SetTreeName("SU2gens");
DC<Constant *>(ans->Read("One Upper Lower Real "))->Set(0.5);
```

```
DC<Constant*>(ans->Read("One Lower Upper Real "))->Set(0.5);


DC<Constant*>(ans->Read("Two Upper Lower Imaginary "))->Set(-0.5);
DC<Constant*>(ans->Read("Two Lower Upper Imaginary "))->Set(0.5);


DC<Constant*>(ans->Read("Three Upper Upper Real "))->Set(0.5);
DC<Constant*>(ans->Read("Three Lower Lower Real "))->Set(-0.5);
```

A.3.3 Specifying A Superpotential And Other Lagrangian Terms

The examples below illustrate the most important elements regarding this part of defining a model for EFFECTIVE.

```
Parameter * Elyukawa = new Parameter;
Elyukawa->SetName("ElectronYukawa");
Elyukawa->SetValue(1.0);
AddParameter(Elyukawa);
Expression * temp = new Expression(new Product);
temp->PushBack(Elyukawa);
temp->PushBack(GetRep("ElectronRB")->ShowField());
temp->PushBack(GetRep("LeptonL")->ShowField());
temp->PushBack(GetRep("Higgs")->ShowField());
IncrementLagrangian(temp->Simplification());
```

In this example, the various fields are being called for from the list of gauge representations (sec. 5.3.3). The supersymmetric "link-fields" are returned, since the fermionic or bosonic part of the field is not requested (sec. 5.3.4).

Family-matrix parameters such as the Yukawa couplings can be created. Instead of making all elements of the matrix parameters, we make only the elements we wish to be non-zero into parameters: this keeps the symbolic calculation fast, since constants of value zero are simplified away, while parameters of value zero are not, since they may later be changed. The texture of zeros in, for example, the Yukawa matrix, then makes the simplifed Lagrangian smaller. The `Morph` method is used to replace one of the constants with a parameter. Note also the `AllocateTree()` method: the constructors used to build up the matrix just set the multiplet-types of the first element of each multiplet, so `AllocateTree()` is used to build storage for the other elements: the default old elements need then be `delete`d. To create a matrix parameter, use the following code as an example:

```
Constant* nc = new Constant;
PhysicalMultiplet * f1 = new Family(nc);
PhysicalMultiplet * ans = new Family(f1);
Base * temp = ans->First();
ans->AllocateTree();
delete temp;
Parameter* tp = new Parameter;
tp->Morph(ans->ReadLoc("Top Top"));
AddParameter(ans->Read("Top Top"));
ans->SetTreeName(treename);
```

Methods to quickly create Family-matrices with defined-to-be-zero off diagonal elements exist: `NewFamilyDiagonalParameter` or `NewComplexFamilyDiagonalParameter`.

A.3.4 The Parameter-Input-File Format

The input file format is based on the idea of a "scan-hierarchy", to control which parameter is varied "most-significantly" and which "least significantly" in a scan.

The commands have the format:

```
Parameter-Name Command-Name Arguments
```

Available commands and their syntaxes are:

```
SET value
SCAN hierarchy-number start end number
RANDOM type <further-arguments>
```

The arguments for the random command depend on the value of `type`:

```
type==1 mean
type==2 lowerlim upperlim
type==3 mean width
```

The argument `hierarchy-number` indicates the order for the scan, zero being most significant. The type argument specifies the distribution to be used for random sampling: a Gaussian for 1 and 3, a flat distribution for 2. An argument of 1 gives a Gaussian with a width equal to a quarter of the mean.

If `RANDOM` is used, an additional command,

```
ALL RANDOMTOTAL hierarchy-number number-samples
```

is used to specify the significance in the hierarchy of the RANDOM commands and the number of samples to be taken. If the hierarchy-number for random sampling is smaller (more-significant) than a SCAN command, the scan will be made for a single value of the random parameters, while if it is larger, different random parameters will be taken for each scanned point.

A.3.5 Output Data

New output data are created by overloading `LoaderModel::PrintUnusualData(ostream &datafile,ostream &indexfile)`. If the member function DoneIndex() returns false, the method must, in addition to writing the datum to `datafile`, write to `indexfile` a line of the form

```
column-number-in-datafile human-readable-label
```

Where the current column-number is available from the method `int LoaderModel::IndexLine()`, and must be incremented afterwards using `void LoaderModel::NextIndexLine()`.

A.3.6 Changing The Extremisation Calculation

The calculation performed for each dataset can be changed by overloading `Model::DoAnyCalculation()`. If parameters are manually changed using the method `SetValue()`, a method `NotifyMassMatricesParametersChanged()` must be called. This allows the diagonalisation of the mass matrices to be done only when necessary. One might, for example, use the techniques of this section to set one parameter to be equal to some constnant times another, to enable two parameters to be scanned simultaneously:

```
void DerivedModel::DoAnyCalculation()
{
  //  lock arg At to arg Ab
  Parameter * iat = GetParameter("UpTrilinear->Top->Top->Imaginary");
  Parameter * iab = GetParameter("DownTrilinear->Top->Top->Imaginary");
  Parameter * rab = GetParameter("DownTrilinear->Top->Top->Real");
  Parameter * rat = GetParameter("UpTrilinear->Top->Top->Real");
  iab->SetValue(iat->Show()*rab->Show()/rat->Show());
  NotifyMassMatricesParametersChanged();
  SolveForZeroTadpolesByVaryingParameters(
   ShowParametersToSolveOver(),false);
}
```

The `GetParameter` method is used to retrieve a parameter from the list in the model by name.

A.3.7 Constructing And Using A Diagram Class

To develop a new diagram, it should be constructed as based on the following example:

```
#define MassCorrection_3Point_Loop1 2
#define MassCorrection_3Point_Loop2 3

#undef ClassName
#define ClassName MassCorrection_3Point_ScalarScalarLoop

class ClassName : public Diagram
{
```

```
double Function() {
    double couprod = Coupling(MassCorrection_Leg2,
     MassCorrection_3Point_Loop1,
     MassCorrection_3Point_Loop2);
    if (couprod==0.0) return 0.0;
    couprod*=Coupling(MassCorrection_Leg1,
     MassCorrection_3Point_Loop1,
     MassCorrection_3Point_Loop2);
    return One_o_32_pi_sq()*couprod*B0(psq(),
     SquareMass(MassCorrection_3Point_Loop1),
     SquareMass(MassCorrection_3Point_Loop2))*-0.25; }
public:
  #include "Diag_Constructors.h"
};
```

The header file `Diag_Constructors.h` defines the usual set of constructor functions for diagrams.

To use a diagram class, one must fill in a structure specifying which fields are to be used for each propagator in the diagram, and set flags specifying whether the interaction eigenstate specified is to be used, or all mass-mixing eigenstates should be summed over. The diagram instance is created using this structure, and then evaluated using `EvaluateAndSum()`. The following example, taken from the routine determining the scalar self-energy, explains this:

```
  ReadyMassMatricesForUse();
  vector<vector<MassMatrix *> > mmfordiag3pt(4);
  vector<int> whichestatefordiag3pt(4);
  vector<int> flagsfordiag3pt(4);
```

```
  mmfordiag3pt[MassCorrection_Leg1]=vector<MassMatrix *>();
  mmfordiag3pt[MassCorrection_Leg1].push_back(GetAssociatedMassMatrix(a));
  flagsfordiag3pt[MassCorrection_Leg1] = DIAGRAM_STATEDINTERESTATE;
  whichestatefordiag3pt[MassCorrection_Leg1]=
   (mmfordiag3pt[MassCorrection_Leg1].front())->WhichNumberInFields(a);
  mmfordiag3pt[MassCorrection_Leg2]=vector<MassMatrix *>();
  mmfordiag3pt[MassCorrection_Leg2].push_back(GetAssociatedMassMatrix(b));
  flagsfordiag3pt[MassCorrection_Leg2] = DIAGRAM_STATEDINTERESTATE;
  whichestatefordiag3pt[MassCorrection_Leg2]=
   (mmfordiag3pt[MassCorrection_Leg2].front())->WhichNumberInFields(b);

  mmfordiag3pt[MassCorrection_3Point_Loop1] = _pblockmassmatricesscalar;
  flagsfordiag3pt[MassCorrection_3Point_Loop1] = DIAGRAM_SUMOVERMASSESTATES;
  mmfordiag3pt[MassCorrection_3Point_Loop2] = _pblockmassmatricesscalar;
  flagsfordiag3pt[MassCorrection_3Point_Loop2] = DIAGRAM_SUMOVERMASSESTATES;

 double runningtotal=0;

 runningtotal += MassCorrection_3Point_ScalarScalarLoop
  (mmfordiag3pt,whichestatefordiag3pt,flagsfordiag3pt,
  this,p2).EvaluateAndSum()
```

The parameter `p2` is the external momentum to be sent for the diagram. The containter `_pblockmassmatricesscalar`, available as a data member of class `Model`, contains all of the scalar fields.

Bibliography

[1] B. C. Allanach, J. P. J. Hetherington, M. A. Parker, and B. R. Webber, *Naturalness reach of the large hadron collider in minimal supergravity*, *JHEP* **08** (2000) 017, [http://arXiv.org/abs/hep-ph/0005186].

[2] J. P. J. Hetherington, *The spectrum of the MSSM with nonstandard supersymmetry breaking*, *JHEP* **10** (2001) 024, [http://arXiv.org/abs/hep-ph/0108206].

[3] D. Bailin and A. Love, *Supersymmetric gauge field theory and string theory.* Graduate student series in physics. IOP, 1994.

[4] S. Weinberg, *Supersymmetry*, vol. 3 of *The quantum theory of fields.* CUP, 2000.

[5] S. P. Martin, *A supersymmetry primer*, http://arXiv.org/abs/hep-ph/9709356.

[6] H. E. Haber, *Introductory low-energy supersymmetry*, http://arXiv.org/abs/hep-ph/9306207.

[7] E. Witten, *Dynamical breaking of supersymmetry*, *Nucl. Phys.* **B188** (1981) 513.

[8] J. R. Ellis, S. Kelley, and D. V. Nanopoulos, *Probing the desert using gauge coupling unification*, *Phys. Lett.* **B260** (1991) 131–137.

[9] D. M. Ghilencea and G. G. Ross, *Precision prediction of gauge couplings and the profile of a string theory*, *Nucl. Phys.* **B606** (2001) 101, [http://arXiv.org/abs/hep-ph/0102306].

[10] C. Kolda and H. Murayama, *The Higgs mass and new physics scales in the minimal standard model*, *JHEP* **07** (2000) 035, [http://arXiv.org/abs/hep-ph/0003170].

[11] **ATLAS** Collaboration, *Detector and physics performance TDR, volume II*, tech. rep., CERN/LHCC, 1999.

[12] **CMS** Collaboration, *Technical proposal*, tech. rep., http://cmsinfo.cern.ch/TP/TP.html.

[13] D. R. Tovey, *Measuring the SUSY mass scale at the LHC*, *Phys. Lett.* **B498** (2001) 1–10, [http://arXiv.org/abs/hep-ph/0006276].

[14] S. Dimopoulos and G. F. Giudice, *Naturalness constraints in supersymmetric theories with nonuniversal soft terms*, *Phys. Lett.* **B357** (1995) 573–578, [http://arXiv.org/abs/hep-ph/9507282].

[15] R. Barbieri and A. Strumia, *About the fine-tuning price of LEP*, *Phys. Lett.* **B433** (1998) 63–66, [http://arXiv.org/abs/hep-ph/9801353].

[16] B. de Carlos and J. A. Casas, *One loop analysis of the electroweak breaking in supersymmetric models and the fine tuning problem*, *Phys. Lett.* **B309** (1993) 320–328, [http://arXiv.org/abs/hep-ph/9303291].

[17] G. W. Anderson and D. J. Castano, *Naturalness and superpartner masses or when to give up on weak scale supersymmetry*, *Phys. Rev.* **D52** (1995) 1693–1700, [http://arXiv.org/abs/hep-ph/9412322].

[18] M. Bastero-Gil, G. L. Kane, and S. F. King, *Fine-tuning constraints on supergravity models*, *Phys. Lett.* **B474** (2000) 103–112, [http://arXiv.org/abs/hep-ph/9910506].

[19] D. Wright, *Naturally nonminimal supersymmetry*, http://arXiv.org/abs/hep-ph/9801449.

[20] J. L. Feng, K. T. Matchev, and T. Moroi, *Focus points and naturalness in supersymmetry*, *Phys. Rev.* **D61** (2000) 075005, [http://arXiv.org/abs/hep-ph/9909334].

[21] H. Baer, C.-H. Chen, F. Paige, and X. Tata, *Signals for minimal supergravity at the CERN large hadron collider II: Multilepton channels*, *Phys. Rev.* **D53** (1996) 6241–6264, [http://arXiv.org/abs/hep-ph/9512383].

[22] J. R. Ellis, K. Enqvist, D. V. Nanopoulos, K. A. Olive, and M. Srednicki, *Su(n,1) inflation*, *Phys. Lett.* **B152** (1985) 175.

[23] B. C. Allanach, A. Dedes, and H. K. Dreiner, *Bounds on R-parity violating couplings at the weak scale and at the GUT scale*, *Phys. Rev.* **D60** (1999) 075014, [http://arXiv.org/abs/hep-ph/9906209].

[24] S. Davidson, M. Losada, and N. Rius, *Neutral Higgs sector of the MSSM without R(p)*, *Nucl. Phys.* **B587** (2000) 118–146, [http://arXiv.org/abs/hep-ph/9911317].

[25] L. J. Hall and L. Randall, *Weak scale effective supersymmetry*, *Phys. Rev. Lett.* **65** (1990) 2939–2942.

[26] J. Rosiek, *Complete set of Feynman rules for the minimal supersymmetric extension of the standard model*, *Phys. Rev.* **D41** (1990) 3464.

[27] I. Jack and D. R. T. Jones, *Non-standard soft supersymmetry breaking*, *Phys. Lett.* **B457** (1999) 101–108, [http://arXiv.org/abs/hep-ph/9903365].

[28] I. Jack and D. R. T. Jones, *Quasi-infra-red fixed points and renormalization group invariant trajectories for non-holomorphic soft supersymmetry breaking*, *Phys. Rev.* **D61** (2000) 095002, [http://arXiv.org/abs/hep-ph/9909570].

[29] F. M. Borzumati, G. R. Farrar, N. Polonsky, and S. Thomas, *Precision measurements at the Higgs resonance: A probe of radiative fermion masses*, http://arXiv.org/abs/hep-ph/9712428.

[30] F. Borzumati, G. R. Farrar, N. Polonsky, and S. Thomas, *Soft Yukawa couplings in supersymmetric theories*, *Nucl. Phys.* **B555** (1999) 53–115, [http://arXiv.org/abs/hep-ph/9902443].

[31] J. L. Diaz-Cruz, *FCNC from non-standard soft-breaking terms in the MSSM*, http://arXiv.org/abs/hep-ph/9906330.

[32] S. P. Martin, *Dimensionless supersymmetry breaking couplings, flat directions, and the origin of intermediate mass scales*, *Phys. Rev.* **D61** (2000) 035004, [http://arXiv.org/abs/hep-ph/9907550].

[33] J. M. Frère, M. V. Libanov, and S. V. Troitsky, *Neutrino masses from nonstandard supersymmetry breaking terms*, *Phys. Lett.* **B479** (2000) 343–346, [http://arXiv.org/abs/hep-ph/9912204].

[34] J. M. Frère, M. V. Libanov, and S. V. Troitsky, *Phenomenological aspects of nonstandard supersymmetry breaking terms*, http://arXiv.org/abs/hep-ph/0006149.

[35] E. Ma and M. Raidal, *Relaxing $b \longrightarrow s$ gamma constraints on the supersymmetric particle mass spectrum*, *Phys. Lett.* **B491** (2000) 297–304, [http://arXiv.org/abs/hep-ph/0006253].

[36] M. Peskin and D. Schröder, *An introduction to Quantum Field Theory.* Perseus Books, 1995.

[37] S. A. Abel and J. M. Frère, *Could the MSSM have no CP violation in the CKM matrix?*, *Phys. Rev.* **D55** (1997) 1623–1629, [http://arXiv.org/abs/hep-ph/9608251].

[38] J. L. Rosner, *CP violation: A brief review*, http://arXiv.org/abs/hep-ph/0005258.

[39] H. P. Nilles, M. Srednicki, and D. Wyler, *Weak interaction breakdown induced by supergravity*, *Phys. Lett.* **B120** (1983) 346.

[40] A. T. Davies, C. D. Froggatt, and A. Usai, *Light Higgs boson in the spontaneously CP violating NMSSM*, *Phys. Lett.* **B517** (2001) 375–382, [http://arXiv.org/abs/hep-ph/0105266].

[41] R. Ellis, W. Stirling, and B. R. Webber, *QCD and collider physics.* Cambridge monographs on particle physics, nuclear physics and cosmology. CUP, 1996.

[42] D. M. Pierce, J. A. Bagger, K. T. Matchev, and R.-J. Zhang, *Precision corrections in the minimal supersymmetric standard model*, *Nucl. Phys.* **B491** (1997) 3–67, [http://arXiv.org/abs/hep-ph/9606211].

[43] S. Weinberg, *Perturbative calculations of symmetry breaking*, *Phys. Rev.* **D7** (1973) 2887–2910.

[44] G. Gamberini, G. Ridolfi, and F. Zwirner, *On radiative gauge symmetry breaking in the minimal supersymmetric model*, *Nucl. Phys.* **B331** (1990) 331–349.

[45] P. M. Ferreira, *Minimisation of a one-loop charge breaking effective potential*, *Phys. Lett.* **B512** (2001) 379–391, [http://arXiv.org/abs/hep-ph/0102141].

[46] V. D. Barger, M. S. Berger, and P. Ohmann, *The supersymmetric particle spectrum*, *Phys. Rev.* **D49** (1994) 4908–4930, [http://arXiv.org/abs/hep-ph/9311269].

[47] M. Claudson, L. J. Hall, and I. Hinchliffe, *Low-energy supergravity: False vacua and vacuous predictions*, *Nucl. Phys.* **B228** (1983) 501.

[48] G. Passarino and M. J. G. Veltman, *One loop corrections for e^+e^- annihilation into $\mu^+\mu^-$ in the Weinberg model*, *Nucl. Phys.* **B160** (1979) 151.

[49] A. Denner, *Techniques for calculation of electroweak radiative corrections at the one loop level and results for W physics at LEP-200*, *Fortschr. Phys.* **41** (1993) 307–420.

[50] I. Jack and D. R. T. Jones, *Infra-red stability of Yukawa and soft-breaking fixed points*, *Phys. Lett.* **B443** (1998) 177–184, [http://arXiv.org/abs/hep-ph/9809250].

[51] F. E. Paige, S. D. Protopopescu, H. Baer, and X. Tata, *ISAJET 7.40: A Monte Carlo event generator for pp, anti-pp, and e^+e^- reactions*, http://arXiv.org/abs/hep-ph/9810440.

[52] B. C. Allanach, *SOFTSUSY: A C++ program for calculating supersymmetric spectra*, http://arXiv.org/abs/hep-ph/0104145.

[53] H. Baer. private communication.

[54] T. Sjöstrand, L. Lönnblad, and S. Mrenna, *PYTHIA 6.2: Physics and manual*, http://arXiv.org/abs/hep-ph/0108264.

[55] G. Corcella *et. al.*, *HERWIG 6: An event generator for hadron emission reactions with interfering gluons (including supersymmetric processes)*, *JHEP* **01** (2001) 010, [http://arXiv.org/abs/hep-ph/0011363].

[56] S. Moretti, K. Odagiri, P. Richardson, M. H. Seymour, and B. R. Webber, *Implementation of supersymmetric processes in the herwig event generator*, *JHEP* **04** (2002) 028, [http://arXiv.org/abs/hep-ph/0204123].

[57] E. Richter-Was, D. Froidevaux, and L. Poggioli, *Atlfast 2.0: A fast simulation package for ATLAS*, ATL-PHYS-98-131. ATLAS internal note.

[58] G. Sterman and S. Weinberg, *Jets from quantum chromodynamics*, *Phys. Rev. Lett.* **39** (1977) 1436.

[59] J. L. Feng, K. T. Matchev, and T. Moroi, *Multi-TeV scalars are natural in minimal supergravity*, *Phys. Rev. Lett.* **84** (2000) 2322–2325, [http://arXiv.org/abs/hep-ph/9908309].

[60] A. Romanino and A. Strumia, *Are heavy scalars natural in minimal supergravity?*, *Phys. Lett.* **B487** (2000) 165–170, [http://arXiv.org/abs/hep-ph/9912301].

[61] W. T. Giele, T. Matsuura, M. H. Seymour, and B. R. Webber, *W boson plus multijets at hadron colliders: HERWIG parton showers versus exact matrix elements*, . Contribution to Proc. of 1990 Summer Study on High Energy Physics: Research Directions for the Decade, Snowmass, CO, Jun 25 - Jul 13, 1990.

[62] B. C. Allanach *et. al.*, *Report of the beyond the standard model working group of the 1999 UK phenomenology workshop on collider physics (Durham)*, *J. Phys.* **G26** (2000) 551–592, [http://arXiv.org/abs/hep-ph/9912302].

[63] H. Baer, C.-H. Chen, M. Drees, F. Paige, and X. Tata, *Probing minimal supergravity at the CERN LHC for large* $\tan(\beta)$, *Phys. Rev.* **D59** (1999) 055014, [http://arXiv.org/abs/hep-ph/9809223].

[64] V. D. Barger, *Supersymmetry phenomenology*, http://arXiv.org/abs/hep-ph/9801440.

[65] W. H. Press, S. A. Teukolsky, W. T. Vettering, and F. B. P., *Numerical Recipes in C*. CUP, 2nd ed., 1992.

[66] T. Hahn, *Loop Tools User's Guide*, July, 2000. www.feynarts.de/looptools.

[67] J. R. Espinosa and I. Navarro, *Scale-independent mixing angles*, *Phys. Rev.* **D66** (2002) 016004, [http://arXiv.org/abs/hep-ph/0109126].

[68] A. Pilaftsis and C. E. M. Wagner, *Higgs bosons in the minimal supersymmetric standard model with explicit CP violation*, *Nucl. Phys.* **B553** (1999) 3–42, [http://arXiv.org/abs/hep-ph/9902371].